โครงการ
การเรียนการสอนเพื่อเสริมประสบการณ์

ชื่อโครงการ	EFFECTS OF CLAY MINERALS AND CARBONATE CONTENT ON HYDROGEN AND OXYGEN INDICES OF SOURCE ROCK – A CASE STUDY OF HUAI HIN LAT FORMATION
ชื่อนิสิต	PONDWIPA SUTHIWORASIN
ภาควิชา	GEOLOGY
ปีการศึกษา	2558

คณะวิทยาศาสตร์ จุฬาลงกรณ์มหาวิทยาลัย

ผลของแร่ดินและปริมาณคาร์บอเนตต่อค่าดัชนีไฮโดรเจนและดัชนีออกซิเจนของหินต้นกำเนิด กรณีศึกษาหมวดหินห้วยหินลาด

นางสาว พรวิภา สุทธิวรสิน

รายงานนี้เป็นส่วนหนึ่งของการศึกษาตามหลักสูตรปริญญาวิทยาศาสตรบัณฑิต
ภาควิชาธรณีวิทยา คณะวิทยาศาสตร์ จุฬาลงกรณ์มหาวิทยาลัย
ปีการศึกษา 2558

EFFECTS OF CLAY MINERALS AND CARBONATE CONTENT ON HYDROGEN AND OXYGEN INDICES OF SOURCE ROCK - A CASE STUDY OF HUAI HIN LAT FORMATION

Miss Pondwipa Suthiworasin

A Report Submitted in Partial Fulfillment of the Requirements

for the Degree of Bachelor of Science in Geology

Department of Geology

Faculty of Science

Chulalongkorn University

Academic Year 2015

Date of submit _____/_____/_____

Date of approve _____/_____/_____

_____

(Dr. Kruawun Jankeaw)

Senior Project Advisor

หัวข้องานวิจัย: ผลของแร่ดินและปริมาณคาร์บอเนตต่อค่าดัชนีไฮโดรเจนและดัชนีออกซิเจนของหินต้นกำเนิด กรณีศึกษาหมวดหินห้วยหินลาด

ผู้ทำการวิจัย: นางสาวพรวิภา สุทธิวรสิน

ภาควิชา: ธรณีวิทยา

อาจารย์ที่ปรึกษา: อาจารย์ ดร.เครือวัลย์ จันทร์แก้ว

ปีการศึกษา: 2558

บทคัดย่อ

ผลจากการศึกษาธรณีเคมีปิโตรเลียมของหมวดหินห้วยหินลาดที่ผ่านมา พบว่ามีค่าดัชนีไฮโดรเจนต่ำและค่าดัชนีออกซิเจนสูง (Chamchoy, 2014) งานวิจัยนี้จึงมีจุดประสงค์เพื่อศึกษาว่าแร่ดินและแร่คาร์บอเนตเป็นสาเหตุทำให้ค่าดัชนีไฮโดรเจนในตัวอย่างมีค่าต่ำ และดัชนีออกซิเจนมีค่าสูงหรือไม่ โดยใช้เครื่องมือ X-Ray Diffractometer และการศึกษาแผ่นหินบาง ในการวิเคราะห์หาชนิดและปริมาณแร่องค์ประกอบโดยประมาณ ซึ่งจะทำให้ได้ชนิดและปริมาณของแร่ดินและแร่คาร์บอเนตในหินตัวอย่าง นอกจากนี้ยังได้ทำการเปรียบเทียบค่าดัชนีไฮโดรเจนและดัชนีออกซิเจนระหว่างตัวอย่างดั้งเดิมและตัวอย่างที่กำจัดแร่คาร์บอเนตออก เพื่อดูผลของแร่คาร์บอเนตที่มีต่อค่าดัชนีออกซิเจน โดยทำการศึกษาชั้นหินบริเวณน้ำตกตาดใหญ่ อยู่ระหว่างอำเภอน้ำหนาว จังหวัดเพชรบูรณ์และอำเภอภูผาม่าน จังหวัดขอนแก่น และเก็บตัวอย่างหินสดทั้งหมด 25 ตัวอย่าง ซึ่งส่วนใหญ่เป็นหินโคลนสีดำสลับหินปูนเนื้อดินของหมู่หินดาดฟ้า หมวดหินห้วยหินลาด

ผลการศึกษาพบว่าหินตัวอย่างประกอบด้วยแร่คาร์บอเนตชนิดโดโลไมต์ (เฉลี่ย 30.76 wt%) และแคลไซต์ (เฉลี่ย 7.96 wt%) และแร่ดินประเภทอิลไลต์ (เฉลี่ย 4.29 wt%) มีศักยภาพในการให้กำเนิดปิโตรเลียมต่ำ (S_2 เฉลี่ย 0.11 mg HC/ g rock) เมื่อพล็อตสมการเส้นตรงระหว่าง S_2 และ TOC เพื่อศึกษาผลของแร่ประกอบหินที่มีต่อค่า S_2 พบว่า ค่าดัชนีไฮโดรเจนที่แท้จริงที่คำนวณได้จากความชันของกราฟ เฉลี่ยเท่ากับ 11.89 mg HC/g TOC ซึ่งอยู่ในช่วงเคอโรเจนชนิดที่ IV และจุดตัดแกน y ของสมการที่บ่งบอกถึงปริมาณไฮโดรคาร์บอนที่ถูกดูดซับไว้ที่ผิวแร่ในระหว่าง pyrolysis มีค่าต่ำ (เฉลี่ย 0.1257 mg HC/ g rock) การที่ตัวอย่างประกอบด้วยแร่ดิน (แร่อิลไลต์) ในปริมาณน้อย ซึ่งแร่ดินนี้เป็นแร่ที่สามารถดูดซับไฮโดรคาร์บอนไว้ได้ที่สุดในหินตัวอย่าง, มีปริมาณ S_2 ต่ำ, มีปริมาณกากคาร์บอน (Carbon residue) ที่เหลือจาก pyrolysis และคาร์บอนที่ไม่สามารถแตกตัวเป็นไฮโดรคาร์บอน (Dead carbon) สูง (1.0386 wt%) และมีระดับความพร้อมในการให้ปิโตรเลียมสูง สันนิษฐานว่าในอดีตเคอโรเจนในหินตัวอย่างอาจแตกตัวให้ไฮโดรคาร์บอนไปมาก คงเหลือไว้แต่คาร์บอนที่ไม่สามารถแตกตัวเป็นไฮโดรคาร์บอนได้ ทำให้ได้ค่า S_2 และ S_3 ต่ำ การตรึงไฮโดรคาร์บอนของแร่ดินในระหว่าง pyrolysis มีผลต่อค่าดัชนีไฮโดรเจนเพียงเล็กน้อยเท่านั้น อีกทั้งยังพบว่าตัวอย่างที่มีการล้างคาร์บอเนตออกมีการกระจายของข้อมูลใน Modified Van-Krevelen diagram น้อยกว่า และโดยรวมมีค่าดัชนีออกซิเจนน้อยกว่าตัวอย่างปกติเล็กน้อย แสดงถึงผลของคาร์บอเนตที่มีต่อค่าดัชนีออกซิเจนเพียงเล็กน้อย

นอกจากนี้ยังได้ทำการวิเคราะห์หาปริมาณอินทรีย์คาร์บอนรวม พบว่ามีปริมาณต่ำถึงสูง (0.47 - 3.55 wt%) หินตัวอย่างส่วนใหญ่จึงจัดว่ามีศักยภาพในการเป็นหินต้นกำเนิดที่ดี และจากค่า T_{max} ทำให้ทราบว่าตัวอย่างมีระดับความพร้อมในการให้ปิโตรเลียมอยู่ในช่วง post mature

คำสำคัญ: หมวดหินห้วยหินลาด, Rock-Eval pyrolysis, ดัชนีไฮโดรเจน, ดัชนีออกซิเจน, ผลของแร่ดินและแร่คาร์บอเนต, การตรึงไฮโครคาร์บอน

TITLE: EFFECTS OF CLAY MINERALS AND CARBONATE CONTENT ON HYDROGEN AND OXYGEN INDICES OF SOURCE ROCK - A CASE STUDY OF HUAI HIN LAT FORMATION

RESEARCHER: PONDWIPA SUTHIWORASIN

DEPARTMENT: GEOLOGY

ADVISOR: DR. KRUAWUN JANKAEW

ACADEMUC YEAR: 2558

ABSTRACT

The study of petroleum geochemistry of Huai Hin Lat Formation cutting samples found that Huai Hin Lat Formation had high hydrogen index and low oxygen index (Chamchoy, 2014). Therefore, this research aims to study whether clay minerals and carbonate content affect the hydrogen and oxygen indices. Petrographic thin sections and X-Ray Diffractometer were used to identify the type and amount of minerals in the samples especially carbonate and clay minerals. Moreover, the comparison between hydrogen and oxygen indices of the original and decarbonated samples could evaluate the effect of carbonate minerals on oxygen index values. The study area is Tat Yai waterfall located on the boundary between Amphoe Phu Pha Man, Changwat Khon Kaen and Amphoe Nam Nao, Changwat Phetchabun. Twenty-five samples of Dat Fa Member laminated black calcareous mudstone interbedded with argillaceous limestone were collected for this study.

The results revealed that Tat Yai samples contain carbonate minerals: dolomite with an average content of 30.76 wt% and calcite with an average content of 7.96 wt% and clay minerals, illite with an average content of 4.29 wt%. The samples have low hydrocarbon generation potential (average S_2 0.11 mg HC/ g rock). The regression lines of S_2 vs. TOC diagram were used to determine mineral matrix effect on S_2 values. True average hydrogen index calculated from slope of the regression lines is 11.89 mg HC/g TOC which falls into kerogen type IV range. Y-intercept which is an amount of hydrocarbons retained by mineral matrix during pyrolysis is low (0.1257 mg HC/ g rock in average). Low content of illite (which is the most active minerals that could retain hydrocarbons on its surface), low S_2 values, high coke from pyrolysis and dead carbons (1.0386 wt%) and high maturation level, all suggest that kerogen might have already cracked to hydrocarbons and only dead carbons are left which cannot generate hydrocarbons. Therefore, hydrocarbon retention during pyrolysis slightly affects the hydrogen index values. From Modified Van-Krevelen diagram, the decarbonated samples have slightly lower oxygen indices than the original samples and have less scatter data showing little effect of carbonate content on oxygen indices.

Tat Yai samples have low - high TOC content (0.47 - 3.55 wt%). Most samples have good source rock potential and are in post-mature stage based on T_{max} values.

Keywords: Huai Hin Lat Formation, Rock-Eval pyrolysis, Hydrogen index, Oxygen index, Mineral matrix and carbonate content effect, Hydrocarbon retention

ACKNOWLEDGEMENT

This research would not be accomplished without kind support and help of many individuals and organizations. I would like to extend my sincere thanks to all of them.

Firstly, I would like to express my deep appreciation to Dr. Kruawun Jankaew, my research advisor, for her patient guidance, enthusiastic encouragement and useful suggestions for this research.

For the field observation, I would like to extend my sincere thanks to Assoc. Prof. Dr. Anat Ruangrassamee and Mr. Sompong Kumchang from Department of Civil Engineering, Faculty of Engineering, Chulalongkorn University and Mr. Andrew Cromarty for kind support.

For the laboratory works, I especially appreciate Ms. Jiraprapa Neampan, Ms. Banjong Puangthong, Ms. Sophit Poomphuang, Mr. Suriya Chokemor, Mr. Prajin Thongprachum and Ms. Wanida Muangnoicharoen (staffs of the Department of Geology, Chulalongkorn University), Assoc. Prof. Dr. Kawee Srikulkit, Dr. Dujreutai Pongkao Kashima and Mr. Wirapong Kornpanom from Department of Materials Science, Chulalongkorn university for their permission to use instruments. I also wish to thank Core Laboratories Malaysia and Dr. Thammanoon Manosuthikij from PTT Research and Technology Institute for the support of TOC and Rock-Eval pyrolysis analyses. Moreover, I am thankful to financial support from PTTEP research grant “Petroleum Geochemistry of the Source rock of the Khorat Basin” awarded.

Finally, I am sincerely grateful for all lecturers, Ms. Chineenart Prachaiboon, Mr. Alongkot Fanka, my friends and juniors in the Department of Geology, Chulalongkorn University and my family for their motivation that encouraged me to complete my research.

CONTENTS

Page

LIST OF FIGURES

Page

Page

LIST OF TABLES

CHAPTER 1

INTRODUCTION

1.1 Background and Rationale

Petroleum exploration in Khorat Plateau began in the early 1960's and was successfully discovered in 1981 by Esso. Today only Nam Phong and Sin Phu Horm gas fields are in production in Northeastern Thailand. The gas had accumulated in Permian fractured limestone (Pha Nok Khao and Hua Na Kham Formation of Saraburi Group). The clastic Late Triassic Pre-Khorat Group (Huai Hin Lat Formation and Kuchinarai Group) and Permian Saraburi Group are believed to be potential source rocks (Racey, 2011).

Huai Hin Lat Formation is the Late Triassic (Carnian-Norian) Pre-Khorat Group exposed along the western edge of Khorat Plateau. It is unconformably overlain by the younger Nam Phong Formation of Khorat Group and underlain by Permian limestone of Saraburi Group with Indosinian I unconformity. Huai Hin Lat Formation comprises 5 Members; Pho Hai, Sam Khaen, Dat Fa, Phu Hi and I Mo Members (Sattayarak, 1978). The depositional environments vary from alluvial fan to fluvio-lacustrine environment in slightly humid to semi-arid condition (กรมทรัพยากรธรณี, 2550). However, Dat Fa Member composes of greyish black calcareous shale interbedded with argillaceous limestone and has a high organic matter content and is thought to be a potential source rock.

Petrographic description of thin sections and X-ray diffraction (XRD) analyses were carried out on black calcareous shale of Huai Hin Lat Formation by Prachaiboon (2014) and Arsairai (2014). The rock is mostly composed of feldspar, carbonate and clay minerals. The study of depositional environment and petroleum source rock potential found that organic-rich rocks of Huai Hin Lat Formation deposited in highly reducing condition with high TOC, which indicates good source rock potential and contains mainly type I kerogen (Sapropelic group) from point counting of organic materials under microscope (Arsairai, 2014). On the contrary, Khositchaisri (2012) concluded that Huai Hin Lat Formation is a gas-prone source rock containing mainly type III kerogen (Vitrinite and Inertinite macerals) from visual kerogen analysis. Chamchoy (2014) studied petroleum source rock potential of Huai Hin Lat Formation cutting samples by Rock-Eval pyrolysis method and found that it has low hydrogen index with some samples have high oxygen index, which might initially contain

kerogen type II, II/III and III but had been converted to kerogen type IV during thermal maturity process.

The inconsistency between results from Rock-Eval pyrolysis study of Chamchoy (2014) and visual kerogen analysis of Arsairai (2014) and Khositchaisri (2012) causes doubt whether carbonate and clay minerals affect hydrogen and oxygen index values of the Huai Hin Lat source rock, leading to different interpretation of kerogen type based on hydrogen and oxygen indices.

1.2 Definitions of specific terms

Source rock is a sedimentary rock, which has quantity of organic matter to generate hydrocarbons and has thermal maturity. Most source rock is grey or black shale. There are some limestones and coal that can generate hydrocarbons too. Quantity, quality and maturation are main parameters used to evaluate potential of source rock.

Kerogen is a mixture of organic matter in sedimentary rocks, that is insoluble in organic solvents. Table 1.1 below lists and defines four kerogen types.

Table 1.1 Kerogen classified by source material (Modified from Law, 1999).

Kerogen type	Name	Predominant hydrocarbon potential	Typical depositional environment
I	Algal kerogen	Oil prone	Lacustrine
II	Liptinitic kerogen	Oil and gas prone	Marine
III	Humic	Gas prone	Terrestrial
IV	Inertinite	Neither (primarily composed of vitrinite) or inert material	Terrestrial(?)

Total Organic Carbon (TOC) is a quantity (amount) of organic carbon present in a sedimentary rock. It is typically used to assess the potential of source rocks (Table 1.2) and help evaluate some unconventional reservoirs.

Table 1.2 Guidelines for classifying potential source rock (Matthis, 1999).

Hydrocarbon Generation Potential	TOC in Shale (wt. %)	TOC in Carbonates (wt. %)
Poor	0.0-0.5	0.0-0.2
Fair	0.5-1.0	0.2-0.5
Good	1.0-2.0	0.5-1.0
Very Good	2.0-5.0	1.0-2.0
Excellent	>5.0	>2.0

Rock-Eval pyrolysis is a method used to identify the quality (kerogen types) and maturation of organic matter. Samples will be heated to 550 ℃ under an inert atmosphere. The amount of free hydrocarbons are volatile at 300 ^{o}C and are measured as a S_1 peak. The hydrocarbons released from thermal cracking of nonvolatile organic matter and very heavy hydrocarbons compounds are recorded as a S_2 peak. T_{max} is the temperature, at which the maximum release of hydrocarbons from kerogen cracking (S_2) occurs. The CO_2 generated from kerogen cracking is trapped in the 300 – 390 ℃ and recorded as a S_3 peak as shown in Figure 1.1.

Modified Van-Krevelen diagram is a diagram used to assess type and maturity of kerogen from hydrogen and oxygen indices. Hydrogen and oxygen indices are calculated from Rock-Eval data.

Hydrogen index (HI) = S_2/TOC x 100

Oxygen index (OI) = S_3/TOC x 100

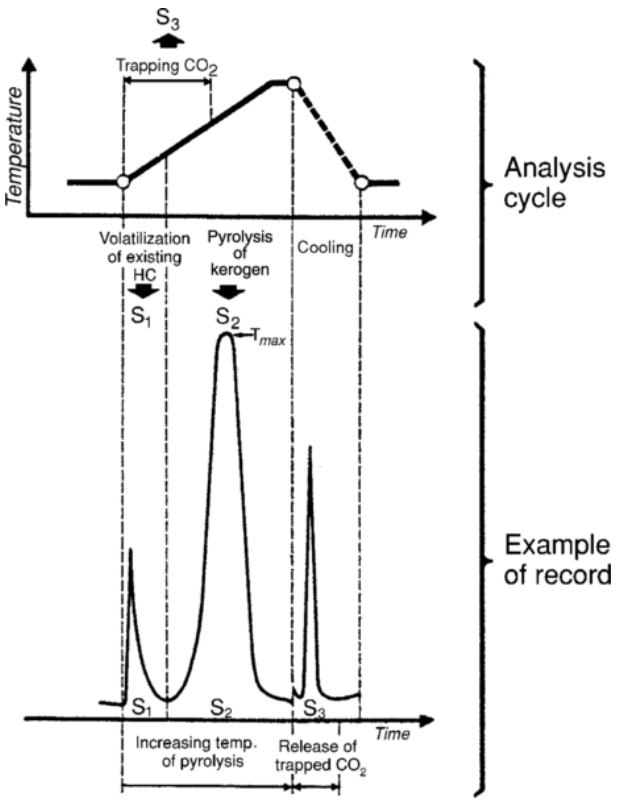

Figure 1.1 Cycle of analysis and the recording of Rock-Eval pyrolysis (Tissot and Welte, 1984).

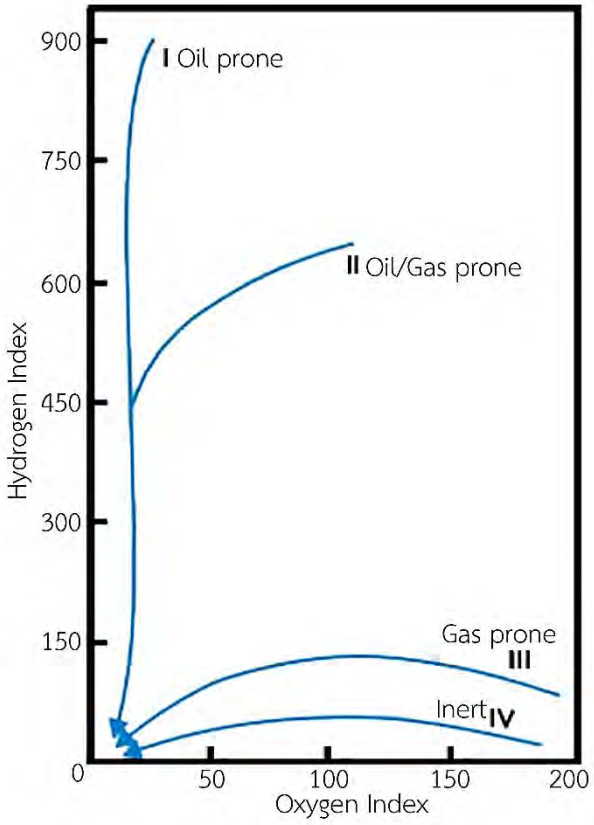

Figure 1.2 Modified Van-Krevelen diagram (Modified from Slat, 2002).

Table 1.3 Guidelines for assessing source rock quality and maturation by Rock-Eval data (Peters and Garrey, 2014).

Quantity	TOC	S_1(mg HC/g rock)	S_2(mg HC/g rock)
Poor	<0.5	<0.5	<2.5
Fair	0.5-1	0.5-1	2.5-5.0
Good	1-2	1-2	5-10
Very Good	2-4	2-4	10-20
Excellent	>4	>4	>20
Quality	HI (mg HC/g TOC)	S2/S3	Kerogen Type
None	<50	<1	IV
Gas	50-200	1-5	III
Gas and Oil	200-300	5-10	II/III
Oil	300-600	10-15	II
Oil	>600	>15	I
Maturation	Ro (%)	Tmax (^{0}C)	TAI
Immature	0.2-0.6	<435	1.5-2.6
Early Mature	0.6-0.65	435-445	2.6-2.6
Peak Mature	0.65-0.9	445-450	2.7-2.9
Late Mature	0.9-1.35	450-470	2.9-3.3
Post Mature	>1.35	>470	>3.3

X-Ray diffraction (XRD) is a unique method in identification and characterization of crystalline materials by measuring the angles and intensities of X-Ray diffracted beams. When X-Ray incident beam interacts with atomic plane, part of the beam is transmitted, absorbed, refracted and scattered and diffracted. The diffraction of X-rays by crystals is described by Bragg's Law.

$n\lambda = 2d \sin\theta$ n = order of the reflection

λ = wavelength of electromagnetic radiation

d = lattice spacing in a crystalline sample

θ = diffraction angle

When samples and detector are rotated, 2-theta angles (twice the diffraction angles) are recorded and all possible diffraction directions of the lattice will be attained due to the random orientation of the powdered material (Figure 1.3). Then, the diffraction peaks are converted to d-spacings for mineral identification because each mineral has a set of unique d-spacings. Typically, this is achieved by comparison of d-spacings with standard reference patterns (Crain, 2015: www.spec2000.net/09-xrd.htm).

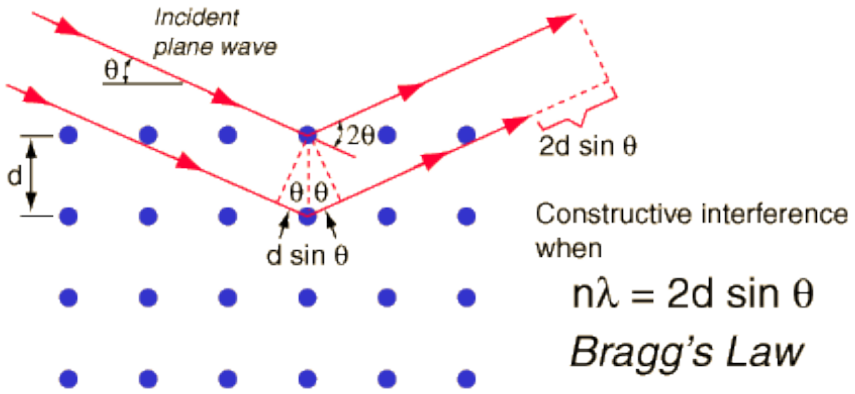

Figure 1.3 Incident X-Rays diffracted by the layers of atoms in a crystalline material (http://hyperphysics.phy-astr.gsu.edu).

1.3 Objective

To determine the effects of clay minerals matrix and carbonate content on hydrogen and oxygen indices of Dat Fa Mamber, Huai Hin Lat Formation from Rock-Eval pyrolysis method which might explain why this black calcareous mudstone has low hydrogen index (HI) but high oxygen index (OI).

1.4 Scope of work

Twenty-five samples were collected from Tat Yai waterfall and ground to perform geochemical analyses. Petrographic thin sections and X-ray diffractometer (XRD) analyses are used for quantitative determination of mineral content. Total Organic Carbon (TOC) analyzer is used to measure organic carbon content in samples and evaluate source rock quality. Rock-Eval pyrolysis is used to measure S_1, S_2, S_3 of original samples and decarbonated samples. Then, hydrogen and oxygen indices are calculated and plotted in Modified Van-Krevelen diagram to identify quality and maturation of organic matter. Moreover, the S_2 – TOC diagram is plotted to determine mineral matrix effect.

1.5 Study area

The study area is Tat Yai waterfall (47Q 796734N 1850785E) in Phu Pha Man National Park which is located on the boundary between Amphoe Phu Pha Man, Changwat Khon Kaen and Amphoe Nam Nao, Changwat Phetchabun. The waterfall is about 100-150 meters high. It consists of Dat Fa Member laminated black calcareous mudstone interbedded with argillaceous limestone (อนุวัชร ตรีโรจนานนท์, 2555).

1.6 Expected outcomes

- Dominant minerals that might affect hydrogen indices as identified from XRD
- Determine if carbonate content affects oxygen index values of Dat Fa Member, Huai Hin Lat Formation from Rock-Eval pyrolysis data

CHAPTER 2

LITERATURE REVIEW

2.1 Geology of the Khorat Plateau Basin

Khorat Plateau is a saucer-shaped landform in Northeastern Thailand occupying about 200,000 km^2 and tilting southeastward. The average elevation is 200 meters above sea level. The plateau is bounded by the Mekong River (north and east on the Laos border), the Phetchabun and Phang Hoei ranges (west), and the Phanom Dong Rak Range (south). The western and southern margins are rimmed by cuesta scarps, which rise between 600 to 1,000 meters above sea level. The plateau can be divided by Phu Phan Anticlinorium into 2 sub-basins: the northern Ubon-Sakhon Nakhon sub-basin and the southern Khorat-Ubon sub-basin which both dip eastward (กรมทรัพยากรธรณี, 2550).

Khorat Plateau mainly consists of the Mesozoic sedimentary rocks of Khorat Group except for the western rim which Triassic Pre-Khorat Group and Permo-Carboniferous rocks are exposed (as shown in Geologic map of Khorat Plateau in Figures 2.1, 2.2). The plateau is composed of an initial rift sequence of Carboniferous to Triassic age sediments and a syn-rift sequence of Late Triassic to Cretaceous age sediments. The syn-rift sequence deposited after Indosinian I unconformity, which represented the main collision between Indochina block and its neighbors (RPS Energy Consultants Limited, 2012).

Khorat Basin was a half-graben basin formed in Late Triassic. Eastward subduction of Shan-Thai block beneath Indochina block began in Late Permian. The collision of these two blocks in the Early Triassic (Nan-Uttaradit Suture) created the Loei-Petchabun Fold Belt and Indosinian Orogeny. In the Late Triassic, an extensional event occurred and thermal subsidence started. Therefore, sediments were deposited in fault-bounded extensional basins on angular unconformity above horst and graben structures of Permian sequence. Thermal subsidence continued in the Late Cretaceous – Early Tertiary. Mesozoic and Tertiary sediments in Northeastern Thailand are continental deposits of Khorat Group (Cooper, 1989). The uplift and erosion of Khorat Plateau may have occurred during 40 Ma, suggesting Paleogene compressional tectonics associated with folding and faulting was a main tectonic event in the plateau and nearby regions (Charusiri, 2012). Tectonic evolution of the Khorat basin is shown in Figure 2.3.

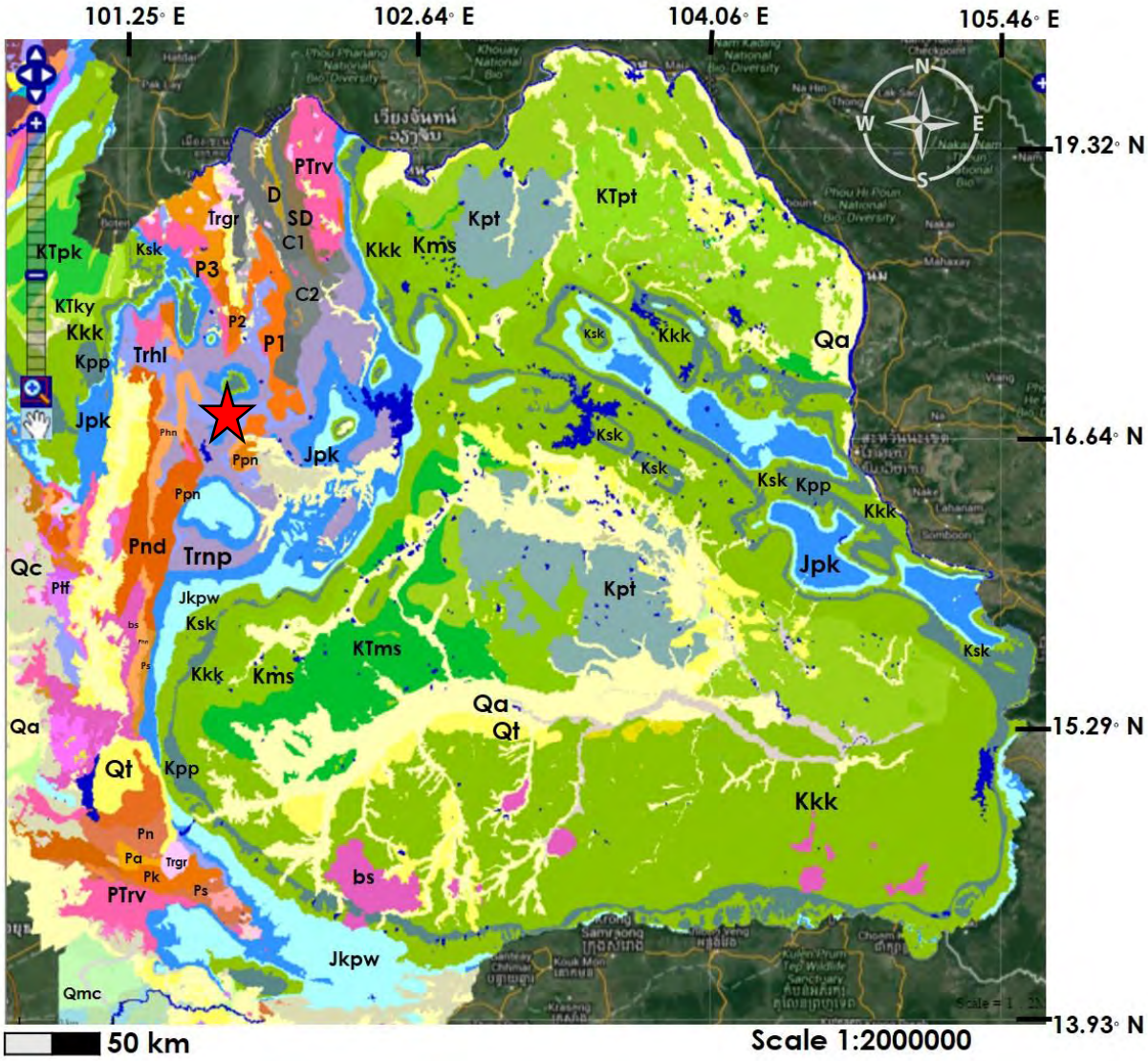

Figure 2.1 Digital geologic map 1:25000 of Northeastern Thailand (Modified from DMR, 2015).

The study area is shown as a star.

SEDIMENT, SEDIMENTARY AND METAMORPHIC ROCKS	FORMATION/GROUP	PERIOD	AGE (my.)
Alluvial deposit : sand, silt, clay and fine-grained gravel Terrace deposits : gravel, sand, silt and clay Colluvial deposits : Gravelly sand to sandy clay, loose bodies of sediment, deposited at the base of mountains or the bottom of a low-grade slope, transported by gravity Coastal tide-dominated deposits : clay, silt, and fine sand of tidal flat, marsh, mangrove swamp, and estuary		Quaternary	0.01-1.6
Mudstone, reddish brown; siltstone, orangish & reddish brown; feldspathic sandstone, brick red, fine grained, small scale cross bedding, with trace fossils of burrows	Phu Thok Fm., Khorat Gp.	Tertiary to Cretaceous	1.6-140
Siltstone, shale, and sandstone, brick red, purplish red, thin -thick bedded with rock salt, potash, gypsum and anhydrite	Maha Sarakham Fm., Khorat Gp.	Cretaceous	66.4-140
Siltstone and sandstone, brownish red and red, calcareous, claystone and conglomerate ; with calcrete horizons	Khok Kruat Fm., Khorat Gp.		
Conglomeratic sandstone, sandstone and conglomerate lens, grayish white, medium-coarse grained, poorly sorted, subangular to subrounded, composed of chert, quartz and siliceous clay, well bedded, cross bedding in common	Phu Phan Fm., Khorat Gp.		
Arkosic sandstone, reddish brown, fine-medium grained interbedded with siltstone, claystone and conglomerate; with abundant calcrete horizons	Sao Khua Fm., Khorat Gp.		
Quartzitic sandstone, grayish white, fine-medium grained, moderately sorted, tabular cross bedding in common, occasionally interbedded with conglomeratic sandstone	Phra Wihan Fm., Khorat Gp.	Cretaceous to Jurassic	66.4-210
Micaceous sandstone, siltstone, and claystone, maroon, intercalated with grayish green sandstone, with calcrete horizons ; trace fossils with small scale cross bedding	Phu Kradung Fm., Khorat Gp.	Jurassic	140-210
Sandstone, reddish brown, fine-medium grained, well sorted subangular-subrounded, interbedded with calcareous siltstone/claystone with purplish gray carbonate nodules	Nam Phong Fm.	Triassic	210-245
Basal conglomerate and local volcanic conglomerate; shale, mudstone, siltstone, gray, yellowish-brown; graywacke.	Huai Hin Lat Fm.		
Shale, sandstone, siltstone, and conglomerate	Pha Dua Fm.	Permian	245-286
Shale intercalated with sandstone, gray limestone lens	E-Lert Fm.		
Limestone, gray, whitish gray, well-beded, fossils in common of fusulinids, corals, sponges, algaes, and crinoids	Nam Maholan Fm.		
Shale, greyish black, brownish-red; sandstone, brownish-yellow, brownish-red, small to medium cross-bedded, highly folded siliceous cementing; limestone lens.	Nam Duk Fm.		
Shale, gray; sandstone, yellowish-brown and limestone, gray lense or bedded; fossils are fusulinids, brachiopods, corals, and plant remains	Hua Na Kham Fm.		
Limestone, gray, massive and bedded; shale, grey, yellowish-brown; and chert, gray; fossils are fusulinids, brachiopods, ammonites and corals	Pha Nok Khao Fm.		
Limestone, gray to black, massive to well bedded; chert, black nodular or thin bedded; with intercalations of thin bedded gray shale	Tak Fa Fm.		
Shale, siltstone, thin-bedded limestone	Wang Saphung Fm.	Carboniferous	286-360
Quartzose sandstone, shale, silty shale, limestone lens and conglomerate	Nong Dok Bua Fm.		
Chert with layer of tuff, limestone lens, and locally shale	Pak Chom Fm.	Devonian	286-360
Phyllite, quartzite, schist, slate and sandstone		Devonian-Silurian	286-360
IGNEOUS ROCKS		PERIOD	AGE (my.)
Basalt, dark gray to black, vesicular and amygdaloidal, with phenocrysts and megacrysts of olivine, pyroxene and spinel locally columna joints		Tertiary	1.6-66.4
Biotite granite, tourmaline granite, granodiorite, biotite-muscovite granite, muscovite-tourmaline granite, biotite-tourmaline granite		Triassic	210-245
Tuff, andesitic tuff, rhyolitic tuff, greenish-gray, light-gray, white; agglomerate, greenish-gray, rhyolitic white, light gray; and andessite, greenish-gray		Triassic-Permian	210-286

Figure 2.2 Explanation of the geologic map of Northeastern Thailand (Modified from กิตติ ขาววิเศษ, 2552).

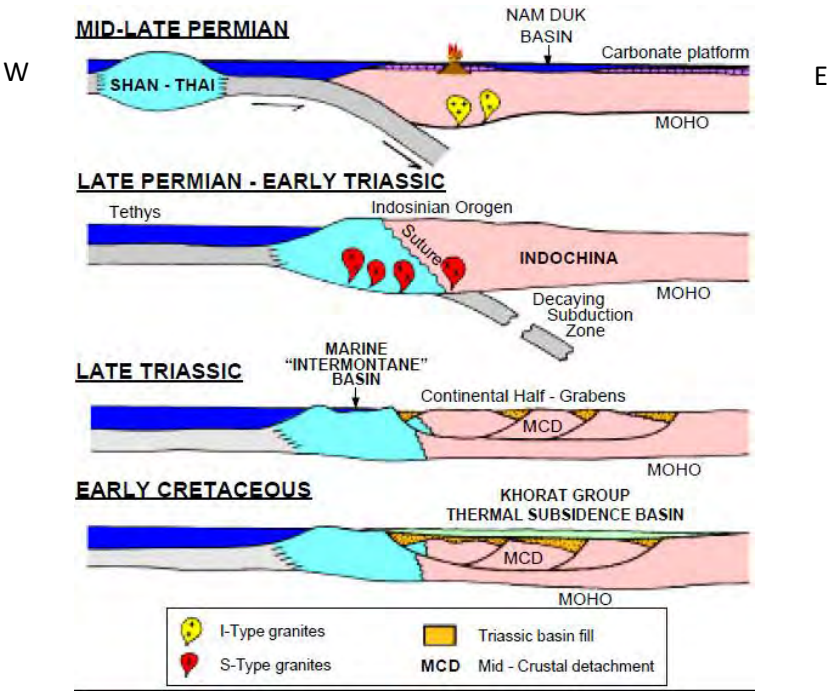

Figure 2.3 Permian and Mesozoic plate tectonic model for NE Thailand (Cooper *et al.*, 1989).

2.2 Stratigraphy and petroleum system of Khorat Plateau

2.2.1 The stratigraphic succession of the Khorat Plateau (Figure 2.4) composes of 3 intervals divided by 2 major unconformities; Indosinian I and Indosinian III unconformities (Racey and Goodall, 2009). Granites and metamorphic rocks are basement rocks underlying Permian sequence.

- Upper Carboniferous to Upper Permian Saraburi Group (extensive marine carbonate and siliciclastics underlying Indosinian I unconformity).
- Upper Triassic Kuchinarai Group and Huai Hin Lat Formation (fluvial - alluvial red beds and lacustrine sediments below Indosinian II unconformity).

  Lower Nam Phong Formation (Uppermost Triassic fluvial - alluvial sediments).
- Khorat Group (Upper Jurassic - Lower Cretaceous continental red beds above Indosinian III unconformity): Upper Nam Phong, Phu Kradung, Phra Wihan, Sao Khua, Phu Phan, Khok Kruat Formation.

  Maha Sarakham Formation (Upper Cretaceous non-marine evaporites and fluvial clastics).

  Phu Tok Formation (Uppermost Cretaceous low energy fluvial clastics and thick bedded aeolian sandstone).

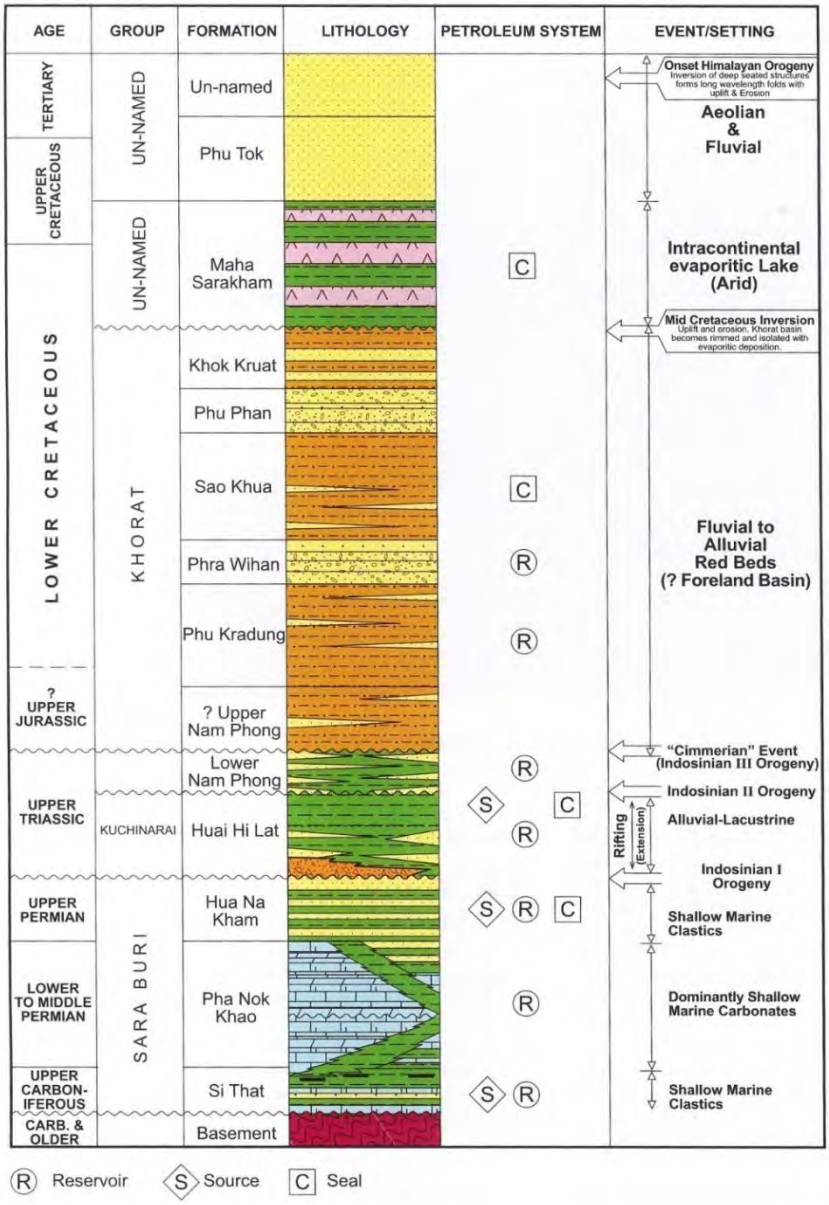

Figure 2.4 Stratigraphy and petroleum system of Northeastern Thailand (Racey, 2011).

2.2.2 Petroleum system of the Khorat Plateau

➢ Source rocks

There are three potential source rocks (Racey, 2011). These potential source rocks had high maturity indicating high geothermal gradient in the past, which might cause oil cracking into gas.

1. Upper Carboniferous to Upper Permian Saraburi Group: main source rock according to Advanced Resources International, Inc. (2013).

Potential source socks in this group are lacustrine - shallow marine shales and micrite limestones deposited after Indochina - South China

collision. Si That Formation, lower part of Saraburi Group has 0.3 to 1.6 wt% TOC values. Grey shales from Hua Na Kham Formation, upper part of Saraburi Group has 0.2 to 1.0 wt% TOC. Both have kerogen type II and III (oil- and gas-prone source rock). Shale in Nam Duk Formation which deposited in structural low (basin) and is equivalent to Pha Nok Khao Formation also has gas generating potential. Permian source rocks are over-mature based on 2 to > 3% R_o (Kozar *et al.*, 1992). While Permian carbonate platform of Saraburi Group (reservoir) deposited in high relief areas such as uplifted horst blocks (Racey, 2011).

2. Upper Triassic Huai Hin Formation and Kuchinarai Group:

Shan Thai - Indochina collision during Upper Permian to Upper Triassic caused the compressional tectonics and inversion. The depositional environment vary from alluvial fan to fluvio-lacustrine environment filling the extensional half-graben and causing the deposition of lacustrine shales of Huai Hin Lat Formation and Kuchinarai Group in structural low areas. These source rocks are oil-prone source rocks consisting mainly of type I kerogen. This study will focus on Huai Hin Lat Formation.

Huai Hin Lat Formation is a Late Triassic (Carnian-Norian) Pre-Khorat Group depositing in a half-graben. It consists of conglomerates and volcanic rocks underlying thick lacustrine shales with some coal seams and fluvial sandstones. Huai Hin Lat source rock is oil-prone source rock consisting of kerogen type I and type II with 0.2-5.0 wt% TOC and 0.8 to 3.0 % R_o. Oil generation from this source rock began in early Jurassic and cracked into gas in late Cretaceous (Sattayarak *et al*., 1989). There are 5 Members in Huai Hin Lat Formation (Chonglakmani and Sattayarak, 1978) and the relationship of each units is shown in Figure 2.5.

- Pho Hai Member: the lowest member, volcanic sedimentary rocks (tuff, agglomerate) and volcanic igneous rock (rhyolite and andesite) interbedded with sandstone and conglomerate.
- Sam Khaen Member: mostly grey basal conglomerate (limestone conglomerate) interbedded with some limestone lens.

- Dat Fa Member (potential source rock): dark grey - black calcareous shale rich in carbon content, well bedded or interbedded with argillaceous limestone.
- Phu Hi Member: grey sandstone, shale and argillaceous limestone (lower part usually has conglomerate).
- I Mo Member: diorite, tuff, agglomerate interbedded with shale, sandstone and grey limestone.

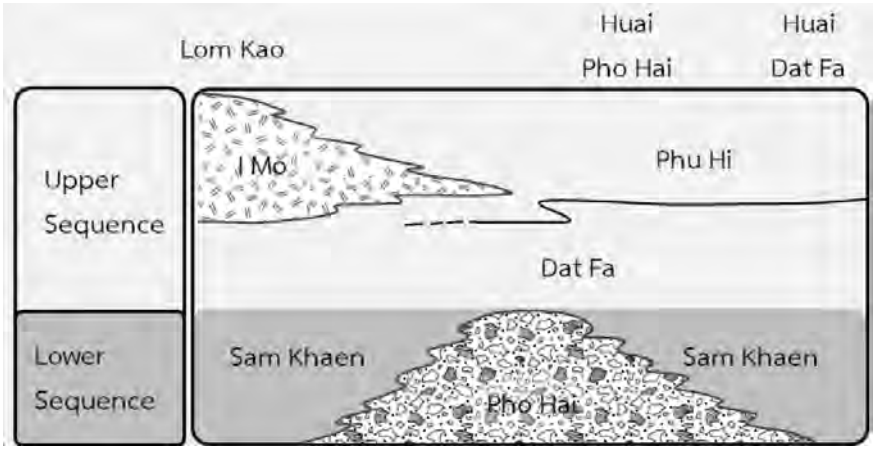

Figure 2.5 Stratigraphic relationship of each rock units in Huai Hin Lat Formation (อนุวัชร ตรีโรจนานนท์, 2555).

3. Lower Nam Phong Formation: minimal gas potential.

➢ Migration

For Permian source rocks, lateral hydrocarbon migration usually occurred from basin into the Permian carbonate-platform rocks. For Late Triassic lacustrine source rocks, vertical migration of hydrocarbon might occur along extensional faults created during Triassic extension into Permian carbonate on the hanging wall blocks.

➢ Reservoir rocks

The primary reservoir target is the Late Carboniferous to Late Permian fractured, dolomitized and hydrothermally altered carbonates (Pha Nok Khao and Hua Na Kham Formations). The secondary target is fluvial sandstones of Late Triassic Kuchinarai Group and Huai Hin Lat Formation. Fractures in these reservoirs mainly associated with Indosinian faults, which were reactivated during Himalayan orogeny and enhanced reservoir quality

(porosity and permeability) from 2% to more than 15% porosity (Chinoroje and Cole, 1995; Booth and Sattayarak, 2011). Moreover, Lower Nam Phong, Phu Kra Dung and Phra Wihan Formations also found some gas shows and dead oil, which might remigrate along reactivated faults during Himalayan orogeny (Racey, 2011).

- Seals and traps

Mudstone, shale and claystone in Permian Group, Late Triassic Group, Nam Phong Formation and Phu Kradung Formation are regional seals overlying carbonate and sandstone reservoirs. Hydrocarbons are also trapped by angular unconformity (between the Permian Saraburi Group and Late Triassic Huai Hin Lat Formation) and structural closures (half-grabens and anticline) at the base Khorat Group (ATOP Technology Co. Ltd., 2006; Booth and Sattayarak, 2011).

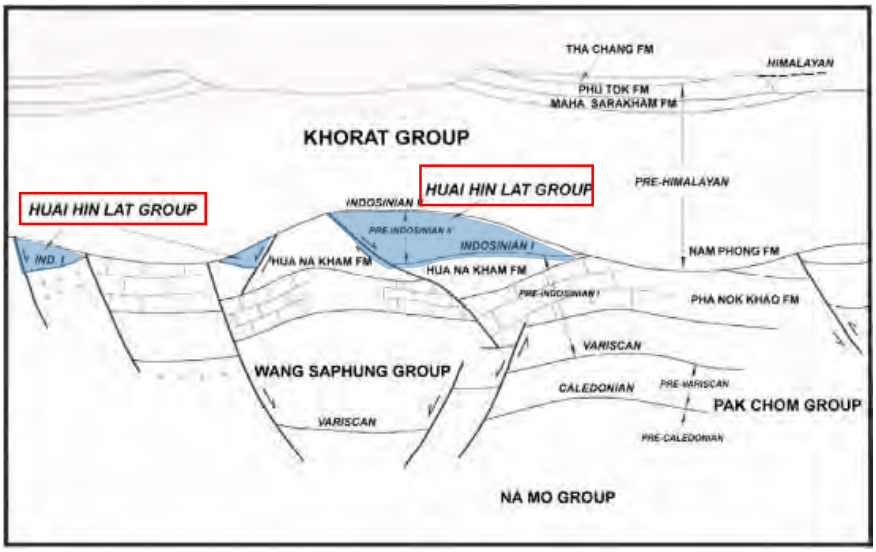

Figure 2.6 Lithostratigraphic units of rock sequences of the Khorat Plateau and their structural setting (after DMR, 1999).

2.3 Studies of source rock potential of Huai Hin Lat Formation

Khositchaisri (2012) collected outcrop samples from Huai Hin Lat Formation in Amphoe Nam Nao, Changwat Phetchabun and Amphoe Chumpae, Changwat Khon Kaen to study geochemical properties of potential source rock. Huai Hin Lat Formation has TOC values of 0.79 - 13.80 wt% with 0.898 - 1.935 $\%R_o$ indicating fair to excellent source rock potential in late to post mature stage. It also has > 200 ppm of extractable organic matter

(EOM), which means adequate amount of petroleum can be generated from this Formation. Moreover, Huai Hin Lat Formation mainly composes of type III kerogen, which were from mixed organic sources between terrigenous and marine organic matters deposited in lacustrine environment in reducing condition from visual kerogen analyses, Pr/Ph, Pr/nC_{17}, Ph/nC_{18} and ternary diagram of C_{27} - C_{29} regular steranes data. From Rock-Eval pyrolysis data, the samples have little potential to generate gas because of low hydrogen index values (1.52 - 81.08 mg HC/ g TOC), which fall in kerogen type III/IV range and contradict to visual kerogen analysis results.

Lithostratigraphy of Huai Hin Lat Formation at Amphoe Nam Nao, Changwat Phetchabun was studied by Prachaiboon (2014). Huai Hin Lat Formation can be classified into 4 units from ascending order as follows;

- Unit A: black calcareous shale with high organic matter, well bedded and likely to be deposited in deep lacustrine environment.
- Unit B: grey calcareous shale, mudstone, siltstone, argillaceous limestone and coal seam which were deposited in the lacustrine margin and swamp environment.
- Unit C: grey calcareous shale, mudstone, siltstone and sandstone which was deposited in the transitional zone from lacustrine to fluvial system.
- Unit D: purplish red sandstone and conglomerate which is not classified into Huai Hin Lat Formation.

Prachaiboon (2014) correlated these rock units with อนุวัชร ตรีโรจนานนท์ (2555) report, Unit A was classified into Dat Fa Member, Unit B and Unit C were classified into Sam Khaen Member and Nam Phong Formation, respectively. St. 5 Tat Yai waterfall and St. 6 Ban Pa Ruak 2 (Unit A), which are believed to be Dat Fa Member consist of a thick section of well bedded black calcareous shale. From thin sections study of Prachaiboon (2014), it comprises about 90% of clay-silt grain of clay minerals with silt size grain of calcite (10%) as shown in Figure 2.7.

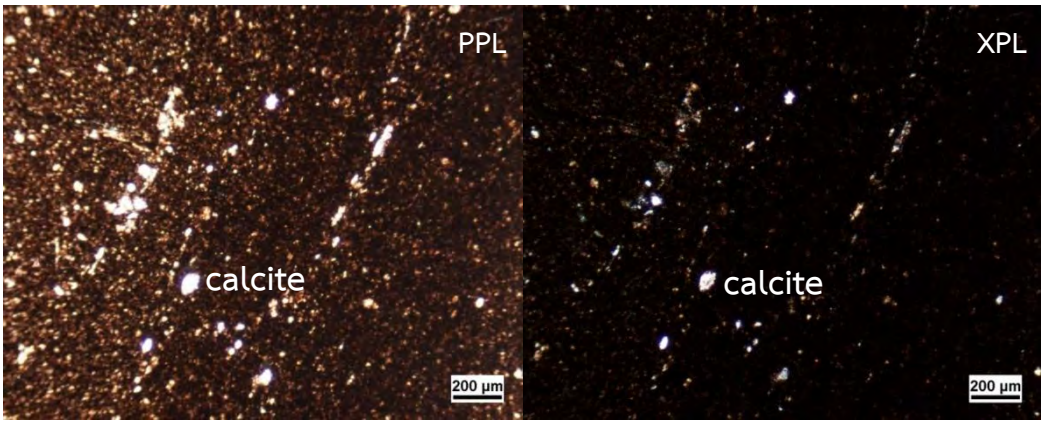

Figure 2.7 Thin section of black calcareous shale from St. 5 Tat Yai waterfall (Prachaiboon, 2014).

Arsairai (2014) studied the depositional environment and petroleum source rock potential of Huai Hin Lat Formation in Sap Phlu Basin (Ban Nong Sai section) and Na Pho Song Basin (Tat Yai section). In Tat Yai section, the average contents of brittle and clay minerals are 50.7% and 23.6%, respectively. High values of palaeoredox condition of Tat Yai section indicates a highly reducing condition. Shales in this section show 4.7 - 10.1 wt% TOC values representing excellent source rock potential and compose mainly type I kerogen (Sapropelic group) from point counting of organic materials under microscope. However, Modified Van-Krevelen diagram (Figure 2.8) shows that samples from Tat Yai section consist of type IV kerogen in post-mature stage. Vitrinite reflectance and T_{max} values are 1.71 $\%R_o$ and 602.8 °C. High maturation level is conformable to the transformation ratios of 99.8 - 99.9%. The total generated hydrocarbon was 16,914.4 mcf/ac-ft. Therefore, this section of the Huai Hin Lat Formation has high gas generating potential for gas accumulation in the Khorat Basin.

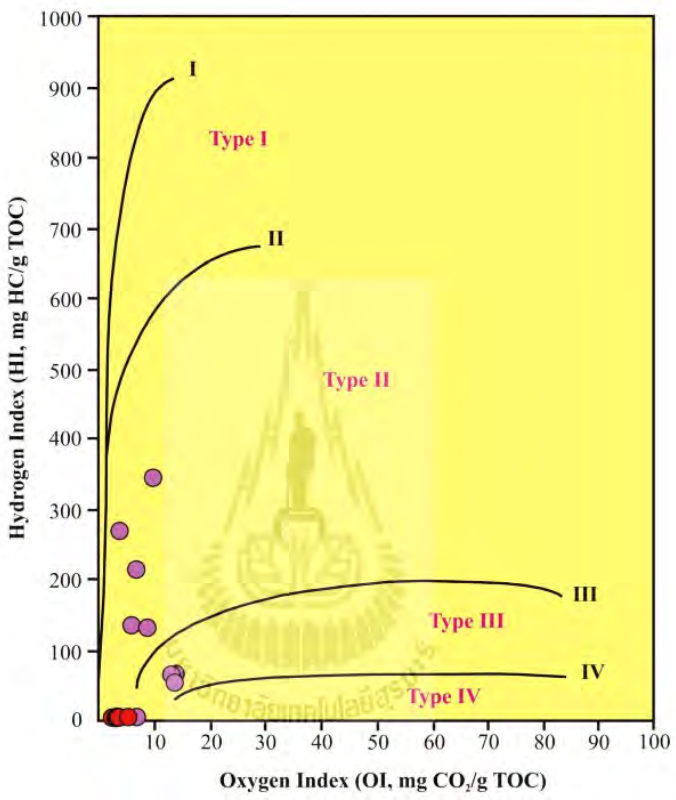

Figure 2.8 Modified Van-Krevelen diagram of the Ban Nong Sai samples (purple solid circles) and the Tat Yai samples (orange solid circles). All samples have low HI and OI values (Arsairai, 2014).

Chamchoy (2014) investigated twenty two cutting samples of Huai Hin Lat Formation from ten exploration wells in the Khorat Plateau to study petroleum geochemistry. Vitrinite reflectance and thermal alteration scale (TAS) indicate that the samples are in late - post mature stage and initially contained kerogen type II, II/III and III but converted to kerogen type IV during thermal maturity process based on hydrogen and oxygen indices (Figure 2.9). TOC contents indicate that samples have poor to excellent source rocks potential. Nonbiomarker, biomarker parameters and bimodal distribution of n-alkane chromatogram suggest that the samples contain organic sources between terrestrial and marine organic matters deposited in reducing conditions but there was greater input of terrestrial organic matter of higher plant than marine organic matter. Chamchoy (2014) concluded that Huai Hin Lat Formation might have been deposited in estuarine and/or marine environment, as supported by a presence of gammacerane in all samples and ternary diagram of C_{27}-C_{28}-C_{29} regular steranes.

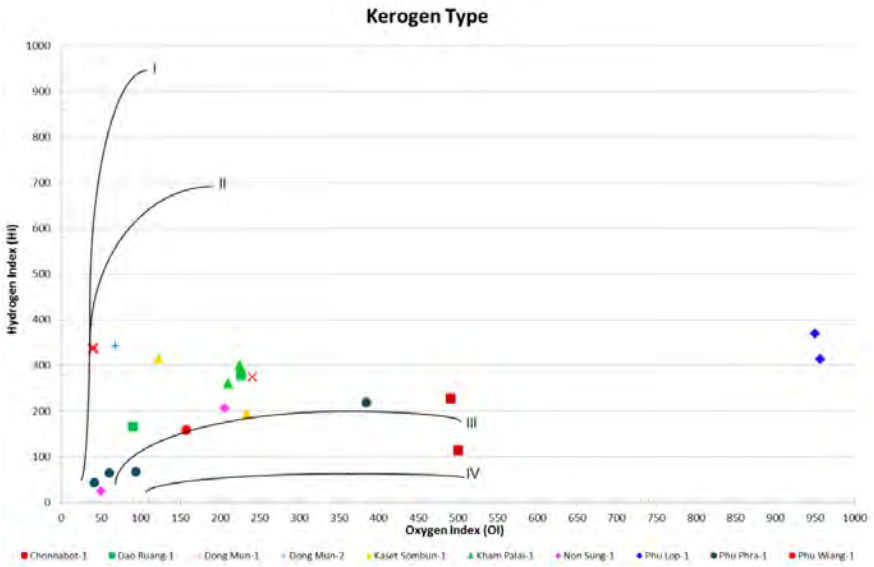

Figure 2.9 Modified Van-Krevelen diagram of the cutting samples of Huai Hin Lat Formation (Chamchoy, 2014).

2.4 Studies of mineral matrix on Rock-Eval pyrolysis

Rock-Eval pyrolysis is a very popular method for source rock evaluation. All pyrolysis parameters (hydrogen index, oxygen index, production index, and T_{max}) vary in kerogen: mineral ratio, type of minerals, and kerogen type (Spiro, 1991).

Espitalie *et al.* (1980) did the comparable pyrolysis experiments on rocks containing organic matter and on kerogen extracted from these rocks (Figure 2.10). Pyrolysable hydrocarbon yield may be affected by the mineral matrix and quantity of organic matter. Mineral matrix can reduce S_1 and S_2 values and increase T_{max}. Therefore, it lowers hydrogen index values and source rock quality. In rock with low organic content or highly active matrix, mineral matrix effect can cause the hydrocarbon retention of heavy hydrocarbon more than lighter hydrocarbons (< C_{15}).

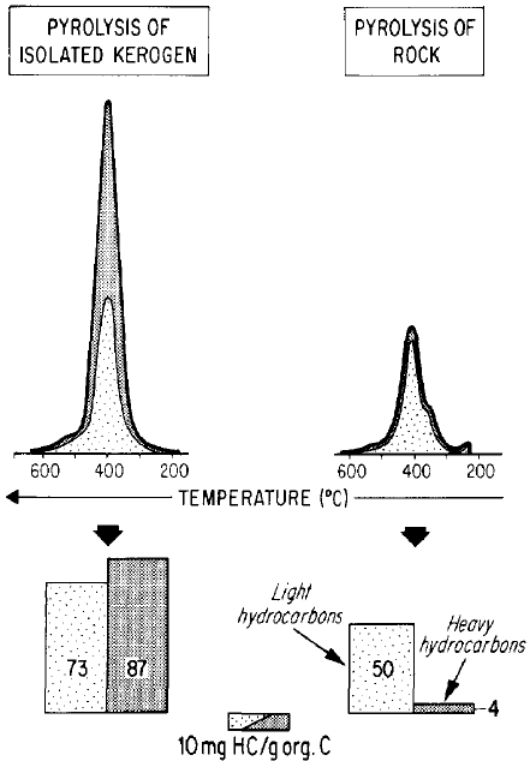

Figure 2.10 Comparison of hydrocarbon yields from immature kerogen and related rock pyrolysis of Upper Cretaceous shales from Douala basin. Heavy hydrocarbons and bitumen are much reduced in rock pyrolysis (Espitalie *et al.*, 1980).

Retention of heavy hydrocarbons occurs on the mineral surfaces. As shown in Figure 2.11, thermal cracking of kerogen generates light and heavy hydrocarbons but only light hydrocarbons can be released. The heavy hydrocarbons and heavier bitumen are trapped on active site of minerals. When temperature and time increase, the trapped hydrocarbons are cracked to light hydrocarbons and hydrogen, which can be released from the samples while carbon residue remains on the active mineral sites. Differences in hydrocarbon yields depend on differences in surface activity (retentive capacity) of minerals. Some argillaceous minerals e.g. illite are more active than other minerals such as carbonates. Clay minerals are the main active minerals for hydrocarbon adsorption (Katz, 1983; Espitalie *et al.*, 1984).

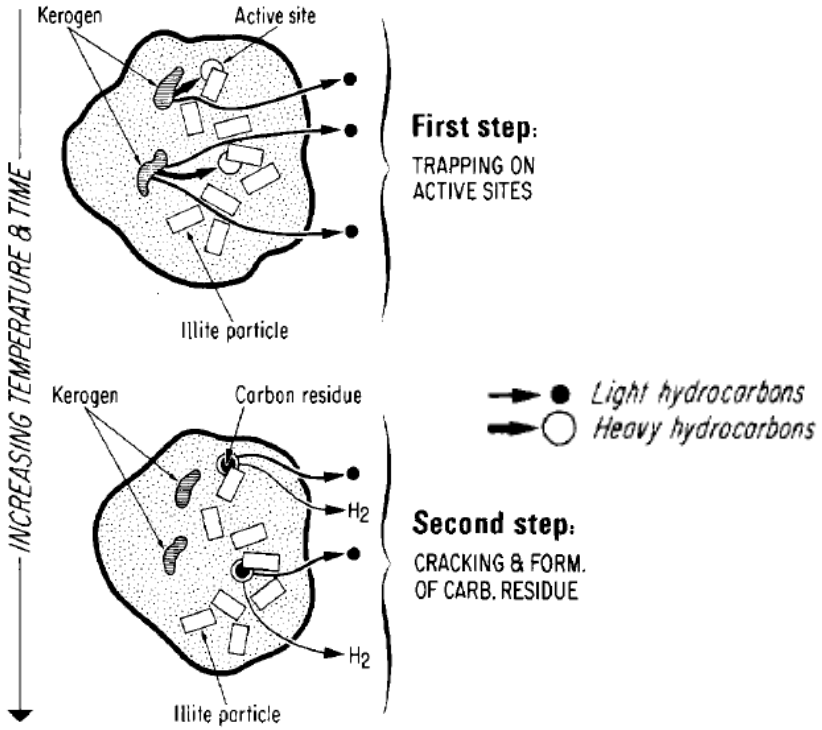

Figure 2.11 Proposed model of hydrocarbon retention (Espitalie *et al.*, 1980).

S_2 vs. TOC diagram is an effective method to determine mineral matrix effect (Katz, 1983). It is usually used to measure the true average hydrogen index from slope of the regression line to avoid the problems in S_3. S_2 vs. TOC diagram is also used to calculate amount of hydrocarbon adsorption by rock matrix from x- and y-intercepts (Figure 2.12). If there are no mineral matrix effects, the regression line should pass through the origin because even very small amounts of organic matter produce hydrocarbons during pyrolysis (Langford and Valleron, 1990).

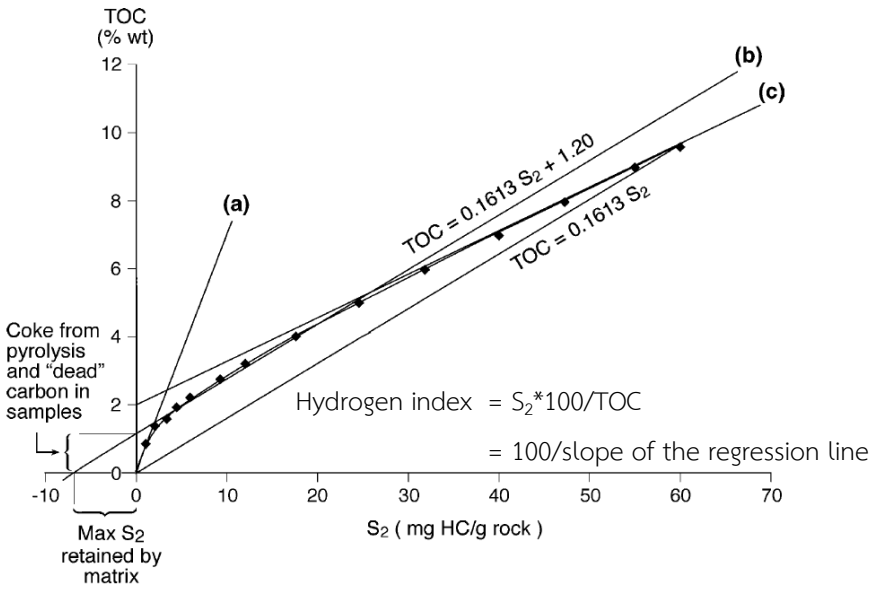

Figure 2.12 S_2 – TOC plot showing the mineral matrix effect occurring during pyrolysis as a result of hydrocarbon retention (Espitalie *et al.*, 1980; Dahl *et al.*, 2004).

Effects of carbonate minerals on oxygen index were observed by Katz (1983). The elevated oxygen indices are usually associated with carbonate rocks containing amount of calcite, dolomite and siderite. The carbonate effects may be caused by normally occurring crystallographic imperfections (atomic substitutions, inclusions and lattice defects), which lower the decomposition temperature of carbonate minerals or lower interactions between matrix and organic matter. During pyrolysis, the decomposition of major carbonate minerals may begin below 390 °C releasing CO_2 and contaminating with CO_2 released from breaking carboxyl group from kerogen. This inorganic CO_2 results in the increased S_3 and scatter in oxygen index which are not observed in decarbonated samples (Figure 2.13).

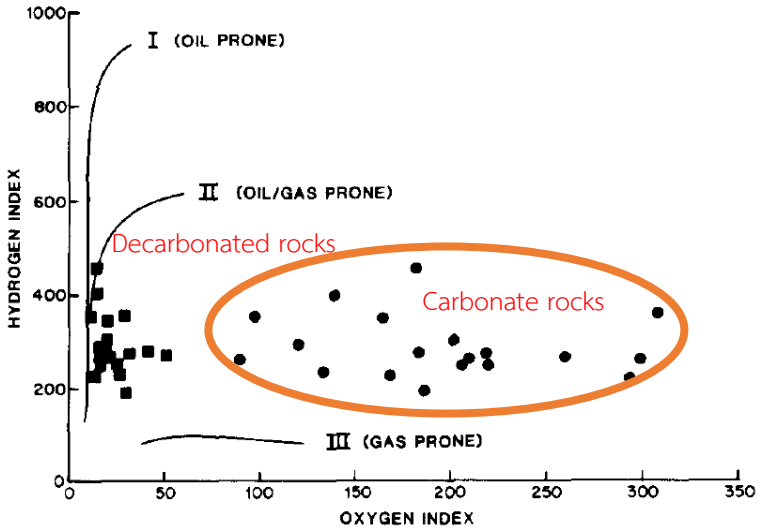

Figure 2.13 Modified Van-Krevelan diagram presenting the results of Rock-Eval pyrolysis ■ for a carbonate-free pyrolysis ● for a suite of carbonate rocks (Katz, 1983).

CHAPTER 3

METHODOLOGY

This flowchart in Figure 3.1 briefly describes the methods used in this research.

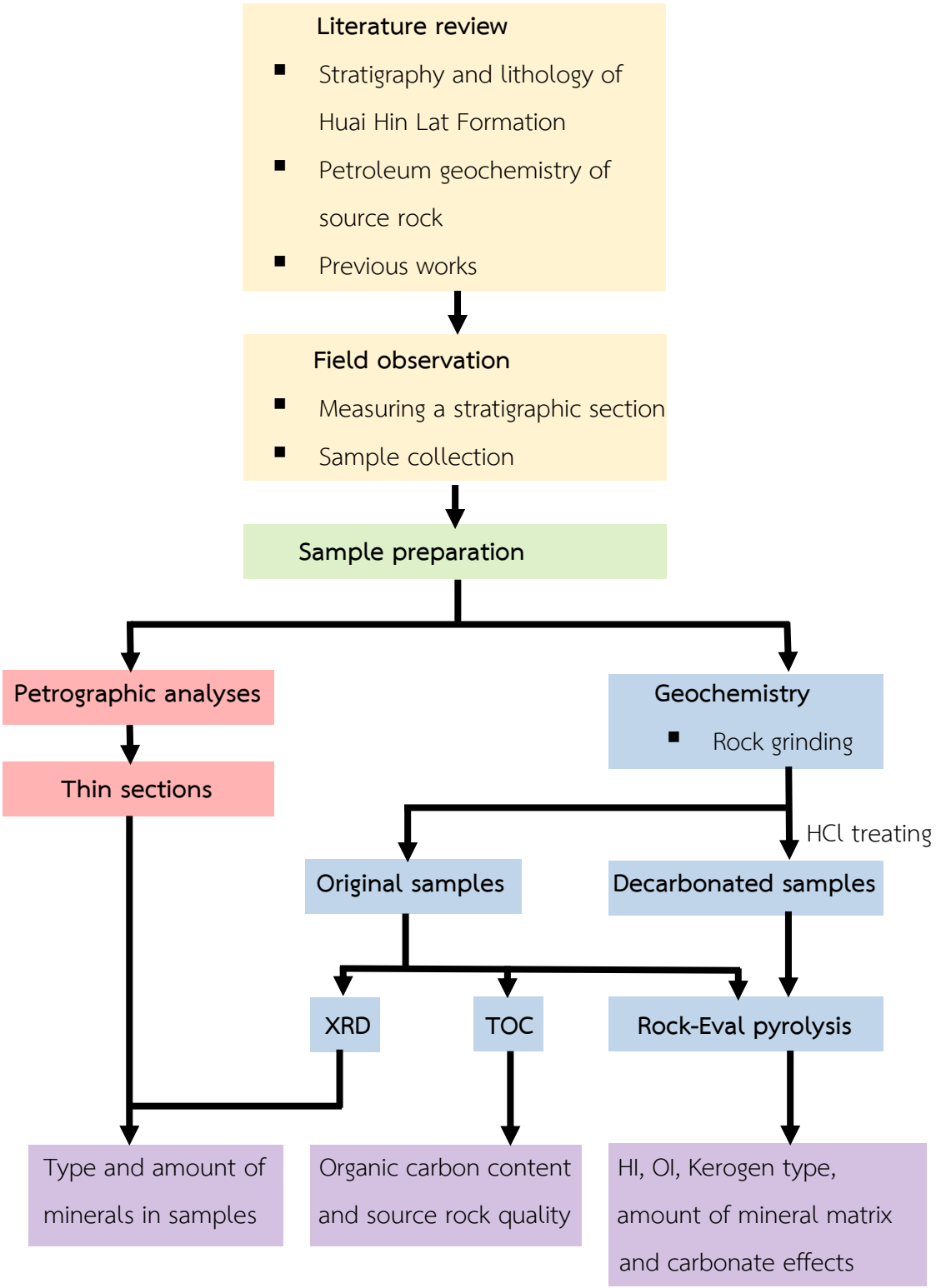

Figure 3.1 Flow chart showing method of study.

3.1 Literature review and field observation

Field survey was done in Na Pho Song basin, which is a Triassic half-graben basin exposed in Phetchabun, Khon Kaen and Chaiyaphum provinces close to Phetchabun Fold Belt. The basin composes of syn-rift sequence of Huai Hin Lat Formation, which deposited in a variety of environments from alluvial fan to fluvio-lacustrine environment in slightly humid to semi-arid condition (กรมทรัพยากรธรณี, 2550).

The study area is Tat Yai waterfall (47Q 796734N 1850785E), which is a part of Na Pho Song Basin located in Phu Pha Man National Park Amphoe Phu Pha Man, Changwat Khon Kaen and Amphoe Nam Nao, Changwat Phetchabun. The location is shown as a star in Figures 3.2, 3.3. The waterfall is about 100 - 150 meters high consisting of Dat Fa Member of sub-horizontal laminated black calcareous mudstone interbedded with thinly argillaceous limestone. Pyrite lens can be observed in these rocks. The outcrop picture is shown in Figure 3.4.

Stratigraphic section, bedding attitude and lithology of rocks in study area were studied and 25 samples were collected at about every 1 meter bedding intervals. Due to the hardness of the rocks, the Jackhammer BOSCH GBH11E and the 1700W generator were used to cut the fresh rocks as shown in Figure 3.5.

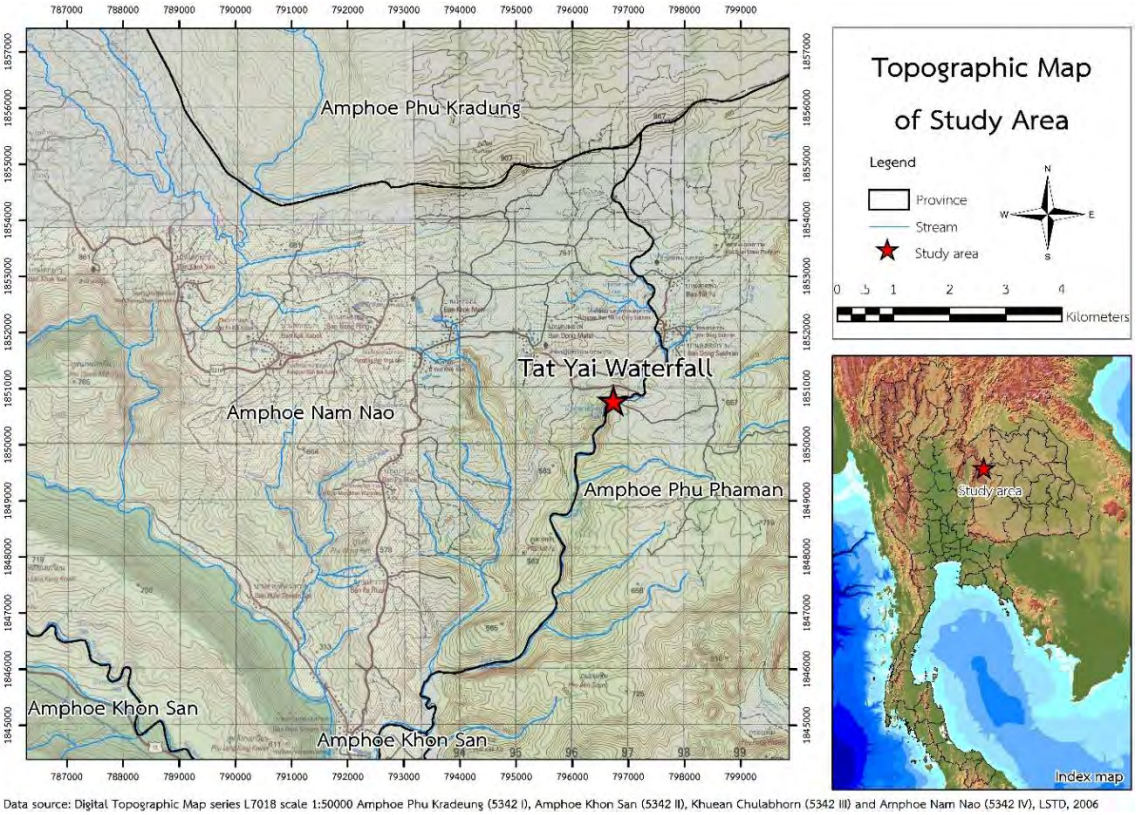

Figure 3.2 Topographic map of study area.

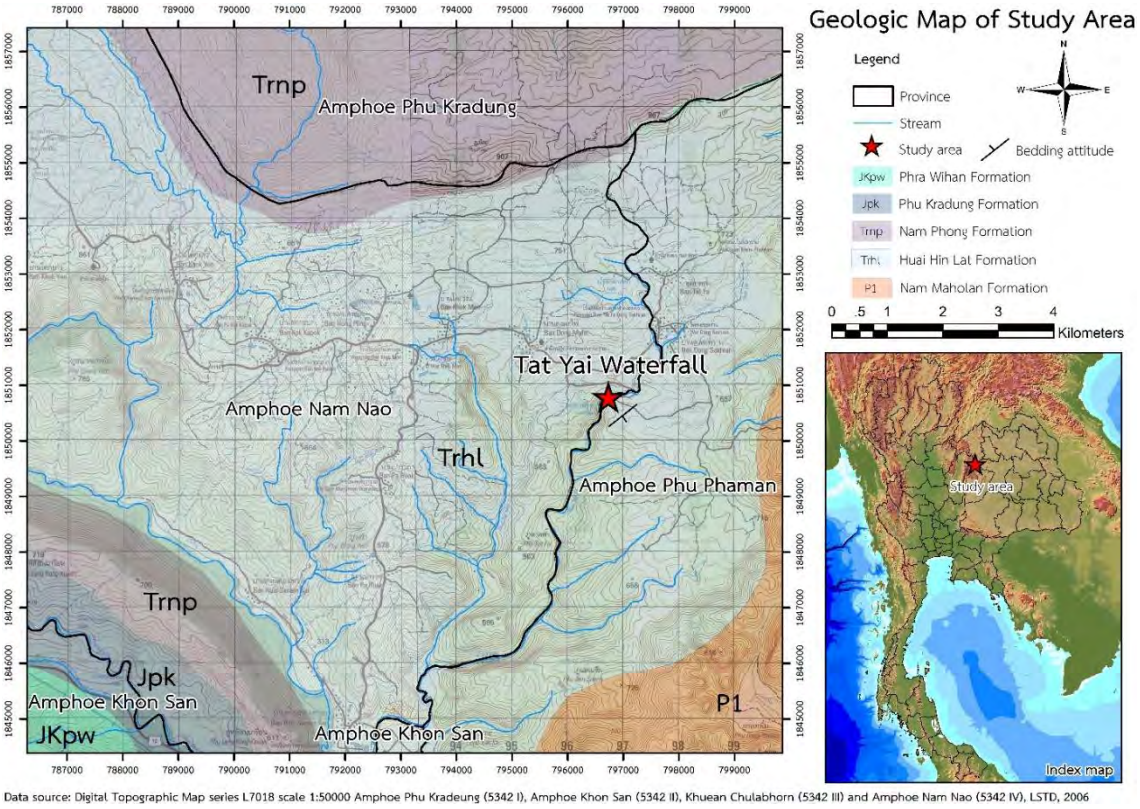

Figure 3.3 Digital geologic map of study area (Modified from DMR, 2007).

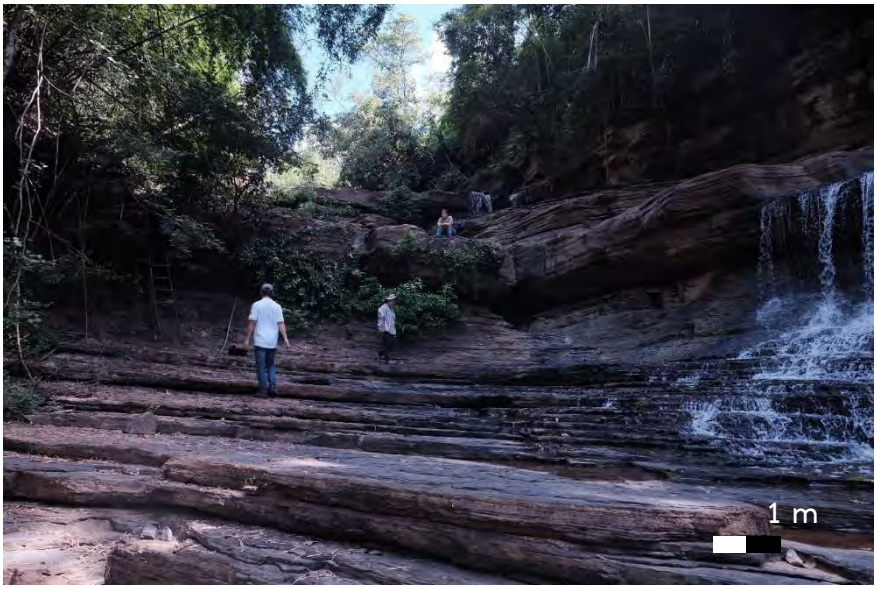

Figure 3.4 Natural outcrop at Tat Yai waterfall with sub-horizontal bedding attitude of black calcareous mudstone interbedded with thinly argillaceous limestone (looking northeast).

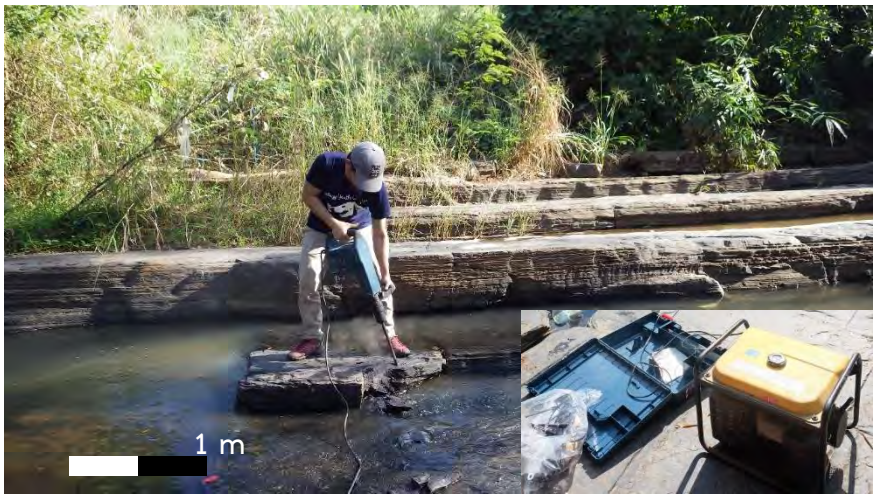

Figure 3.5 Collecting process by using Jackhammer BOSCH GBH11E and the 1700W generator (looking east).

3.2 Sample preparation

Fresh samples (Figure 3.6) were crushed into small pieces by stonecutter and jaw crusher. For geochemical analyses, about 20 grams of each sample was ground into fine powder by using an agate mortar. For XRD analysis, tin/tungsten disc mill was used to ground about 5 grams of each samples into very fine powder (less than 0.044 millimeters). For TOC analysis and Rock-Eval pyrolysis, an agate mortar is used to grind the samples into fine powder to avoid contamination of carbon from tungsten carbide ball mill (Figure 3.7).

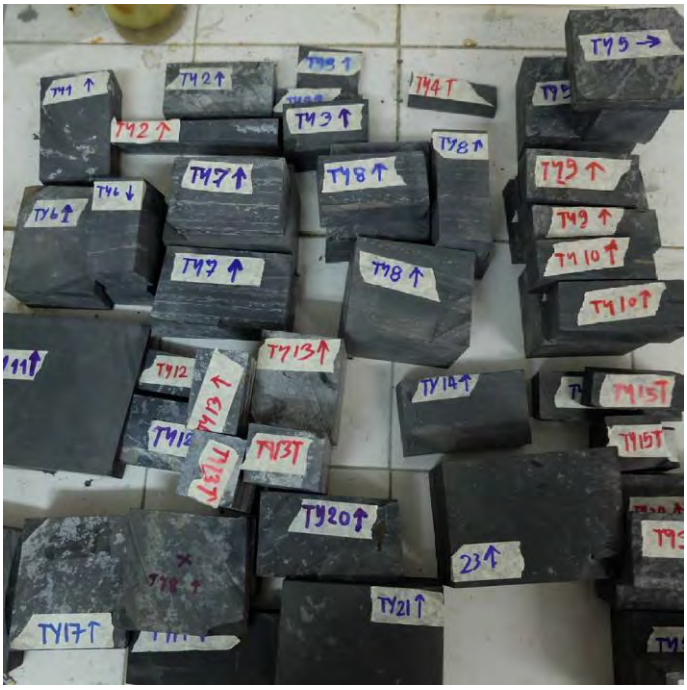

Figure 3.6 Fresh samples cut by a stonecutter.

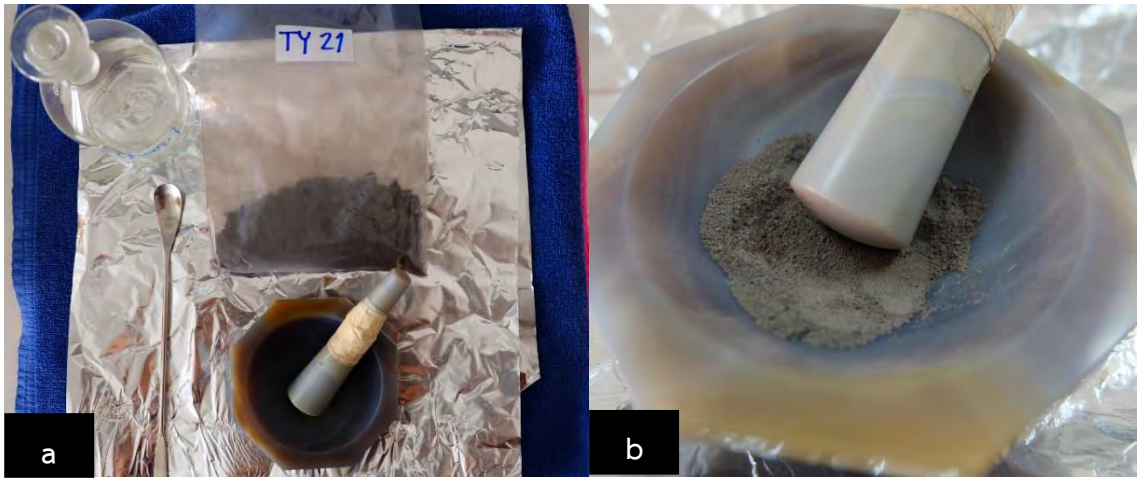

Figure 3.7 (a) Preparation for rock grinding by using agate mortar.
(b) Fine powder sample from rock grinding.

3.3 Petrographic and XRD analyses

Thin section of 4 rocks with different lithologic textures observed from hand specimens (TY 5, 13, 18 and 25) were studied for type and amount of minerals under polarizing petrographic microscope. The samples were cut and ground flat. Then, they were attached on a glass slide with balsum and smoothly ground using progressively finer abrasive grit until the translucent samples are only 30 μm thick (Figure 3.8). Micrographs were taken of the selected samples with a Fuji X-A2 mirrorless camera.

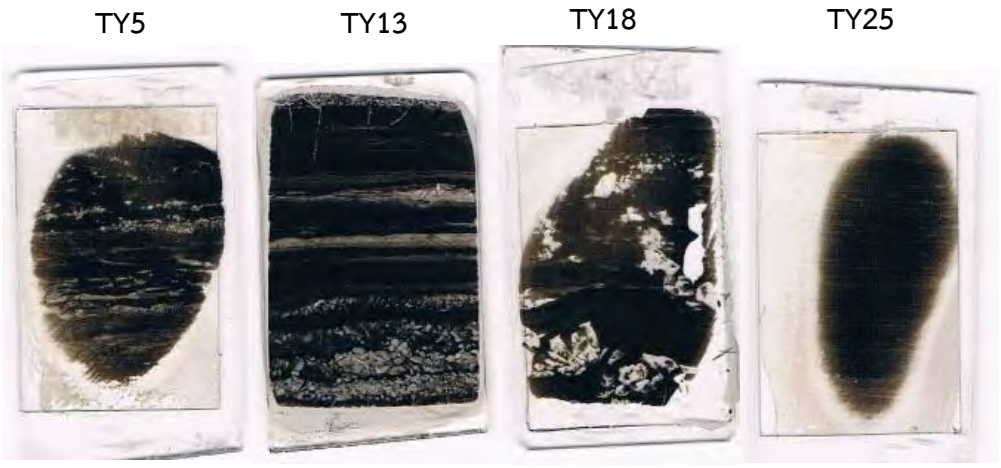

Figure 3.8 Pictures of thin section slides of 4 different lithologic textures.

For powder XRD analyses, about 1 gram of powdered samples ground by tin/tungsten disc mill were pressed into plastic sample holders with the smooth surfaces by using a glass slide as shown in Figure 3.9. Using the Bruker D8 Advance with CuKa radiation at the Department of Geology, Chulalongkorn University (Figure 3.10), samples were investigated to identify different minerals present in rocks. The samples were run from 5° to 55° 2-theta, increment 0.01° and step time 1 sec. Wavelength to compute d-spacing is 1.54 A°. Data interpretation was done by using EVA, XCH and MAUD programs.

Oriented XRD analyses were also conducted to identify clay minerals. Bulk sample (about 5 grams) was treated with 15% hydrogen peroxide and 10% hydrochloric acid to remove organic matter and carbonate minerals. Centrifugation is very important for these processes. Then, 2 grams of Sodium Hexametaphosphate (Calgon) was added to disperse the sample in 45 ml. distilled water. Clay suspension was extracted on a glass slide. When dry, the samples were run in XRD from 5° to 30° 2-theta, increment 0.01° and step time 1 sec. However, the results were not satisfactory as samples contain low content of clay minerals and are not detected by XRD.

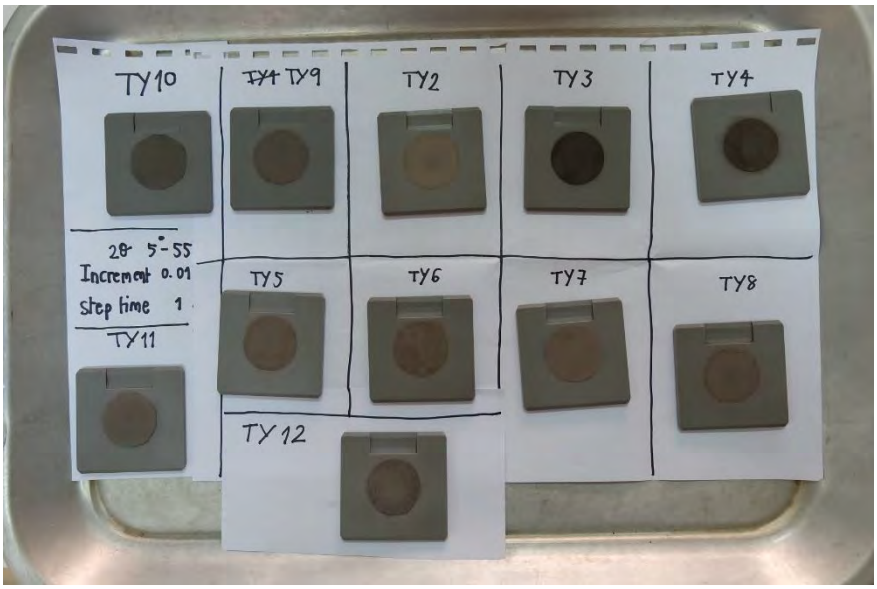

Figure 3.9 Pictures of samples for powder XRD analyses.

Figure 3.10 Bruker D8 Advance X-Ray Diffractometer.

3.4 Petroleum geochemistry

For TOC analyses, powdered samples of the original samples were treated with hot and cold hydrochloric acid to remove carbonates, which are inorganic carbons. Then, the organic carbon content is determined by combustion of the samples in LECO WC 230 Carbon Analyzer (Figure 3.11) in Core laboratories Malaysia.

Figure 3.11 LECO WC 230 Carbon Analyzer (http://leco-korea.com).

For Rock-Eval pyrolysis, 50 - 70 mg of powdered samples (both original and decarbonated samples) were analyzed by the Rock-Eval-6 Instruments (Figure 3.12) in Core Laboratories Malaysia and PTT Research & Technology Institute which provide a rapid (37 min/sample) source rock analysis by heating over a temperature range of 300 - 650 °C, after an initial gas purge at 90 °C. This analysis records the concentration of volatile and soluble

organic matter, the amount of pyrolysable organic matter and thermal maturity. The results were interpreted by plotting in Modified Van-Krevelen diagram and S_2 - TOC diagram to classify kerogen type, maturation stage and mineral matrix effects.

Figure 3.12 Rock-Eval-6 Instrument (http://in.bgu.ac.il).

CHAPTER 4

RESULTS

From the field observation, Tat Yai waterfall composes of laminated black calcareous mudstone interbedded with argillaceous limestone. Twenty-five samples were collected from the outcrop at intervals of about 1 meter. Overall thickness of the studied section is about 31 meters. Lithologic description and petrographic analyses of thin sections were studied on TY 5, 13, 18 and 25, which represent 4 main lithologic textures of the rocks. X-Ray diffraction analyses of 25 samples were used to identify composition and quantity of minerals in the samples especially carbonate and clay minerals. All 25 samples were examined for their TOC content and then were analyzed by Rock-Eval 6 pyrolyzer.

4.1 Mineral composition

4.1.1 Lithologic description

Stratigraphic section of Tat Yai waterfall is shown in Figure 4.1. There are 4 main lithologic textures of the rocks as shown in Figure 4.2. Almost all samples have pyrite lens in carbonate layers or in the laminated mudstones.

- Group 1: laminated calcareous mudstone interbedded with very thin (about 1 mm) carbonate layers (TY 5, 6, 7, 8, 14, 20 and 21)
- Group 2: laminated calcareous mudstone interbedded with thick (about 1 cm) carbonate layers: TY 2, 13, 17, 22 and 23
- Group 3: laminated calcareous mudstone with carbonate lens (TY 1, 9, 10, 12, 18 and 24)
- Group 4: laminated calcareous mudstone (TY 3, 4, 11, 15, 16, 19 and 25)

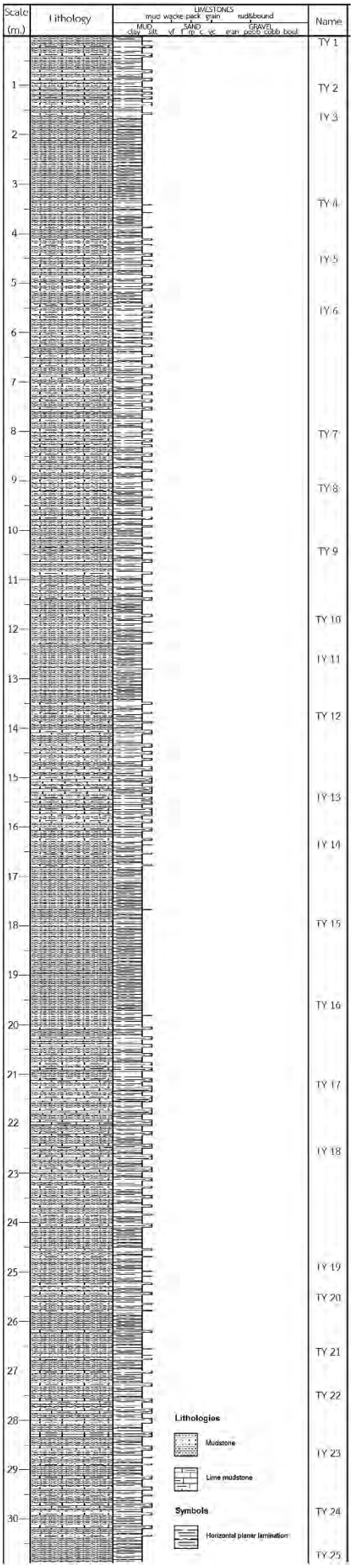

Figure 4.1 Stratigraphic section of Tat Yai waterfall.

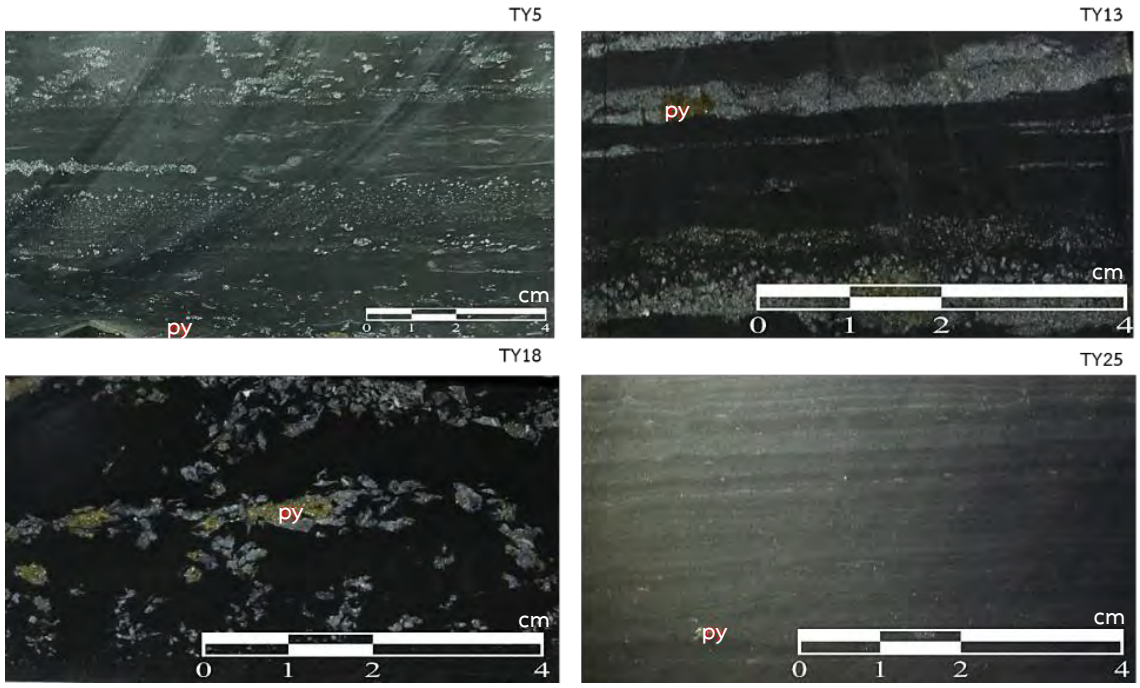

Figure 4.2 Four main lithologic textures of the rocks (py=pyrite).

Petrographic analyses of the 4 thin sections from 4 samples representing each lithologic textures were carried out and described in Table 4.1 and in Figures 4.4 - 4.7. Comparison of mineral composition from 4 thin sections is shown in Figure 4.3.

Table 4.1 Petrographic description of thin sections.

Sample name	Description
TY 5 (Figure 4.4)	The sample is a calcareous mudstone with very thin carbonate layers. It composes of unidentified clay-sized minerals approximately 45%, subhedral carbonate crystals (0.04 - 0.1mm) approximately 35%, subangular quartz grains (0.01 - 0.12 mm) approximately 15%, and opaque minerals (0.02 - 0.6 mm) approximately 3%. Quartz grains and opaque minerals are both found in carbonate layers and in rock matrix.
TY 13 (Figure 4.5)	The sample is a calcareous mudstone with thick carbonate layers. It composes of unidentified clay-sized minerals approximately 32%, subhedral carbonate crystals (0.1 - 1.3 mm) approximately 55%, subangular quartz grains (0.02 - 0.10 mm) approximately 10%, and opaque minerals (0.04 - 0.14 mm) approximately 3%. Stylolite is observed in the thin section. Some subangular-subrounded carbonate grains, quartz grains and opaque minerals are found in carbonate layers and in rock matrix.

Sample name	Description
TY 18 (Figure 4.6)	The sample is a calcareous mudstone with carbonate lens. It composes of unidentified clay-sized minerals approximately 46%, anhedral carbonate minerals (0.06 - 4 mm) approximately 30%, subangular quartz grains (0.02 - 0.18 mm) approximately 20%, and opaque minerals (0.04 - 0.6 mm) approximately 3%. Some subangular-subrounded carbonate grains, quartz grains and opaque minerals are found in carbonate layers and in rock matrix.
TY 25 (Figure 4.7)	The sample is a calcareous mudstone. Lamination is very clear in thin section. It composes of unidentified clay-sized minerals approximately 73%, carbonate minerals (0.04 - 0.10 mm) approximately 10%, subangular quartz grains (0.04 - 0.12 mm) approximately 15%, and opaque minerals (0.02 - 0.04 mm) approximately 2%.

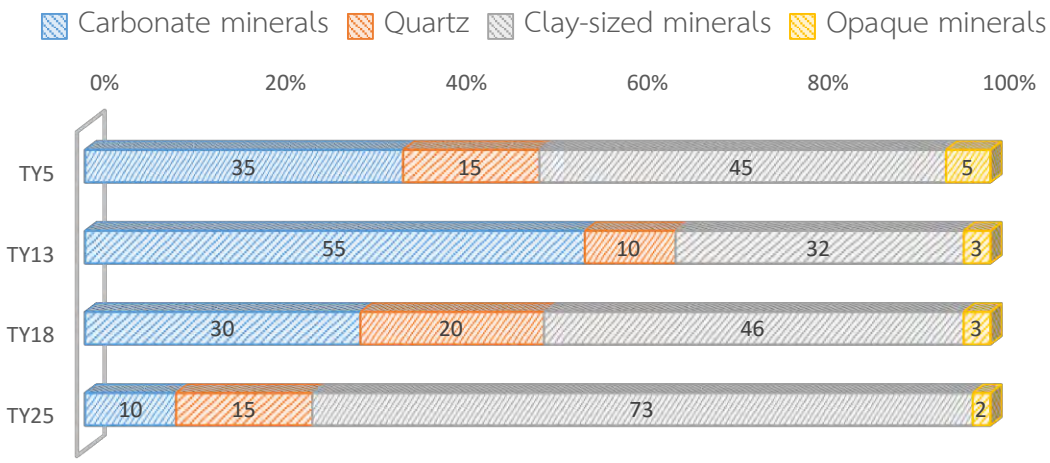

Figure 4.3 Mineral composition from thin sections.

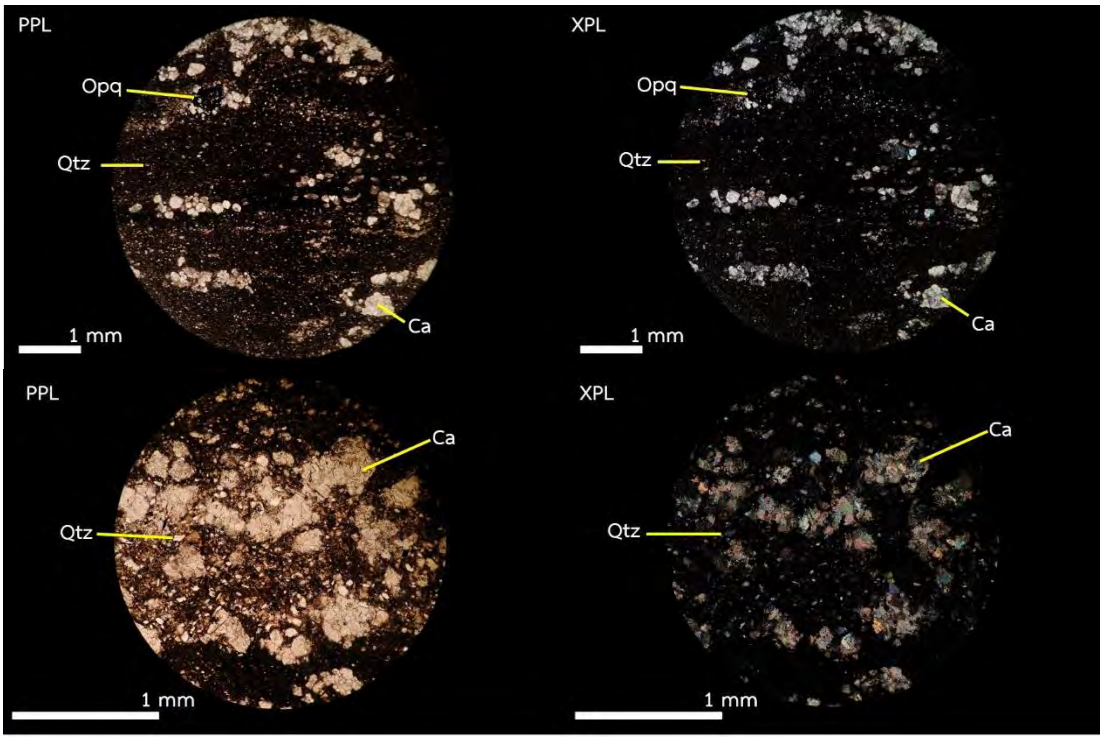

Figure 4.4 Photomicrographs of TY 5 in plane-polarized light (PPL) and cross-polarized light (XPL) showing calcareous mudstone with very thin carbonate layers and subangular quartz grains in carbonate layers and rock matrix. The sample composes of carbonate minerals (Ca), quartz (Qtz), opaque minerals (Opq) and unidentified clay-sized minerals (rock matrix).

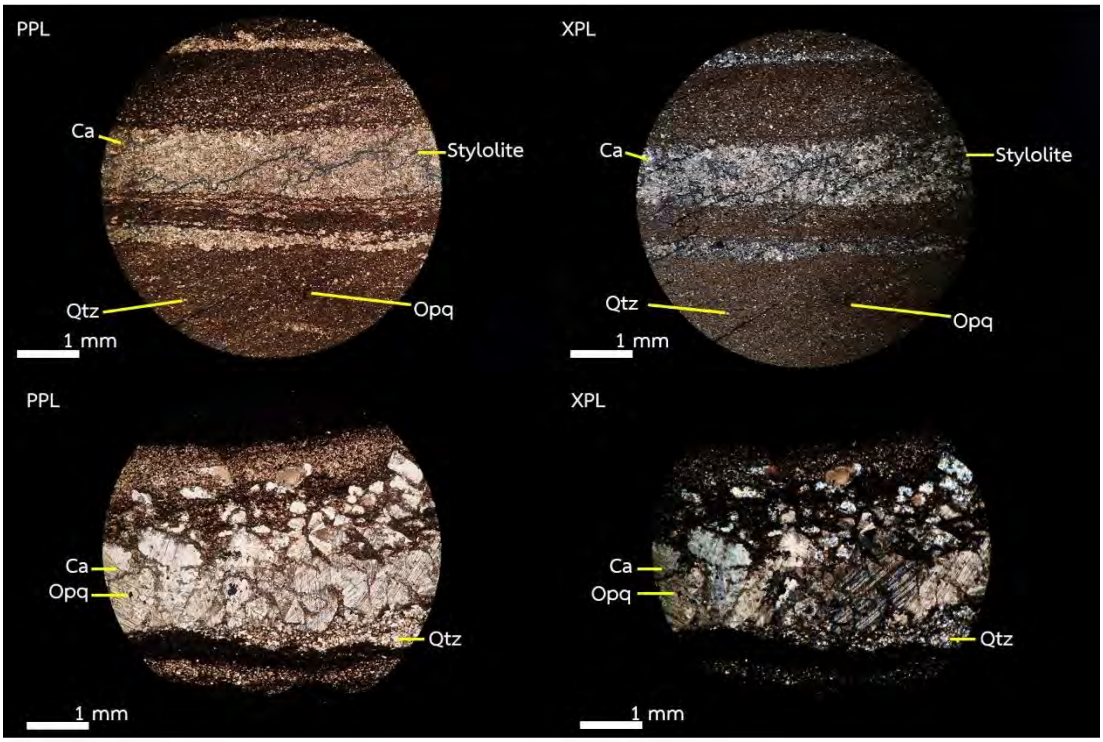

Figure 4.5 Photomicrographs of TY 13 in plane-polarized light (PPL) and cross-polarized light (XPL) showing calcareous mudstone with thick carbonate layers. Subrounded carbonate and subangular quartz grains are in carbonate layers and rock matrix. The sample composes of carbonate minerals (Ca), quartz (Qtz), opaque minerals (Opq) and unidentified clay-sized minerals (rock matrix).

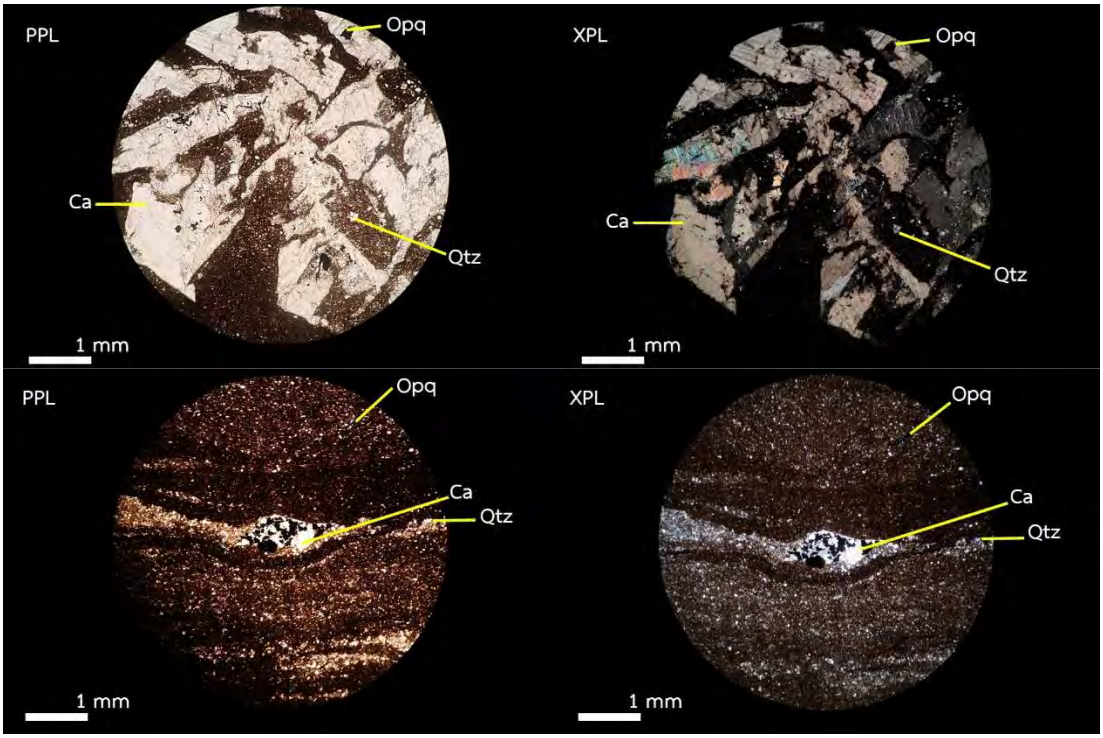

Figure 4.6 Photomicrographs of TY 18 in plane-polarized light (PPL) and cross-polarized light (XPL) showing calcareous mudstone with carbonate lens. The sample composes of carbonate minerals (Ca), quartz (Qtz), opaque minerals (Opq) and unidentified clay-sized minerals (rock matrix).

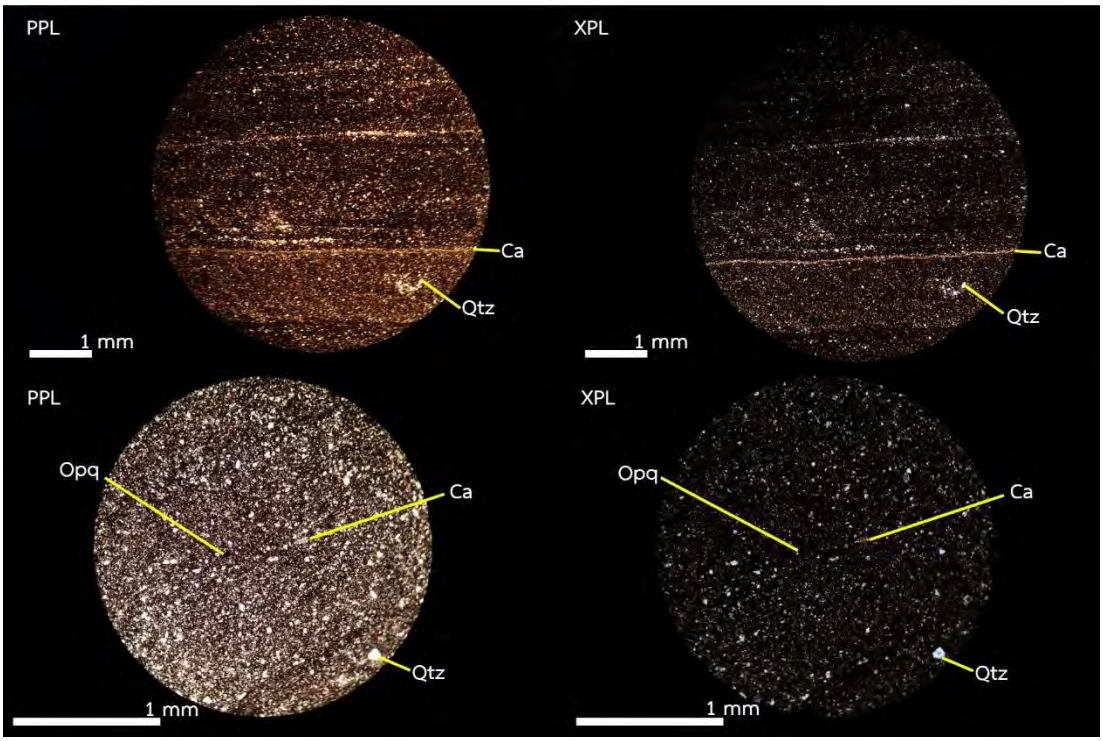

Figure 4.7 Photomicrographs of TY 25 in plane-polarized light (PPL) and cross-polarized light (XPL) showing laminated calcareous mudstone and subangular quartz grains in rock matrix. The sample composes of carbonate minerals (Ca), quartz (Qtz), opaque minerals (Opq) and unidentified clay-sized minerals (rock matrix).

4.1.2 XRD analyses

X-ray diffraction data were used to analyze type and quantity of minerals in the samples using EVA and MAUD softwares (Figures 4.8 - 4.9). Minerals found in the samples are albite (low), dolomite, microcline, calcite, quartz, illite and pyrite. The most abundant minerals are carbonate minerals and albite (low). Illite is present in some samples mostly in the middle to lower section. Pyrite is quite rare and only found in a few samples, which contrasts with observation from fresh samples. Samples contain albite (low) 25.73 - 50.04 wt% with an average of 37.73 wt%. Dolomite is found 19.61 - 39.18 wt% with an average of 30.76 wt%. Microcline is found from 0 - 21.67 wt% with an average 13.69 wt%. Calcite ranges from 0 - 23.26 wt% with an average of 7.96 wt%, while quartz is found 0 - 15 wt% with an average of 5.38 wt%. Illite presents from 0 - 10.19 wt% with an average of 4.29 wt% whereas pyrite is from 0 - 1.33 wt% with an average of 0.18 wt%.

The detection limit of X-Ray diffractometer is about 2% of the sample for mixed and non-homogeneous materials, so clay minerals and pyrite in the samples may be less than 2% and undetected by XRD readings. Moreover, background noise could obscure the minor reference peaks. So the observed XRD pattern and calculated XRD pattern from MAUD software may not match perfectly. Figure 4.10 shows the comparison of mineral composition of 25 samples while average percentage of minerals in samples is shown in Figure 4.11. X-ray powder diffraction pattern of all samples computed by MAUD software can be seen in Appendix A.

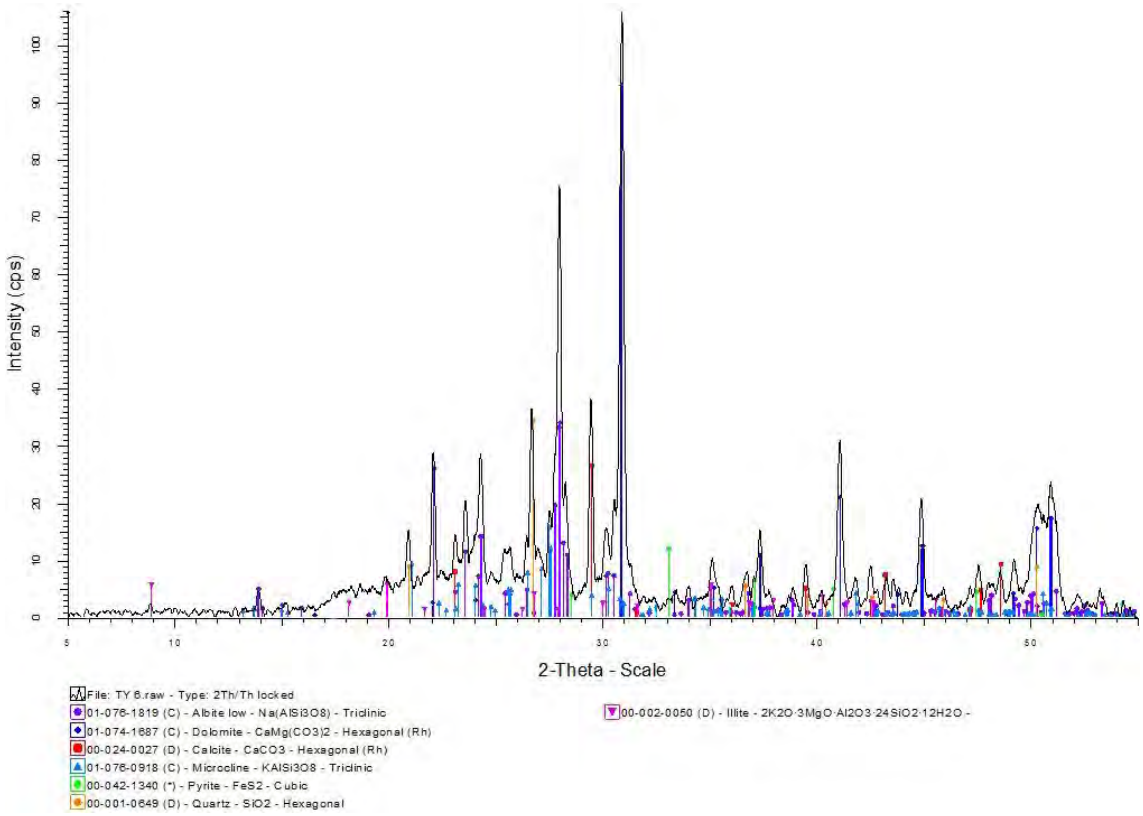

Figure 4.8 X-ray powder diffractogram of TY 6 from EVA software.

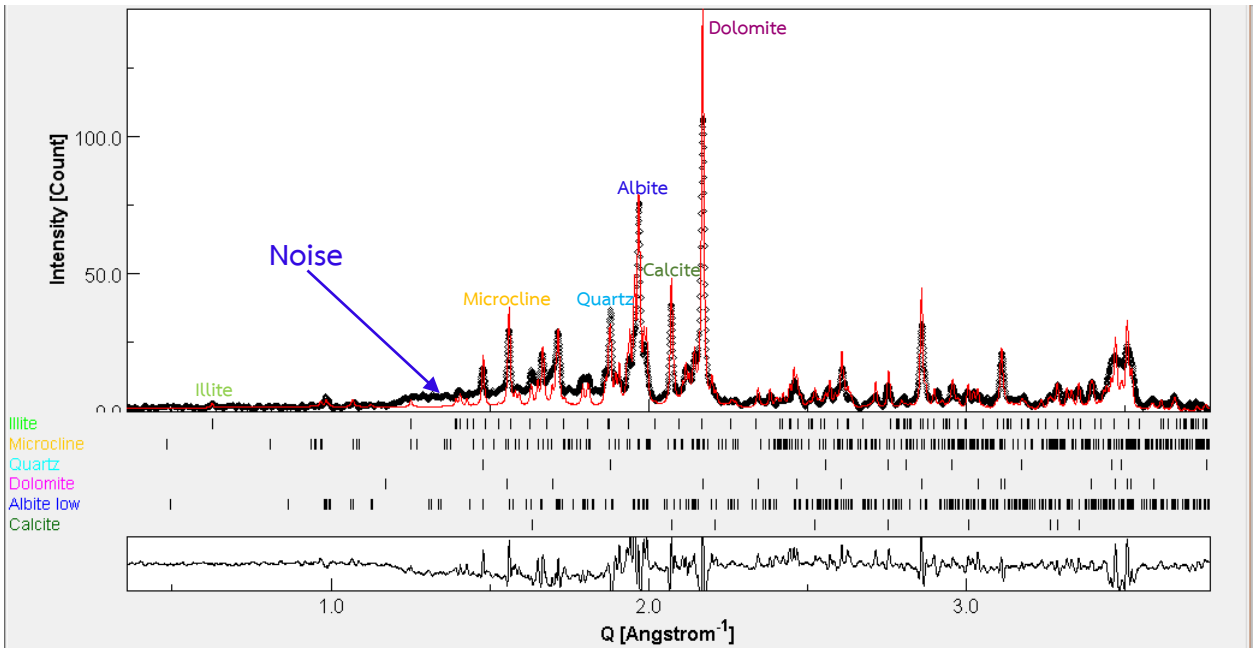

Figure 4.9 X-ray powder diffraction pattern of TY 6 refined by MAUD software. The calculated pattern (red line) is superimposed on the observed profile (black line).

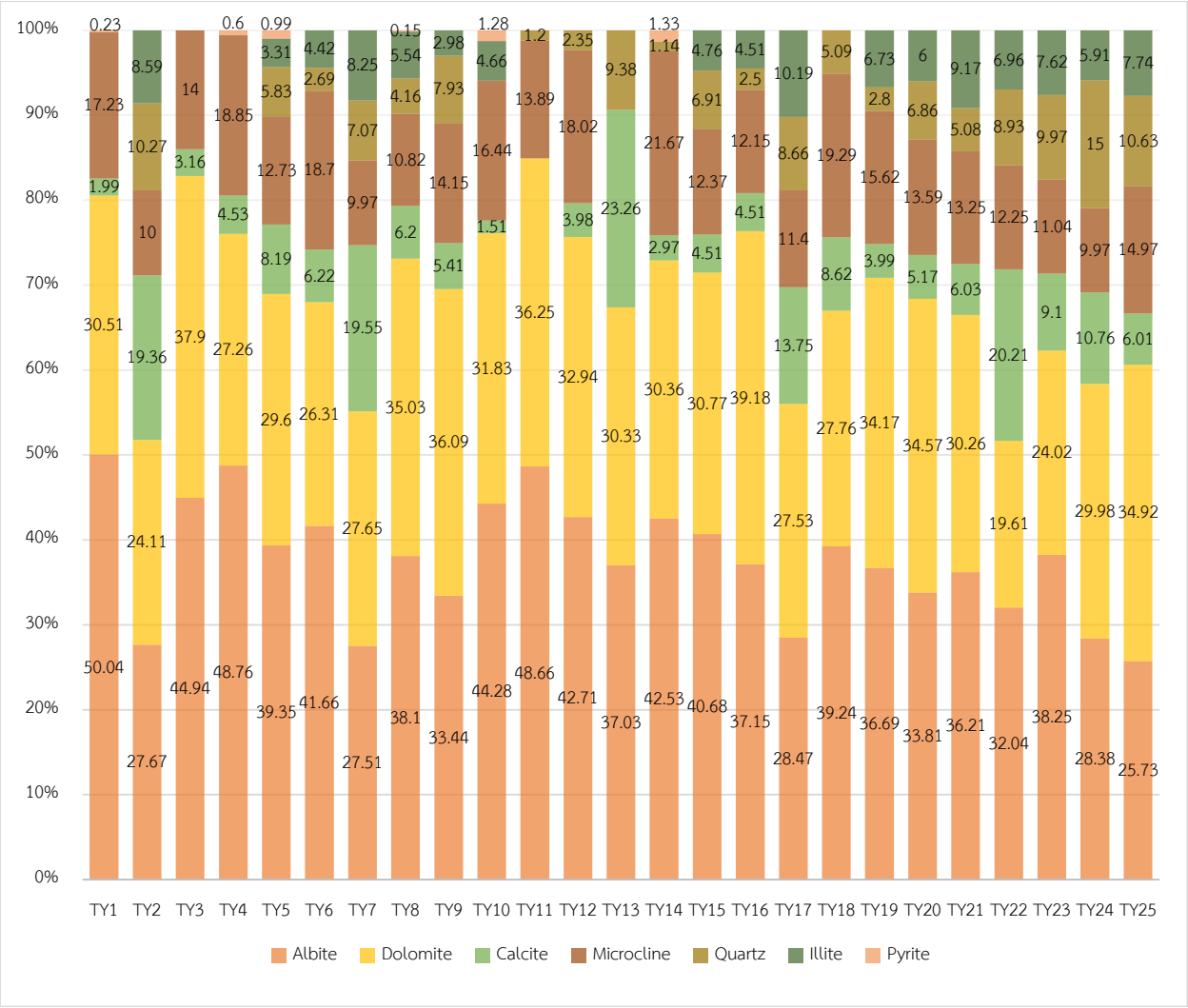

Figure 4.10 Mineral composition of the samples computed by MAUD software. Quantity of minerals are in weight percent.

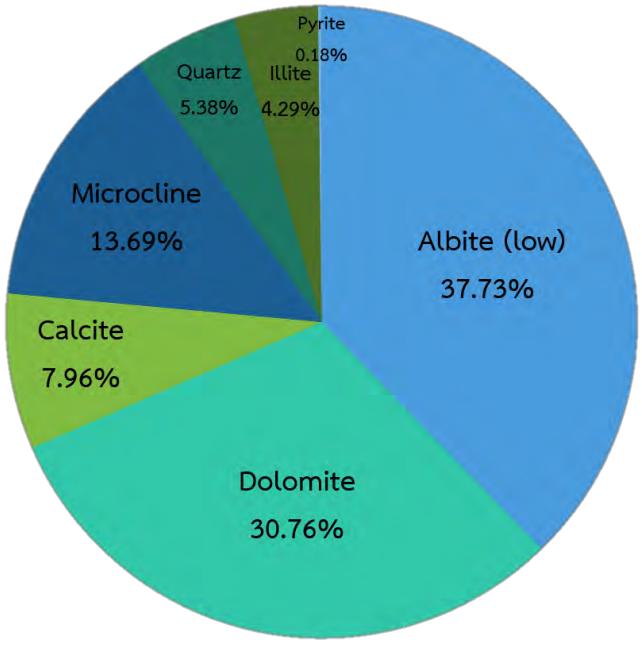

Figure 4.11 Average percentage of minerals in samples.

Average carbonate content of all samples determined from decarbonating process is about 41 wt%, which is similar to the average percentage of carbonate minerals analyzed by MAUD software (38.72 wt%). However, there might be some sample loss during the decarbonating process, that caused the difference in percentages of carbonates when compared to those obtained from XRD results.

From Figures 4.3 and 4.10, carbonate contents observed from thin sections TY 5, 13 and 18 are similar to carbonate contents calculated from XRD results. Carbonate content of TY 25 computed by MAUD software is 40.95 wt% while those observed from thin section is 10%, which means most carbonate minerals in TY 25 are in clay-sized grains that cannot be separated from other clay-sized minerals in the thin section.

Although the lithologic textures of the rocks are different, there is no significant difference in mineral composition between these textural groups. Average percentage of minerals in each groups (Figure 4.12) is quite similar except for Group 2: laminated calcareous mudstone interbedded with thick carbonate layers group which has the lowest average content of albite (low), dolomite and microcline but has the highest average content of quartz and illite.

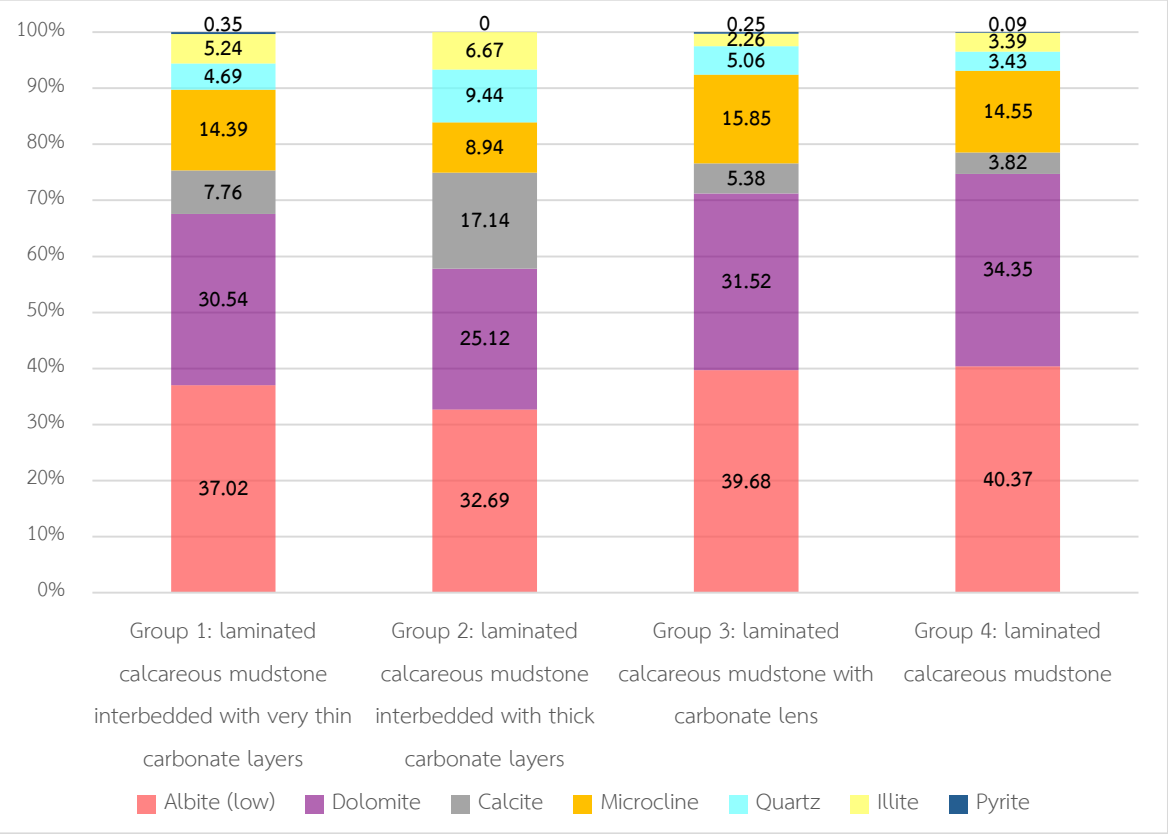

Figure 4.12 Average percentage of minerals in 4 different lithologic textures.

4.2 Petroleum geochemistry

4.2.1 TOC results

The TOC values of Tat Yai waterfall range from 0.47 - 3.55 wt% (Figure 4.13) indicating poor to very good source rock potential with the average TOC of 1.65 wt%. Most samples have good source rock potential (1 - 2 wt% TOC). The highest TOC value is in TY 15 and the lowest TOC value is in TY 13, both of which are in the middle of the studied section.

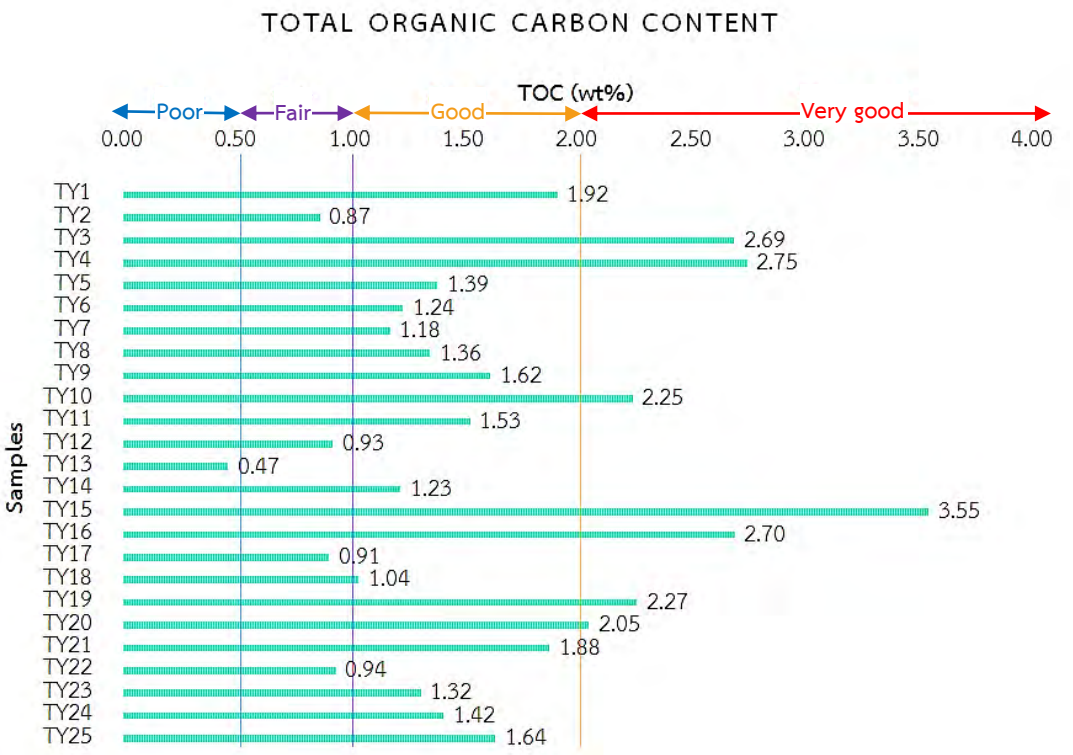

Figure 4.13 TOC values of Tat Yai samples.

4.2.2 Rock-Eval pyrolysis results

➢ Original samples

Only samples with TOC > 1 wt% were pyrolyzed by Rock Eval 6 in Core Laboratories Malaysia, because low TOC may lead to abnormally high values of hydrogen and oxygen indices. Moreover, they might not give reproducible results for hydrogen index and T_{max} mainly because the interference from bitumen in the samples (Marshall *et al.*, 1985). From the results in Table 4.2, S_1 values range from 0.03 - 0.22 mg/g rock and S_2 values range from 0.03 - 0.25 mg/g rock which are very low. In addition, S_3 values range from 0.01 - 0.49 mg/g rock. All samples have S_2 values less than 2.5 mg/g rock, which

indicates poor source rock potential according to Peters and Garrey (2014). From Tissot and Welte (1984), all samples with less than 2 mg/g rock of productive yield (PY) are considered to be low potential source rock. TOC and Rock-Eval results of all original samples can be seen in Appendix B.

All samples have hydrogen index values ranging from 1.57 - 9.86 mg HC/ g TOC which indicate kerogen type IV (Inert) and have oxygen index values ranging from 0.76 - 17.81 mg CO_2/g TOC. Modified Van-Krevelen diagram of the samples is shown in Figure 4.14.

S_2 vs. TOC diagram (Figure 4.15) is an effective diagram to evaluate source rock quality by avoiding S_3 values. All samples fall into type IV kerogen despite good source rock potential from TOC results.

A cross plot of hydrogen index vs. T_{max} (Figure 4.16) is a convenient method for examining the decrease in hydrogen index with an increase in source rock maturation level. The T_{max} values (ranging from 301 to 601 ^{o}C) show that almost all samples exposed on the surface today are in post-mature stage. TY 1 has 301 ^{o}C T_{max} which falls into immature stage. If the S_2 value is less than 0.5 mg HC/g rock and the S_2 peak does not have a definitive peak (e.g. is broad and flat), T_{max} values may not be reliable because they are affected by low organic matter content (Espitalié *et al*., 1985). TY 15 and TY 16 which have S_2 > 0.5 mg HC/g rock have T_{max} 600 ^{o}C and 582 ^{o}C, respectively. High T_{max} values (> 500 ^{o}C) can result from mineral decomposition and pyrobitumen component, which is a residue substance converted from petroleum cracking in the samples.

Table 4.2 S_1, S_2, S_3, T_{max}, OPI, PY, HI and OI values from Rock-Eval pyrolysis of the Tat Yai samples.

Sample name	Lithology	TOC (wt%)	mg/gm rock			T_{max} (°C)	OPI	PY	HI	OI
			S_1	S_2	S_3					
TY 1	brnsh gy, calc	1.92	0.22	0.03	0.24	301	0.88	0.25	1.57	12.52
TY 2	lt brnsh gy, calc	0.87								
TY 3	brnsh blk, calc	2.69	0.10	0.13	0.05	599	0.43	0.23	4.83	1.86
TY 4	brnsh blk, calc	2.75	0.10	0.12	0.49	601	0.45	0.22	4.36	17.81
TY 5	brnsh gy, calc	1.39	0.11	0.07	0.03	598	0.61	0.18	5.05	2.16
TY 6	brnsh gy, calc	1.24	0.06	0.06	0.02	597	0.50	0.12	4.84	1.61
TY 7	brnsh gy, calc	1.18	0.05	0.07	0.01	593	0.42	0.12	5.92	0.85
TY 8	brnsh gy, calc	1.36	0.04	0.07	0.03	598	0.36	0.11	5.16	2.21
TY 9	brnsh gy, calc	1.62	0.05	0.16	0.07	581	0.24	0.21	9.86	4.31
TY 10	brnsh blk, calc	2.25	0.03	0.10	0.05	600	0.23	0.13	4.45	2.23
TY 11	brnsh gy, calc	1.53	0.07	0.14	0.05	575	0.33	0.21	9.14	3.26
TY 12	lt brnsh gy, calc	0.93								
TY 13	lt brnsh gy, calc	0.47								
TY 14	brnsh gy, calc	1.23	0.09	0.06	0.11	598	0.60	0.15	4.89	8.96
TY 15	brnsh blk, calc	3.55	0.07	0.20	0.30	600	0.26	0.27	5.64	8.46
TY 16	brnsh blk, calc	2.7	0.13	0.25	0.04	582	0.34	0.38	9.27	1.48
TY 17	lt brnsh gy, calc	0.91								
TY 18	lt brnsh gy, calc	1.04	0.03	0.04	0.01	600	0.43	0.07	3.84	0.96
TY 19	brnsh blk, calc	2.27	0.04	0.09	0.25	600	0.31	0.13	3.97	11.03
TY 20	brnsh gy, calc	2.05	0.10	0.17	0.05	595	0.37	0.27	8.28	2.43
TY 21	brnsh gy, calc	1.88	0.06	0.1	0.04	599	0.40	0.15	4.78	2.13
TY 22	lt brnsh gy, calc	0.94								
TY 23	brnsh gy, calc	1.32	0.04	0.10	0.01	578	0.29	0.14	7.6	0.76
TY 24	brnsh gy, calc	1.42	0.04	0.12	0.02	582	0.25	0.16	8.48	1.41
TY 25	brnsh gy, calc	1.64	0.05	0.12	0.03	592	0.29	0.17	7.31	1.83

Remark: OPI = Oil Production Index = Transformation Ratio = $S_1/(S_1+S_2)$

PY = Potential Yield = (S_1+S_2)

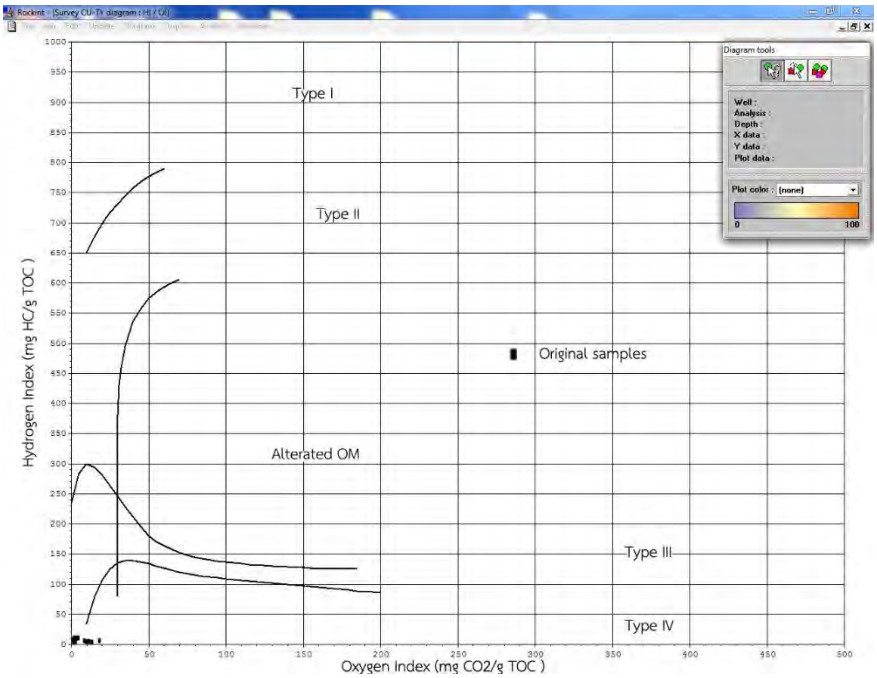

Figure 4.14 Modified Van-Krevelen diagram showing HI and OI of Tat Yai samples.

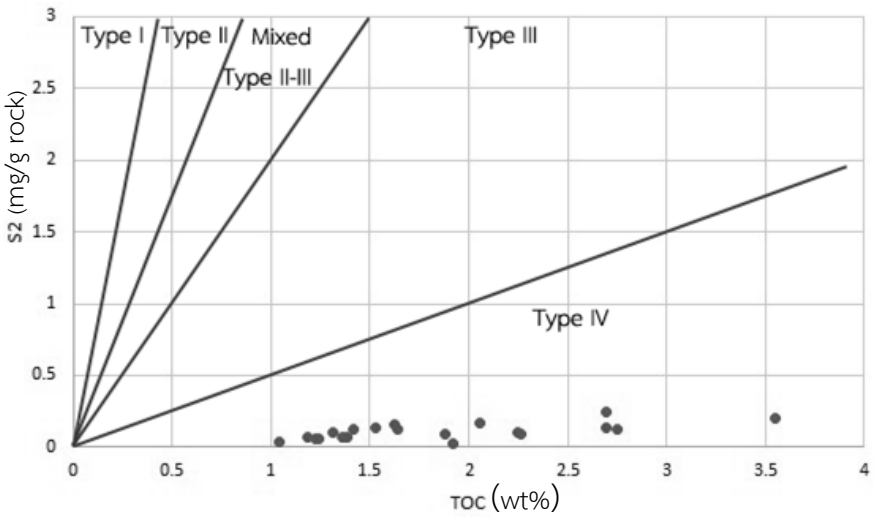

Figure 4.15 Plot of remaining hydrocarbon potential (S_2) versus TOC.

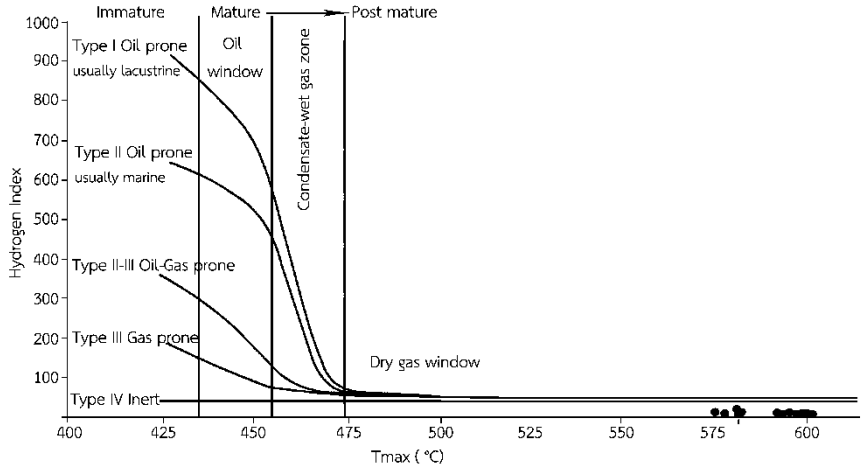

Figure 4.16 Plot of HI vs. Rock-Eval T_{max} for all samples except TY 1 which has T_{max} < 400°C.

➢ Decarbonated samples

The decarbonated samples were pyrolyzed by Rock Eval 6 at the PTT Research and Technology Institute. Excluding the samples with < 1 wt% TOC, S_1 values range from 0.03 - 0.27 mg/g rock and S_2 values range from 0.01 - 0.52 mg/g rock which are quite higher than the values obtained from the original samples but still indicate poor source rock potential. In addition, S_3 values range from 0.03 - 0.36 mg/g rock (Table 4.3). All samples have less than 2 mg/g rock of productive yield (PY), hence are considered to be low potential source rock. Rock-Eval results of all decarbonated samples can be seen in Appendix B.

Hydrogen index values of all samples range from 0.52 to 26.22 mg HC/ g TOC, which indicates kerogen type IV (Inert) and the oxygen index values range from 2.27 to 12.78 mg CO_2/ g TOC. Both hydrogen and oxygen indices of the decarbonated samples do not significantly differ from the values of original samples. Modified Van-Krevelen diagram of the decarbonated samples is shown in Figure 4.17.

Based on TOC results, the samples have good source rock potential but S_2 - TOC diagram (Figure 4.18) of the decarbonated samples shows that samples contain type IV kerogen, which has low hydrocarbon generating potential.

Most decarbonated samples are in post-mature stage identified from T_{max} values (Figure 4.19) which are 283 to 608 ^{o}C. From Table 4.3, only TY 16 has S_2 > 0.5 mg HC/g rock and has T_{max} 598 ^{o}C. Decarbonated samples of TY 1, 5, 6, 10, 14, 18, 21 have T_{max} less than 435 ^{o}C and fall in immature stage. But the T_{max} of original samples TY 5, 6, 10, 14, 18, 21 are in post-mature level (about 600 ^{o}C T_{max}). These conflict T_{max} results may be because of an incorrect selection of the S_2 peak by the program or broad S_1 peak from non-indigenous free hydrocarbons (migrated hydrocarbons), which increase rock weight and lead to reduction in S_2 values (mg HC/ g rock) causing lower T_{max} (less than 380 °C) (Hall *et al.*, 2016).

Table 4.3 S_1, S_2, S_3, T_{max}, OPI, PY, HI and OI values from Rock-Eval pyrolysis of the decarbonated samples.

Sample name	Lithology	TOC (wt%)	mg/gm rock			T_{max} (°C)	OPI	PY	HI	OI
			S_1	S_2	S_3					
TY 1	brnsh gy, calc	1.92	0.08	0.01	0.07	324	0.09	0.89	0.52	3.65
TY 2	lt brnsh gy, calc	0.87	0.03	0.03	0.05	608	0.06	0.5	3.45	5.75
TY 3	brnsh blk, calc	2.69	0.13	0.07	0.07	608	0.20	0.65	2.60	2.60
TY 4	brnsh blk, calc	2.75	0.09	0.13	0.31	608	0.22	0.41	4.73	11.27
TY 5	brnsh gy, calc	1.39	0.10	0.05	0.10	303	0.15	0.67	3.6	7.19
TY 6	brnsh gy, calc	1.24	0.06	0.04	0.05	304	0.10	0.6	3.23	4.03
TY 7	brnsh gy, calc	1.18	0.14	0.03	0.03	462	0.17	0.82	2.54	2.54
TY 8	brnsh gy, calc	1.36	0.10	0.05	0.06	607	0.15	0.67	3.68	4.41
TY 9	brnsh gy, calc	1.62	0.18	0.17	0.05	602	0.35	0.51	10.49	3.09
TY 10	brnsh blk, calc	2.25	0.12	0.02	0.10	283	0.14	0.86	0.89	4.44
TY 11	brnsh gy, calc	1.53	0.20	0.15	0.04	606	0.35	0.57	9.80	2.61
TY 12	lt brnsh gy, calc	0.93								
TY 13	lt brnsh gy, calc	0.47								
TY 14	brnsh gy, calc	1.23	0.11	0.01	0.04	304	0.12	0.92	0.81	3.25
TY 15	brnsh blk, calc	3.55	0.27	0.48	0.36	607	0.75	0.36	13.52	10.14
TY 16	brnsh blk, calc	2.7	0.25	0.52	0.08	598	0.77	0.32	19.26	2.96
TY 17	lt brnsh gy, calc	0.91								
TY 18	lt brnsh gy, calc	1.04	0.06	0.02	0.05	375	0.08	0.75	1.92	4.81
TY 19	brnsh blk, calc	2.27	0.19	0.19	0.29	607	0.38	0.5	8.37	12.78
TY 20	brnsh gy, calc	2.05	0.27	0.20	0.05	608	0.47	0.57	9.76	2.44
TY 21	brnsh gy, calc	1.88	0.15	0.02	0.06	325	0.17	0.88	1.06	3.19
TY 22	lt brnsh gy, calc	0.94								
TY 23	brnsh gy, calc	1.32	0.08	0.05	0.03	608	0.13	0.62	3.79	2.27
TY 24	brnsh gy, calc	1.42	0.17	0.14	0.05	608	0.31	0.55	9.86	3.52
TY 25	brnsh gy, calc	1.64	0.24	0.43	0.10	608	0.67	0.36	26.22	6.1

Remark: OPI = Oil Production Index = Transformation Ratio = $S_1/(S_1+S_2)$

PY = Potential Yield = (S_1+S_2)

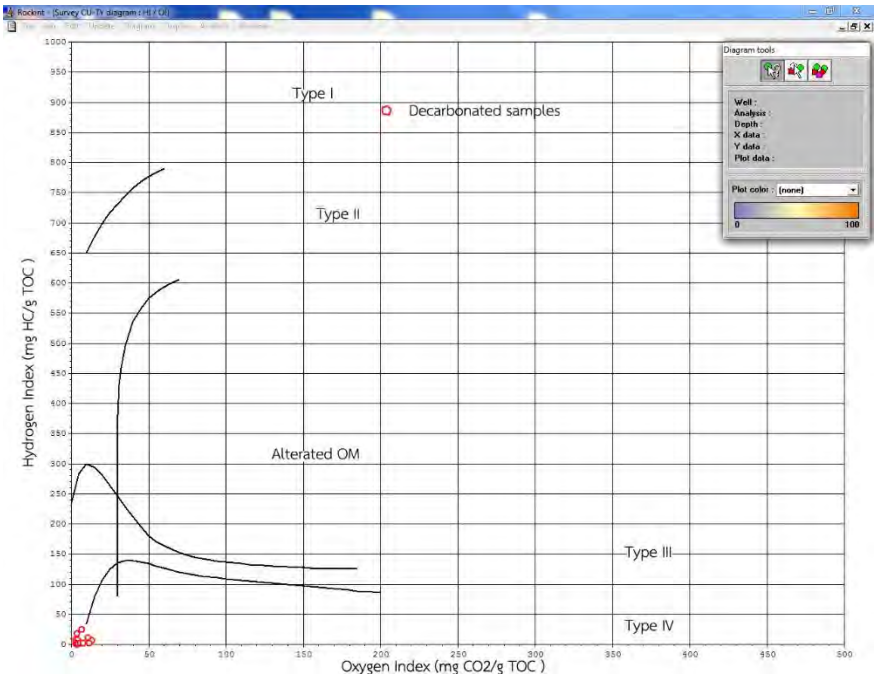

Figure 4.17 Modified Van-Krevelen diagram showing HI and OI of decarbonated Tat Yai samples.

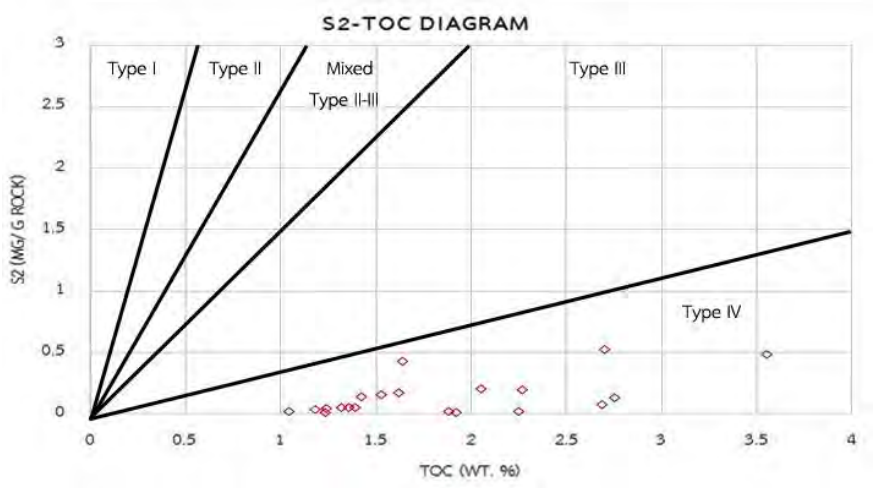

Figure 4.18 Plot of remaining hydrocarbon potential (S_2) versus TOC.

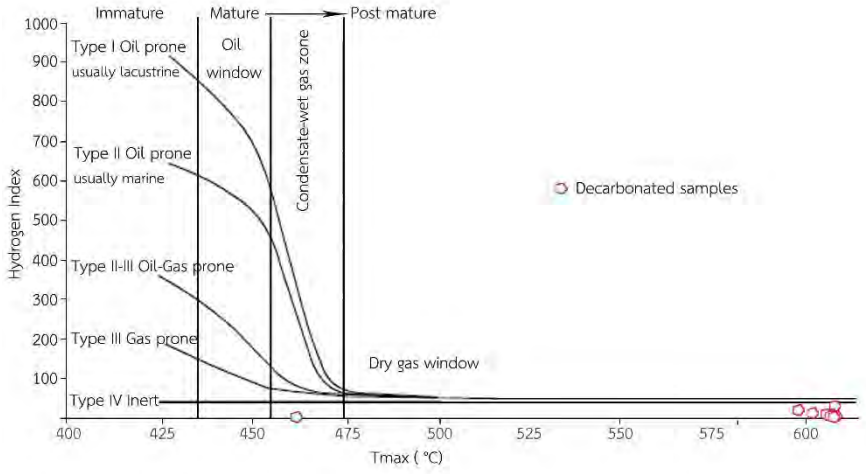

Figure 4.19 Plot of HI versus Rock-Eval T_{max} for all samples except TY 1, 5, 6, 10, 14, 18 and 21 which have T_{max} < 400°C.

CHAPTER 5

DISCUSSION AND CONCLUSION

5.1 Discussion

Both the original and decarbonated samples have similar hydrogen index and oxygen index values and fall into the areas of type IV inert kerogen in post-mature stage (as shown in Figures 5.1 - 5.4). Samples with oxygen index values greater than 10 mg CO_2/g TOC may have TOC_{inert} or mineral matrix effects or carbonate decomposition during Rock-Eval pyrolysis (Erik *et al.*, 2010). Almost all of the Tat Yai samples have oxygen index values less than 10 mg CO_2/g TOC suggesting minimal mineral matrix effect and likely no carbonate decomposition happened during pyrolysis. From Modified Van-Krevelen diagram in Figures 5.1 and 5.2, most of the decarbonated samples show a slight decrease of oxygen index values from the originals. For the original samples, there might be a little carbonate decomposition during pyrolysis and mixed with CO_2 generated from kerogen cracking, which causes higher S_3 and oxygen index values than decarbonated samples.

Figure 5.5 shows stratigraphic summary of Tat Yai waterfall with sample positions, TOC and Rock-Eval pyrolysis results of the original samples compared with those of the decarbonated samples. Rock-Eval pyrolysis results of Tat Yai samples and cutting samples of Huai Hin Lat Formation from exploration wells from Chamchoy (2014) are plotted together in Figure 5.6, Tat Yai samples falls into a different range of kerogen type and maturation level compared with cutting samples. Tat Yai samples are in post-mature level and fall into type IV kerogen range. While the cutting samples are in a wide range of maturation level (late-post mature stage) and most samples fall in kerogen type II/III range. These differences may be resulting from spatial variability of Huai Hin Lat Formation and surface oxidation from long exposure of Tat Yai waterfall causing a decrease in hydrogen and oxygen indices.

From Figure 5.7, hydrogen and oxygen indices of the original and decarbonated samples are plotted together with other Tat Yai samples from Khositchaisri (2012) and Arsairai (2014). The diagram shows that all samples were cluster together in the bottom-left corner of the diagram indicating type IV kerogen with high maturation stage.

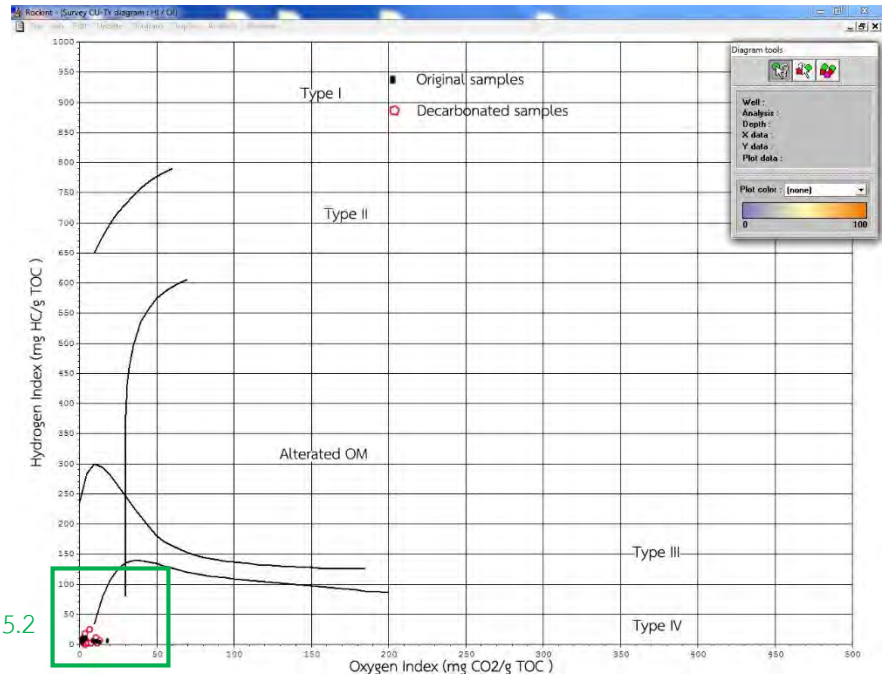

Figure 5.2

Figure 5.1 Modified Van-Krevelen diagram showing HI and OI of Tat Yai original samples compared with the decarbonated samples. Close up of the area in the green box is shown in Figure 5.2.

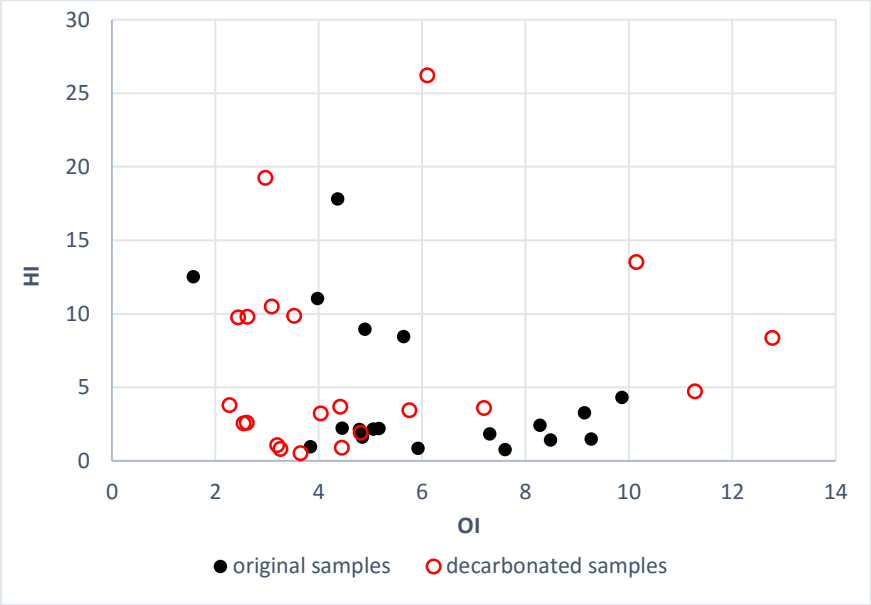

Figure 5.2 HI-OI plot of the Tat Yai original samples compared with the decarbonated samples.

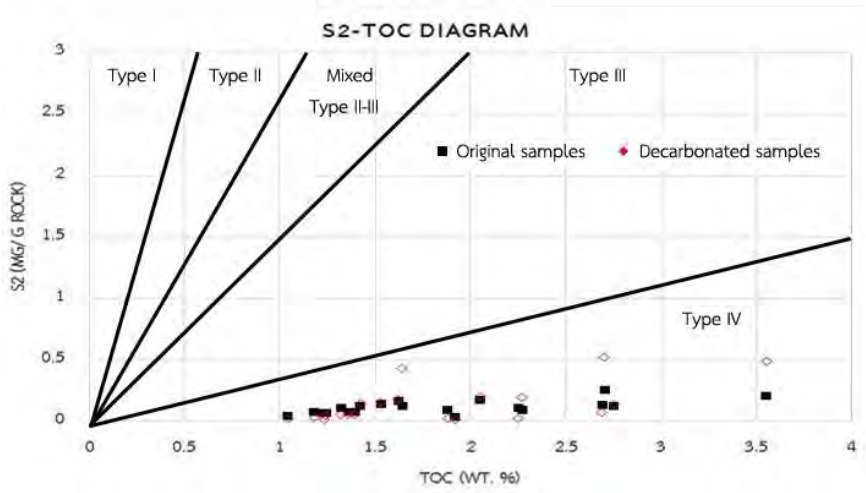

Figure 5.3 Plot of remaining hydrocarbon potential (S_2) versus TOC of the original Tat Yai samples compared with the decarbonated samples.

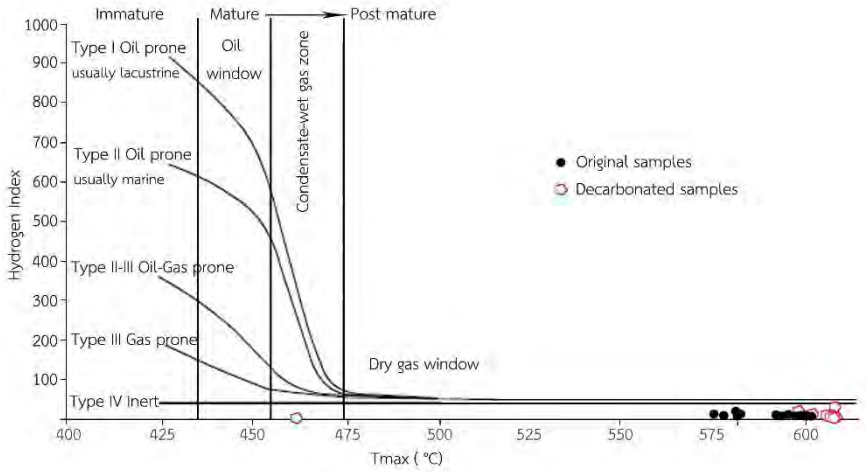

Figure 5.4 Plot of HI versus Rock-Eval T_{max} of the original Tat Yai samples compared with the decarbonated samples.

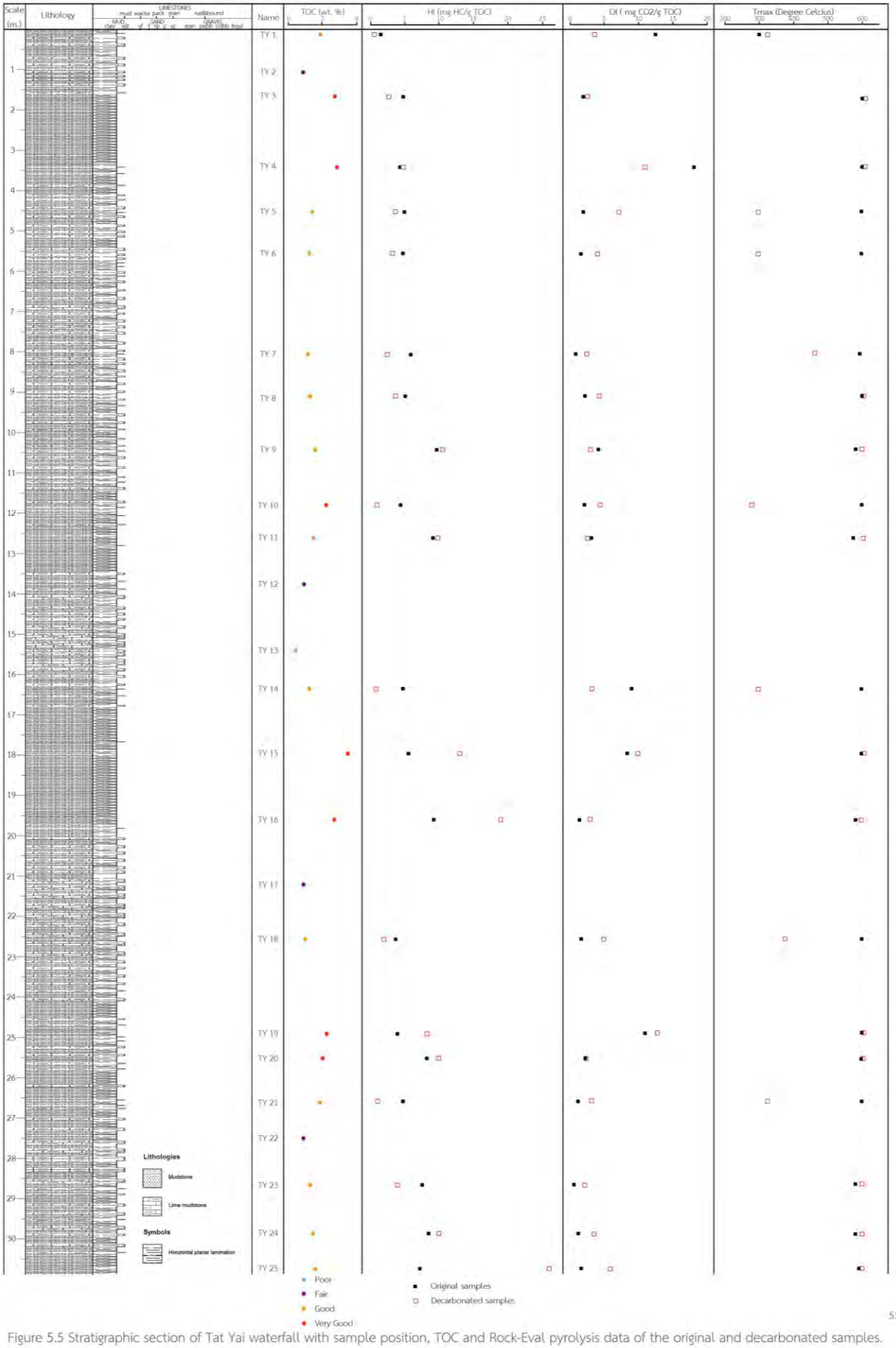

Figure 5.5 Stratigraphic section of Tat Yai waterfall with sample position, TOC and Rock-Eval pyrolysis data of the original and decarbonated samples.

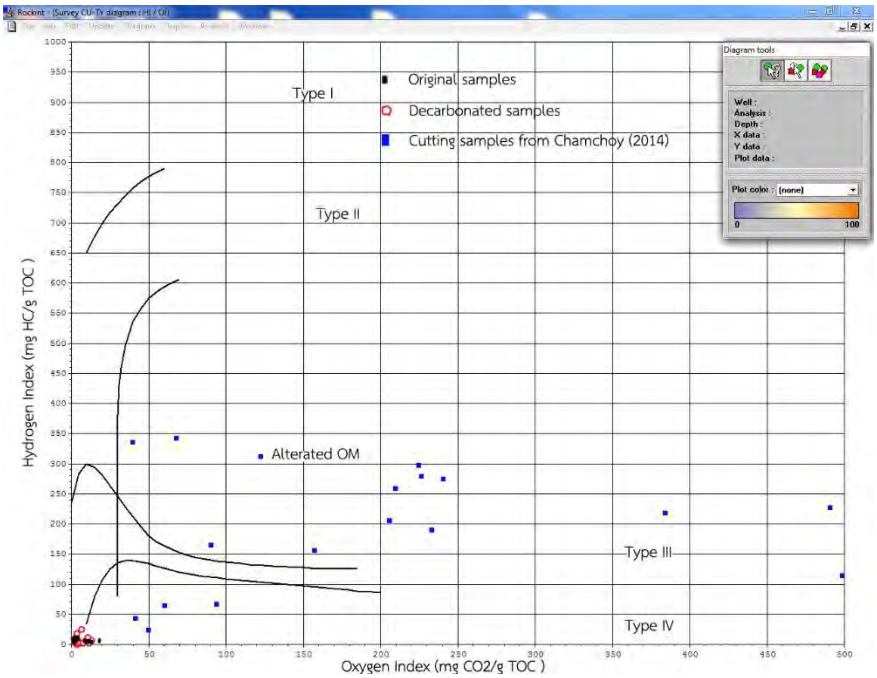

Figure 5.6 Modified Van-Krevelen diagram showing HI and OI of Tat Yai original and decarbonated samples compared with the cutting samples from exploration wells (Chamchoy, 2014).

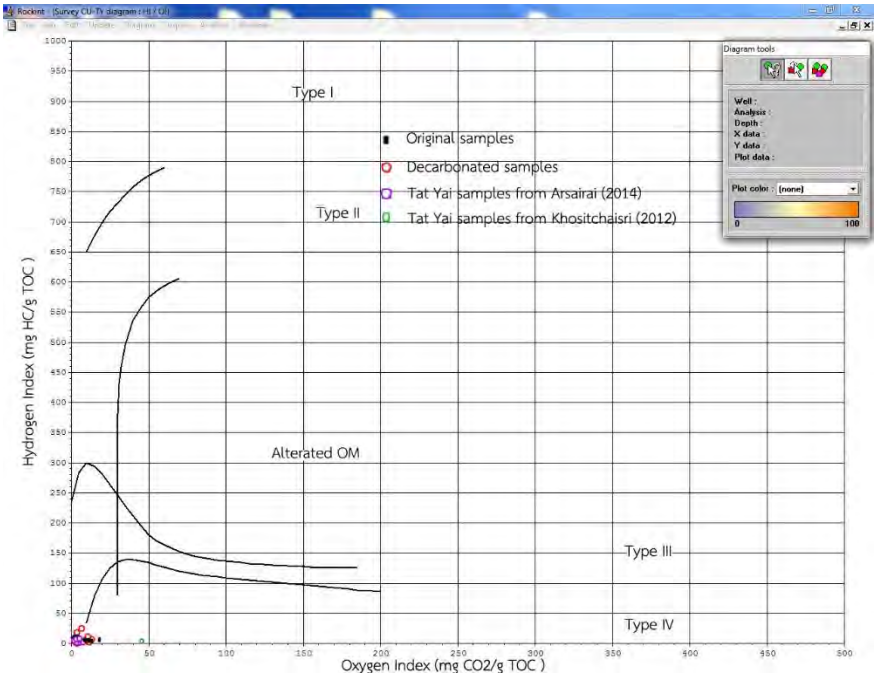

Figure 5.7 Modified Van-Krevelen diagram showing HI and OI of Tat Yai original and decarbonated samples compared with other Tat Yai samples from Khositchaisri (2012) and Arsairai (2014).

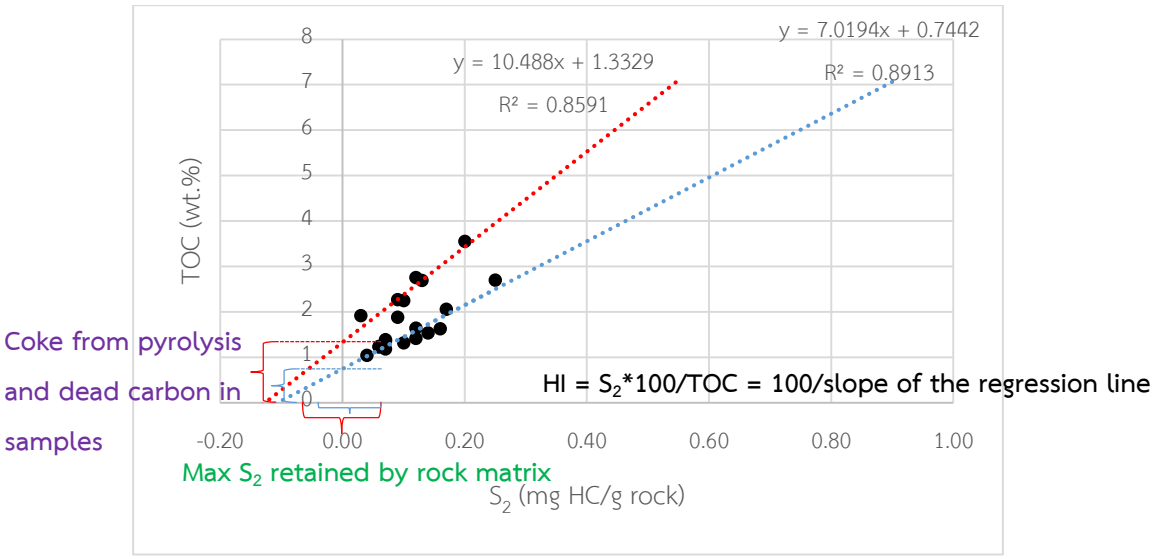

Figure 5.8 S_2 vs. TOC plot showing effects of hydrocarbon retention by mineral matrix in Tat Yai samples.

To determine mineral matrix effect on Rock-Eval pyrolysis results, S_2 vs. TOC diagram of the original samples in Figure 5.8 is used to interpret Rock-Eval pyrolysis data and estimate amount of the matrix effect and inert carbon. The regression slopes of Tat Yai samples are high, resulting from lack of S_2 hydrocarbons. Although only fresh samples were collected in this study, due to long exposure of the outcrops, surface oxidation cannot be ruled out. This may contribute to low S_2 values in samples to a small degree. According to Langford and Valleron (1990), the regression line of the S_2 vs. TOC diagram should pass the origin if there is no rock-matrix absorption. The y-intercept is amount of carbon residue trapped on the minerals during pyrolysis and dead carbon in samples, which cannot generate hydrocarbons. The x-intercept means maximum S_2 retained by rock matrix. From Figure 5.7, Tat Yai samples have mineral matrix effect from a small positive intercept on the y-axis. The resulting plot can be separated into 2 groups (red and blue regression lines). Max S_2 values retained by rock matrix from the x-intercept are 0.1271 mg HC/ g rock for the samples in red line group and 0.1060 mg HC/ g rock for the samples in blue line group with an average of 0.1166 mg HC/g rock. TOC_{inert} is a coke from pyrolysis plus dead carbon which cannot generate hydrocarbons. The TOC_{inert} can be obtained from the y-intercept which is 1.3329 wt% for the samples in red line group and 0.7442 wt% for the samples in blue line group with an average of 1.0386 wt%. The $TOC_{observed}$ is obtained from the total average sample and gives the value of 1.65 wt%. It influences quantity and compositions of pyrolysates especially when the samples have high clay and carbonate contents (Peters,

1986). The pyrolysable TOC_{live} is 0.6114 wt%. This number reflects the percent of carbon that can generate hydrocarbons ($TOC_{observed}$ - TOC_{inert}). The true average hydrogen index calculated from slopes of the regression lines are 9.53 and 14.25 mg HC/g TOC with an average of 11.89 mg HC/g TOC. All are in kerogen type IV range.

The mineral matrix effect usually occurs in lean samples with S_2 0 - 3 mg HC/g rock and high mineral to organic matter ratio (Spiro, 1991). According to Espitalie et al. (1984), hydrocarbon retention is more intense when the sample has clayey matrix (especially illite), or when samples are in low maturation stage (low T_{max}). From XRD results, Tat Yai samples compose of albite (low) about 37.79 wt.%, carbonate minerals about 38.8 wt.%, microcline about 13.72 wt.%, quartz about 5.40 wt.%, illite about 4.12 wt.%, and pyrite about 0.18 wt.%. The average TOC is 1.65 wt%, which is much less than the minerals in the samples. Illite is the only active mineral in the samples that could retain hydrocarbons during pyrolysis. However, there is a low percentage of illite in all samples (less than 30%). Inert carbons in samples are quite high compared with the $TOC_{observed}$ and high T_{max} values indicating post-maturation level. Therefore, it is assumed that kerogen may have already cracked to hydrocarbons during the early stages of hydrocarbon generation and presently contains mainly dead hydrocarbons, which cannot generate petroleum. Another explanation is that the samples may contain type III/IV kerogen, which have low hydrogen/ carbon ratio and contain many aromatic rings in the structure. Surface oxidation of organic matter due to the long exposure of Tat Yai waterfall could also be the cause of high inert carbon in the samples. If an organic molecule is oxidized, it loses a bond, and decomposes resulting in lower hydrogen index and oxygen index values.

An amount of hydrocarbon retention by mineral matrix is considered to be low (0.1257 mg HC/ g rock, less than 1 mg HC/ g rock) due to its kerogen type IV and high maturation stage based on hydrogen and oxygen indices. Heavy hydrocarbons may have already cracked to lighter hydrocarbons and left an amount of dead carbon in samples (Espitalie, 1980). Long exposure of the outcrop may cause surface oxidation that reduces hydrogen and oxygen index values.

5.2 Conclusion

Tat Yai samples of Huai Hin Lat Formation contain low to high organic content (TOC 0.47 - 3.55 wt%) with low hydrocarbon generating potential (low S_2 and low hydrogen index). Modified Van-Krevelen diagram and hydrogen index - T_{max} plot indicate kerogen type IV with high maturity level (post mature stage). Comparison of hydrogen index vs. oxygen index diagram between the original and decarbonated samples shows that there might be a small effect of carbonate minerals on S_3 and oxygen index values that cause oxygen index values of the original samples to be slightly scattered. S_2 vs. TOC diagram help identify mineral matrix effect on Rock-Eval pyrolysis data. The average S_2 retained by rock matrix is 0.1166 mg HC/ g rock. An average of the coke from pyrolysis and dead carbon in samples is 1.0386 wt%. The true average hydrogen index is 11.89 mg HC/g TOC. From XRD data, illite is the only active mineral able to retain pyrolysable hydrocarbons. It was reported to be responsible for heavy hydrocarbon (> C_{15}) retention (Espitalie, 1980). The trapped heavy constituents are released as lighter hydrocarbons and carbon residue (coke from pyrolysis) instead. Due to a low content of illite (0 - 10.19 wt%), type IV kerogen, and high maturation stage, mineral matrix effect in Tat Yai samples caused by Illite is thought to be low.

5.3 Limitations & Recommendations

➢ Limitations

- Noisy X-ray diffraction (XRD) patterns might cause an error in data analyses of quantity of minerals in samples. The computed pattern from MAUD software may not match the observed pattern perfectly.

- The unsuccessful oriented XRD samples may be a result of the very low content of clay minerals in the glass slides that cannot be detected by X-Ray Diffractometer.

➢ Recommendations

- More accurate instrument is needed to analyze type and quantity of minerals in samples.

- Different instruments used in pyrolysis (Rock-Eval 6 instruments from Core Labolatories Malaysia and PTT Research and Technology Institute) may cause the results to be difficult to compare.

- In order to gain more accurate data about Rock-Eval pyrolysis results, kerogen should be isolated from the samples prior to pyrolysis.

- Visual kerogen typing should be conducted to confirm type of kerogen of Tat Yai samples.

- It is difficult to compare hydrogen index and oxygen index values of Tat Yai samples with the cutting samples of Huai Hin Lat Formation from Chamchoy (2014) due to surface oxidation and long exposure of Tat Yai waterfall.

REFERENCES

กรมทรัพยากรธรณี, 2550. ธรณีวิทยาประเทศไทย. พิมพ์ครั้งที่2 ฉบับปรับปรุง. โรงพิมพ์ดอกเบี้ย: สำนักธรณีวิทยา กรมทรัพยากรธรณี.

กิตติ ขาววิเศษ และ นรินทร์ จันทร์ฟู, 2552. แผนที่ธรณีวิทยาจังหวัดเพชรบูรณ์ มาตราส่วน 1:250000: กรมทรัพยากรธรณี.

อนุวัชร ตรีโรจนานนท์, 2555. ลำดับชั้นหินของหมวดหินห้วยหินลาด. พิมพ์ครั้งที่ 1. รายงานสำนักธรณีวิทยา ฉบับที่ มธ 3/2555: สำนักธรณีวิทยา, กรมทรัพยากรธรณี.

อนุวัชร ตรีโรจนานนท์, 2554. ลำดับชั้นหินของกลุ่มหินโคราชบริเวณขอบตะวันตกของที่ราบสูงโคราช. พิมพ์ครั้งที่ 1. รายงานวิชาการ มาตรฐานลำดับชั้นหิน ฉบับที่ 3/2554: สำนักธรณีวิทยา, กรมทรัพยากรธรณี.

Advanced Resources International, Inc. Technically Recoverable Shale Oil and Shale Gas Resources: Thailand. [Online]. 2013. Available from: https://www.eia.gov/analysis/studies/worldshalegas/pdf/Thailand_2013.pdf [2015, January 26]

Arsairai, B., 2014. Depositional environment and petroleum source rock potential of the late Triassic Huai Hin Lat Formation, Northeastern Thailand. Doctoral dissertation, Department of Geotechnology, Faculty of Engineering, Suranaree University of Technology.

Chamchoy, P., 2014. Petroleum Geochemistry of Huai Hin Lat Formation, Northeastern Thailand. Master's Thesis, Department of Geology, Faculty of Science, Chulalongkorn University.

Charusiri, P., Cenozoic Tectonic Evolution of Northeastern Thailand. [Online]. 2012. Available from: http://www.eatgru.sc.chula.ac.th/Thai/interest/pdf/Cenozoic_tectonic_NE_Thailand.pdf [2016, January 5]

Chonglakmani C., and Sattayarak N., 1978. Stratigraphy of the Haui Hin Lat Formation (Upper Triassic) in Northeastern Thailand. Proceeding on the third conference on geology and mineral resources of Southeast Asia: 739-762.

Cooper, M., *et al*., Mesozoic and Cenozoic thick-skinned deformation in Northeastern Thailand. [Online]. 1989. Available from: http://webapp1.dlib.indiana.edu/virtual_disk_library/index.cgi/2870166/FID3366/PDF/650.PDF [2016, February 10]

Crain, E.R., X-Ray diffraction methods. [Online]. 2015. Available from: https://spec2000.net/09-xrd.htm [2016, January 6]

Dahl, B., Bojesen-Koefoed, J., Holm, A., *et al*., 2004. A new approach to interpreting Rock-Eval S_2 and TOC data for kerogen quality assessment. Organic Geochemistry V. 35 No. 11-12: 1461-1477.

Demirel, I.H., 2005. Whole-Rock, Clay Mineral Contents and Matrix Effect on the Cenomanian/Turonian Petroleum Source Rocks in the Lower Antalya Nappe, Western Taurus Region of Turkey. Petroleum Science and Technology V. 23: 1183-1197.

Department of Mineral Fuels. Thailand Petroleum Provinces. [Online]. 2000. Available from: http://www2.dmf.go.th/petro_focus/files/info3.pdf [2015, December 15]

Department of Mineral Resources. WMS on the Geology and Mineral Resourecs. [Online]. 2015. Available from: www.dmr.go.th/main.php?filename=wms_en [2015, November 21]

Downs, R.T., and Hall-Wallace, M., 2003. The American Mineralogist Crystal Structure Database. American Mineralogist V. 88: 247-250.

Erik, N.Y., Özçelik, O., and Altunsoy, M., 2006. Interpreting Rock--Eval pyrolysis data using graphs of S_2 vs. TOC: Middle Triassic--Lower Jurassic units, eastern part of SE Turkey. Journal of Petroleum Science and Engineering, V. 53: 34-46.

Espitalié, J., Madec, M., and Tissot, B., 1980. Role of mineral matrix in kerogen pyrolysis: influence on petroleum generation and migration. American Association of Petroleum Geologists Bulletin V. 64: 59-66.

Espitalié, J., Senga Makadi, K., and Trichet, J., 1984. Role of the mineral matrix during kerogen pyrolysis. Organic Geochemistry V. 6: 365–382.

Hall, L.S., Boreham, C.J., Edwards, D.S., Palu, T.J., Buckler, T., Hill, A.J., and Troup, A., 2016. Cooper Basin Source Rock Geochemistry: Regional Hydrocarbon Prospectivity of the Cooper Basin, Part 2. Geoscience Australia Record V.6.

Katz, B.J., 1983. Limitations of Rock-Eval pyrolysis for typing of organic matter. Organic Geochemistry V. 4: 195–199.

Khositchaisri, W., 2012. Petroleum Geochemistry of Huai Hin Lat Formation in Amphoe Nam Nao, Changwat Phetchabun and Amphoe Chumpae, Changwat Khon Kaen, Thailand. Master's Thesis, Department of Geology, Faculty of Science, Chulalongkorn University.

Kozar, M. G., Crandall. G. F., and Hall. S. E., 1992. Integrated structural and stratigraphic study of the Khorat Basin, Rat Buri Limestone (Permian), Thailand. Proceedings of a National Conference on Geologic Resources of Thailand: Potential for Future Development. Department of Mineral Resources: 682-736

Law, C. A., 1999. Evaluating Source Rocks. AAPG Special Volumes. Treatise of Petroleum Geology/ Handbook of Petroleum Geology: Exploring for Oil and Gas Traps: 6-1 - 6-41.

Langford, F.F., and Blanc-Valleron, M.M., 1990. Interpreting Rock-Eval pyrolysis data using graphs of pyrolizable hydrocarbons vs. total organic carbon. American Association of Petroleum Geologists Bulletin V. 74: 799–804.

Lafargue, E., Espitalié, J., Marquis, F., and Pillot, D., 1998. Rock-Eval 6 applications in hydrocarbon exploration, production and in soil contamination studies. In Revue de I'Institut Francais du Pétrole V. 53: 421-437.

Peters, D., and Garrey, P., 2014. Source rock evaluation and hydrocarbon potential in the Tano Basin, South Western Ghana, West Africa. International Journal of Oil, Gas and Coal Engineering. V. 2 No. 5: 66-77.

Peters, K.E., 1986. Guidelines for evaluating petroleum source rock using programmed pyrolysis. American Association of Petroleum Geologists Bulletin V. 70: 318–329.

Phiri, C., Pujun, W., Nguimbi, G.R., and Hassan, I., 2014. Interpreting effects of TOC_{inert} organic content on source rock potential using S_2 vs. TOC graph in Maamba Coalfield, southern Zambia. Global Geology V. 17.

Phrachaiboon, C., 2014. Lithostratigraphy of the Late Triassic Huai Hin Lat formation at Amphoe Nam Nao, Changwat Phetchabun. Senior Project, Department of Geology, Faculty of Science, Chulalongkorn University.

Poppe, L.J., Paskevich, V.F., Hathaway, J.C., and Blackwood, D.S. A Laboratory Manual for X-Ray Powder Diffraction. [Online]. 2001. Available from: https://www.bucknell.edu/Documents/Geology/USGS-XRD-Manual.pdf [2015, December 26]

Racey A., 2011. Chapter 13. Petroleum Geology. Geology of Thailand. The Geological Society of London: 251-392.

Racey, A., and Goodall, J., 2009. Palynology and Stratigraphy of the Mesozoic Khorat Group Red Bed Sequences from Thailand. Geological Society of London Special Publication V. 315: 41-68.

Racey, A., Love, M. A., Canham, A. C., Goodall, J. G. S., and Polachan, S., 1996. Stratigraphy and reservoir potential of the Mesozoic Khorat Group, NE Thailand Part 1: Stratigraphy and sedimentary evolution. Journal of Petroleum Geology V. 18, 5–39.

RPS Energy Consultants Limited, 2012. Reserves and Resources Certification for the Sinphuhorm Gas Field as of 1st January 2012.

Spiro, B., 1991. Effects of minerals on Rock Eval pyrolysis of kerogen. Journal of thermal analysis, V. 37: 1513-1522.

Tissot, B., and Welte, D., 1984. Petroleum formation and occurrence. New York: Springer-Vferlag.

Wiriyasakpaisan, N., 2012. Geochemistry of Continental Mesozoic sedimentary rocks in Khorat Plateau. Senior Project, Department of Geology, Faculty of Science, Chulalongkorn University.

Appendices

Appendix A: X-ray powder diffractogram

Sample name: TY 1

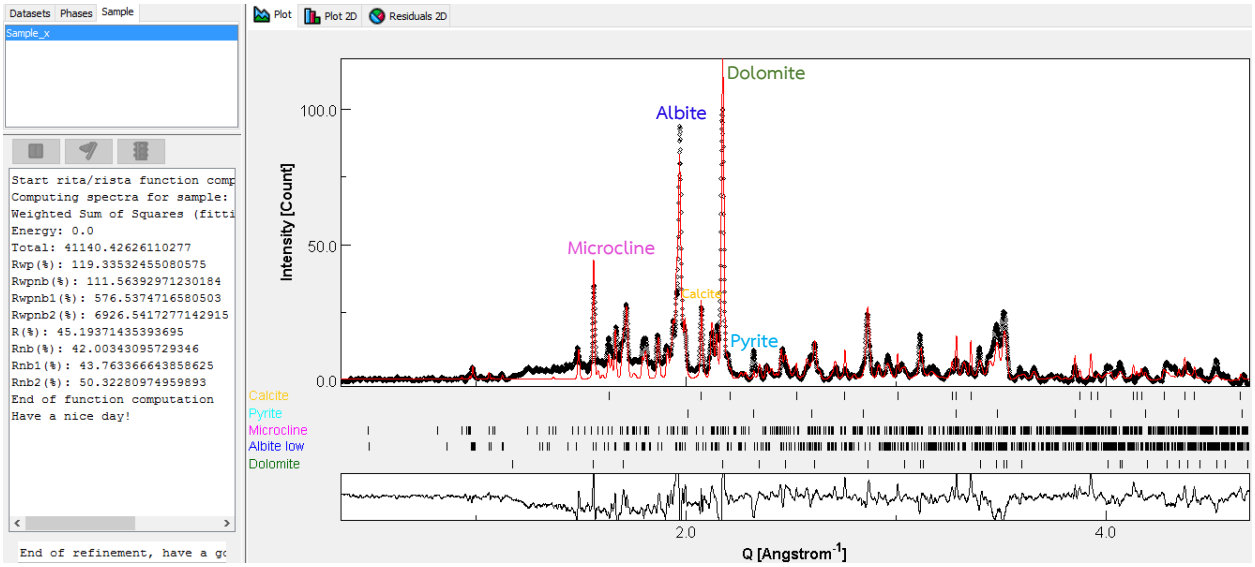

Sample name: TY 2

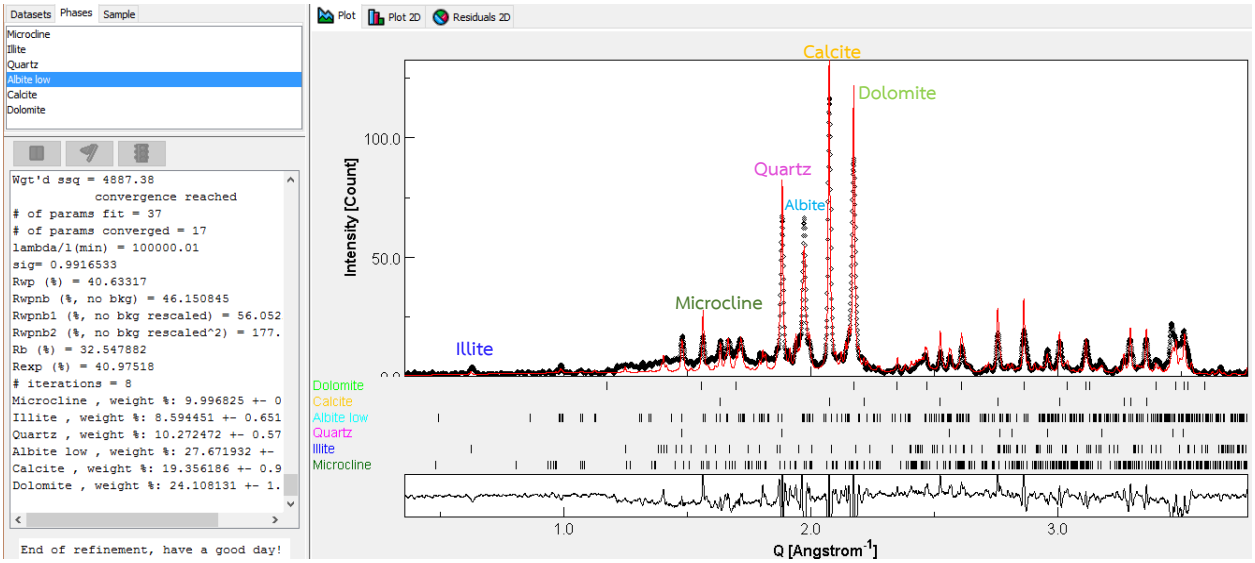

Sample name: TY 3

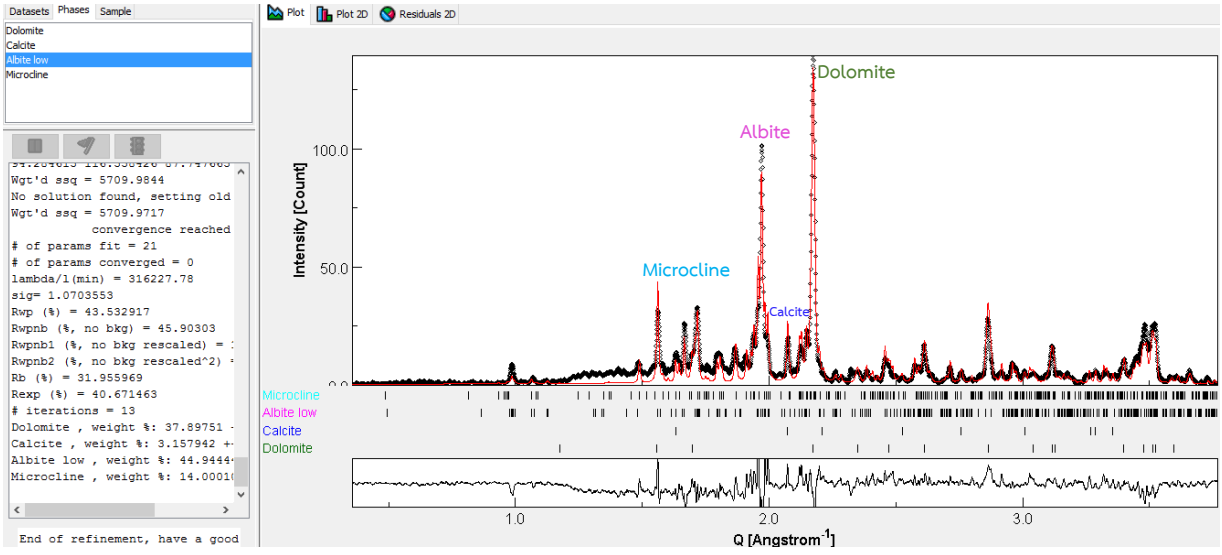

Sample name: TY 4

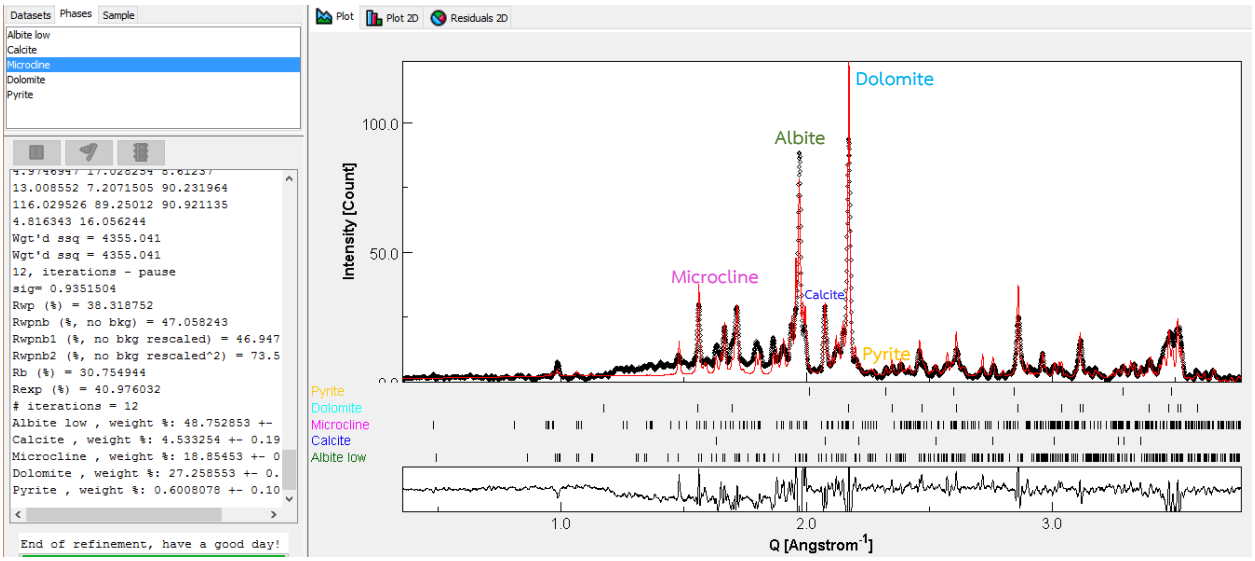

Sample name: TY 5

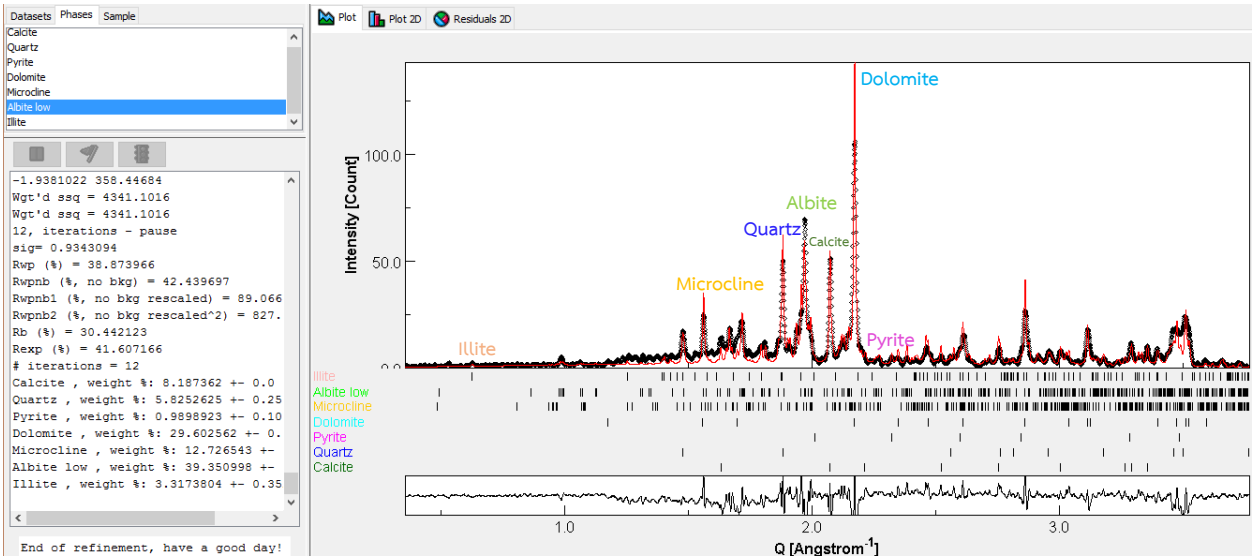

Sample name: TY 6

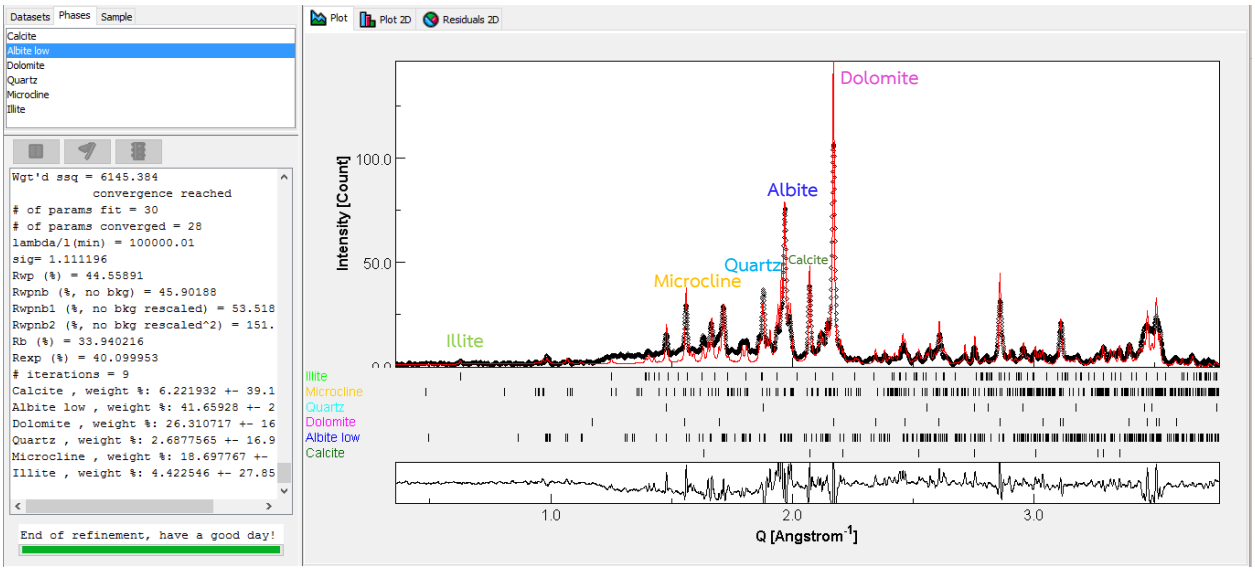

Sample name: TY 7

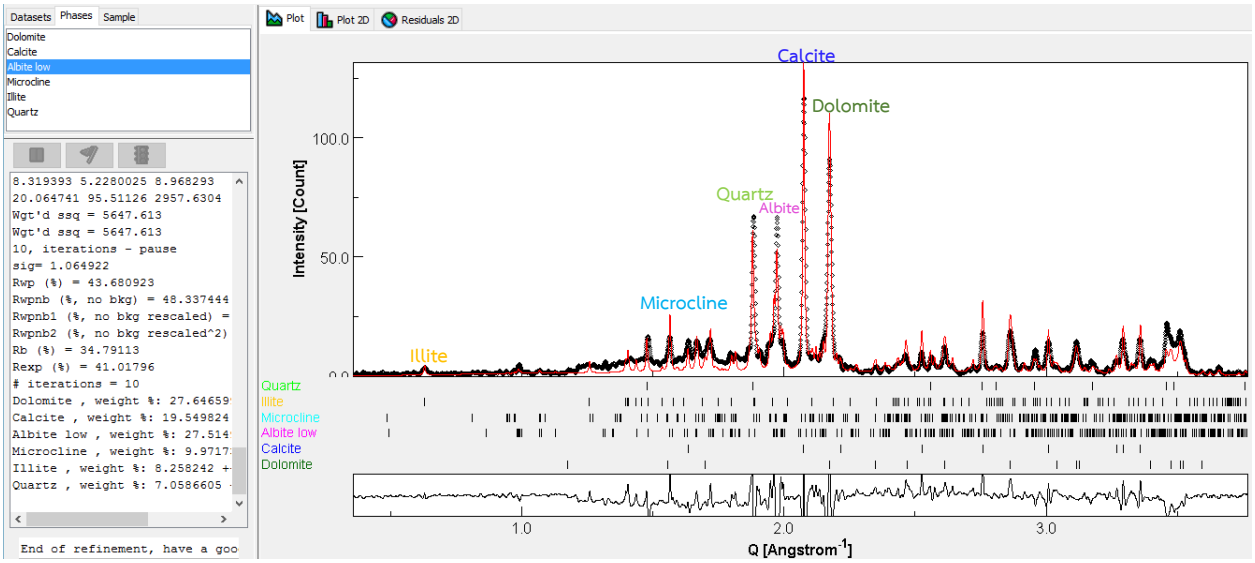

Sample name: TY 8

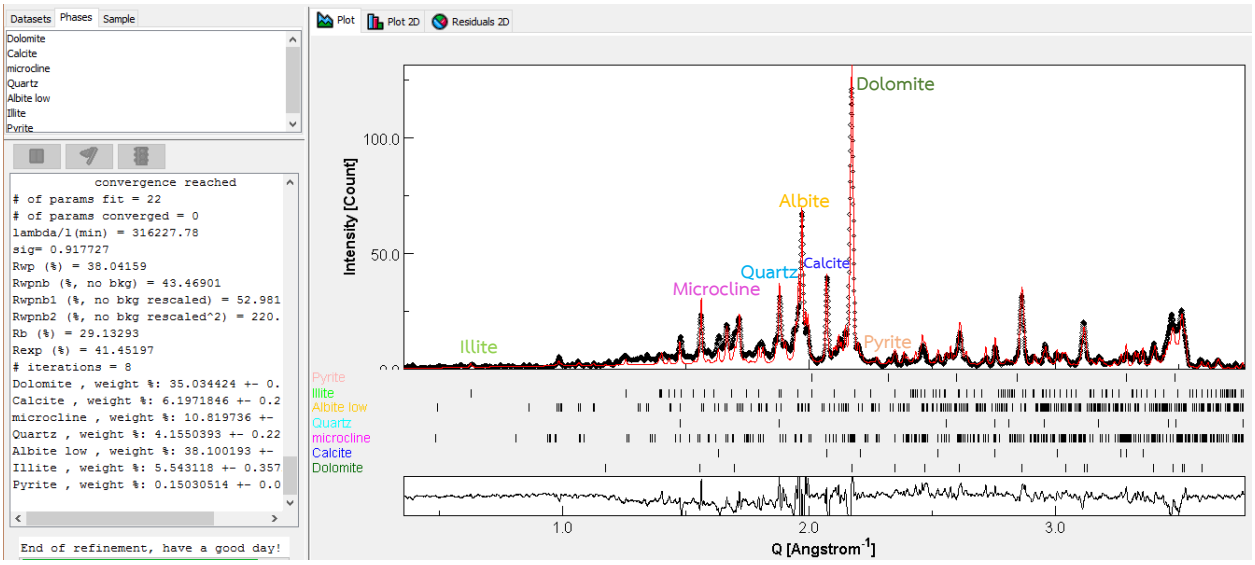

Sample name: TY 9

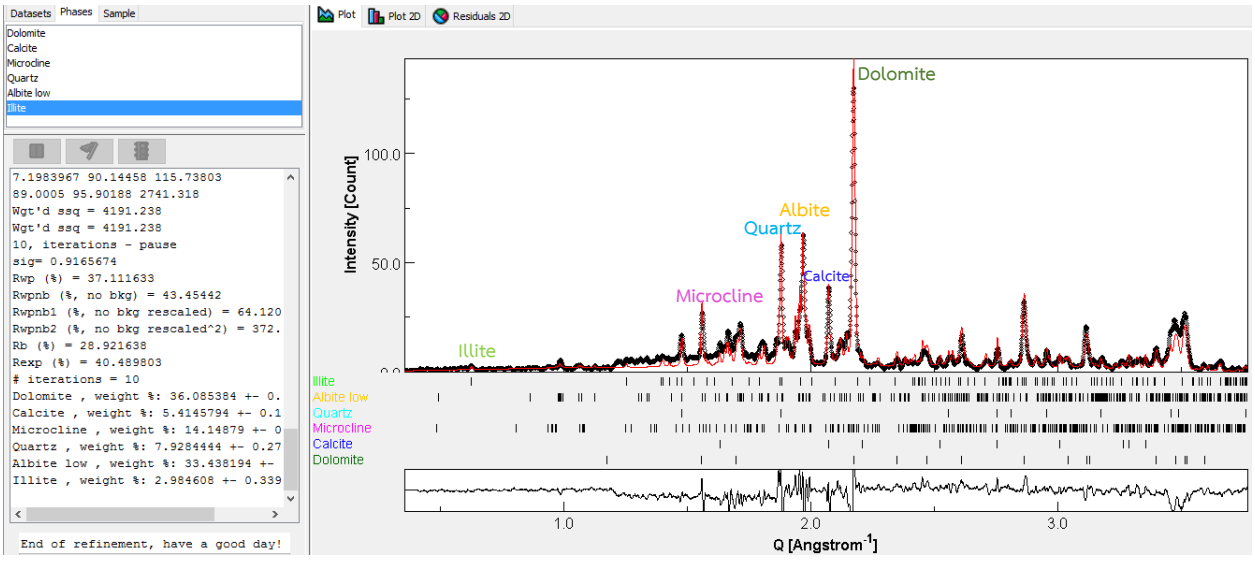

Sample name: TY 10

- Oriented XRD

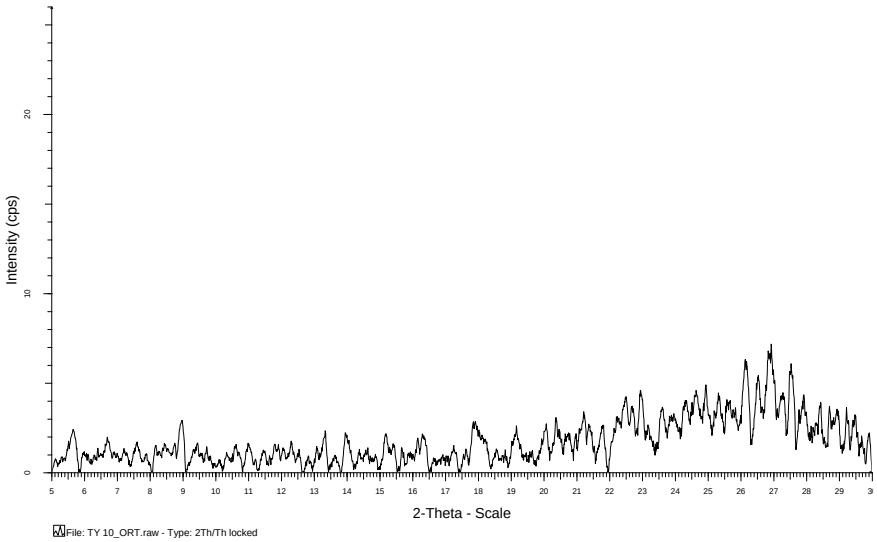

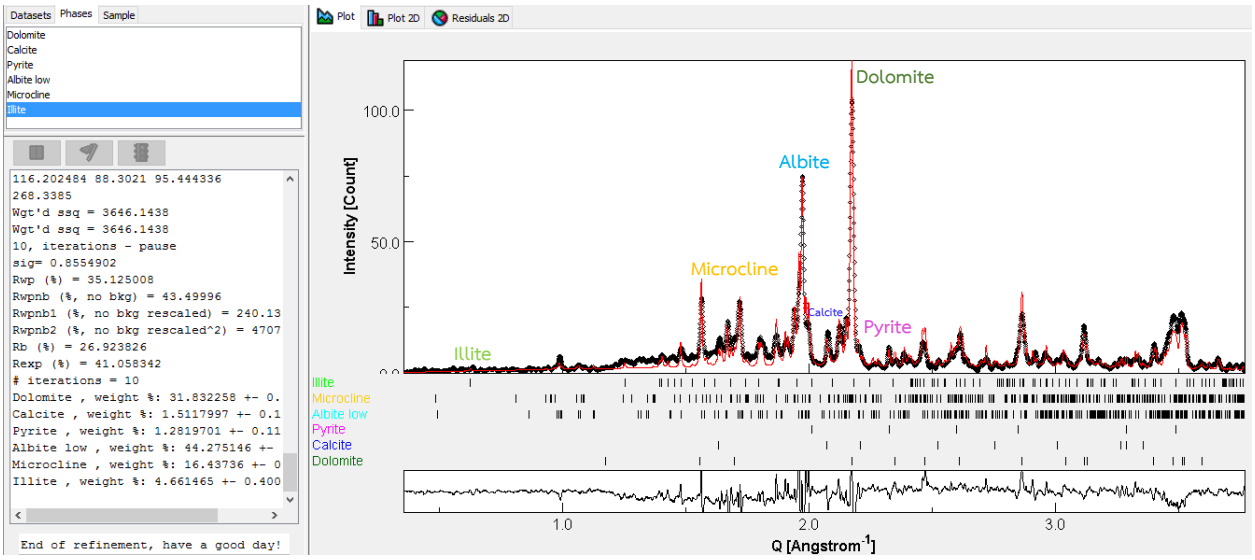

Sample name: TY 11

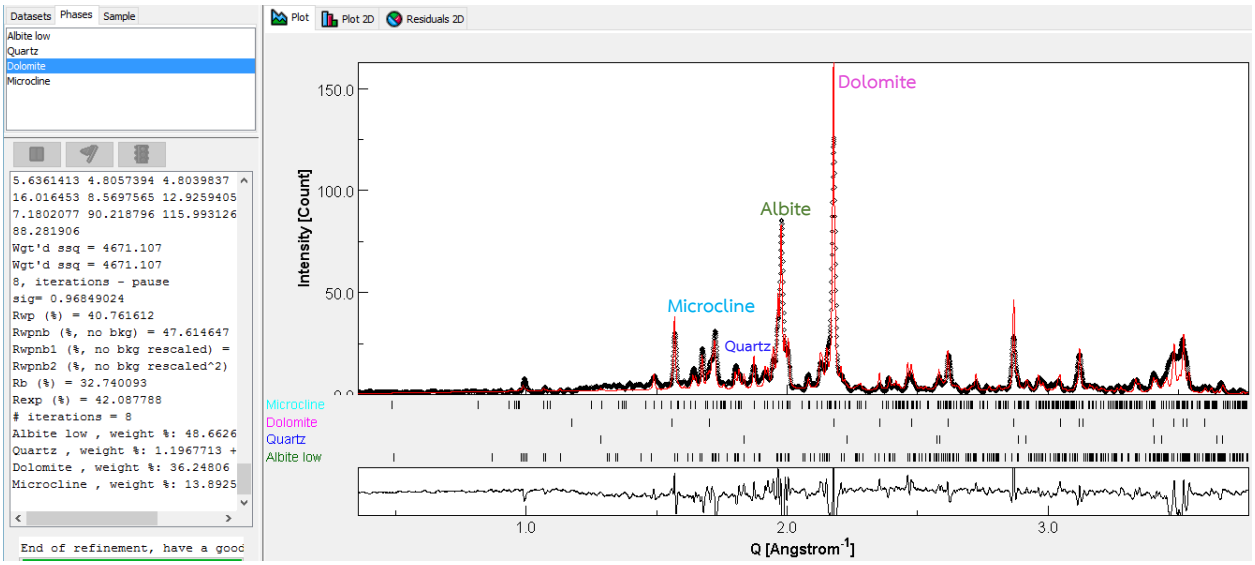

Sample name: TY 12

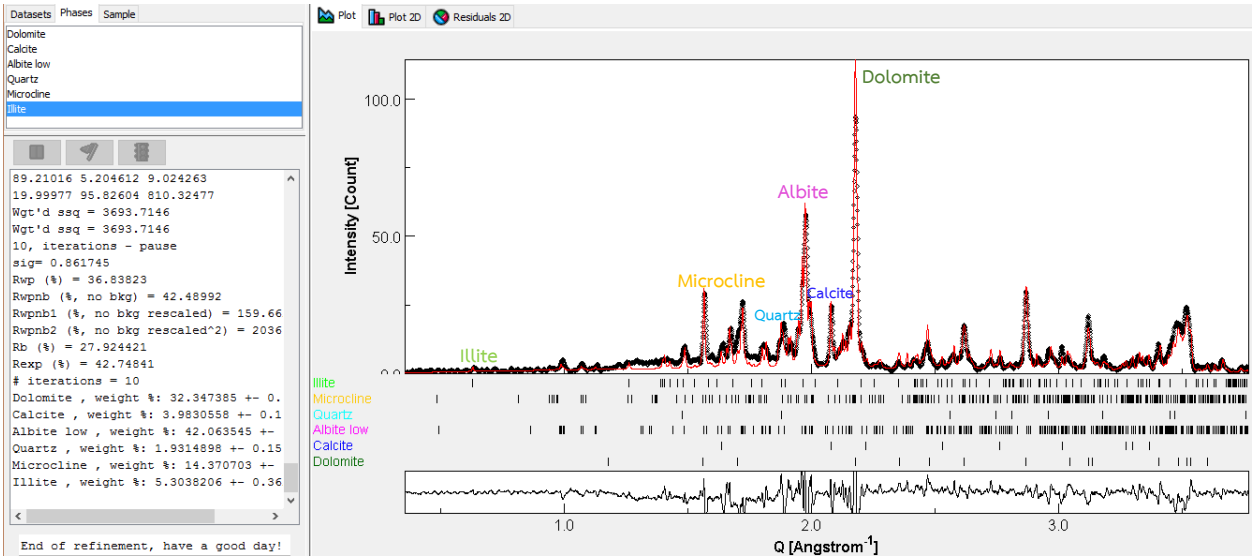

Sample name: TY 13

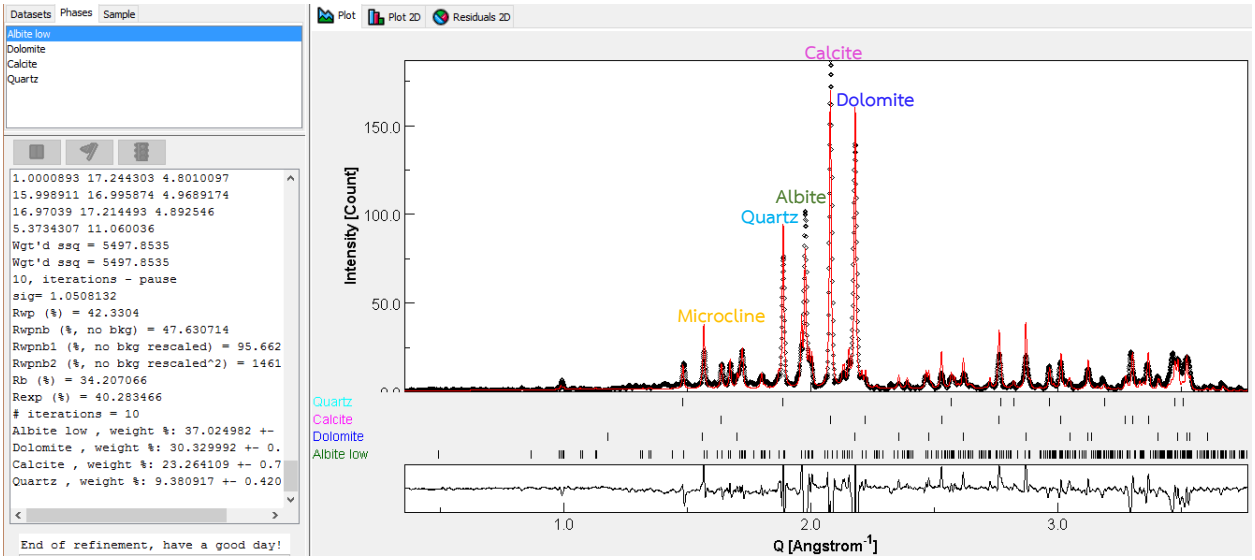

Sample name: TY 14

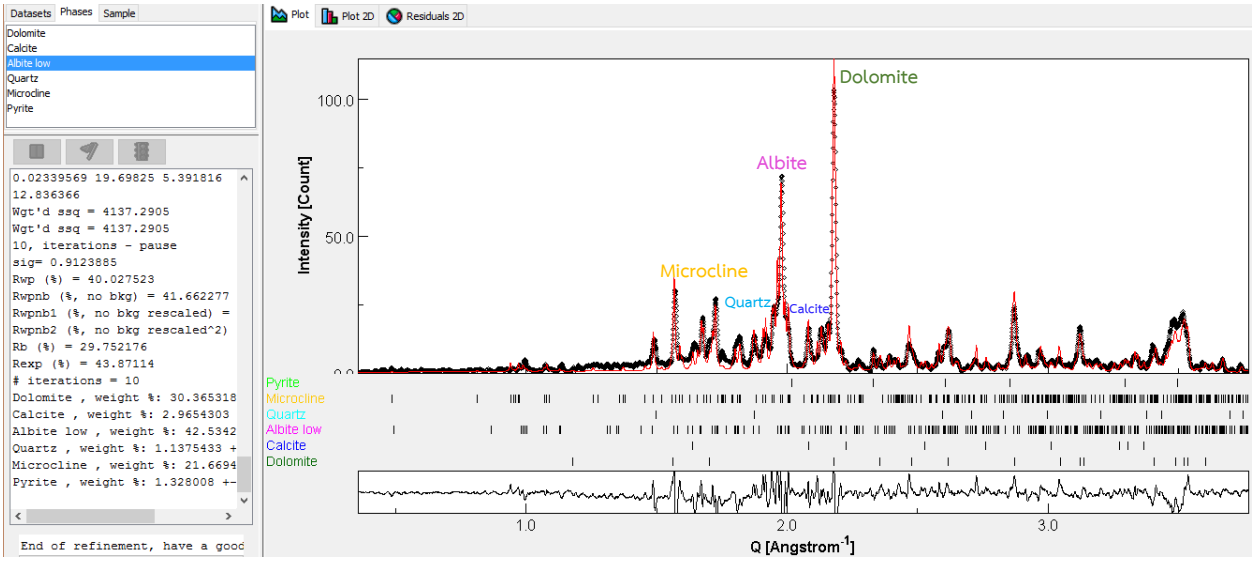

Sample name: TY 15

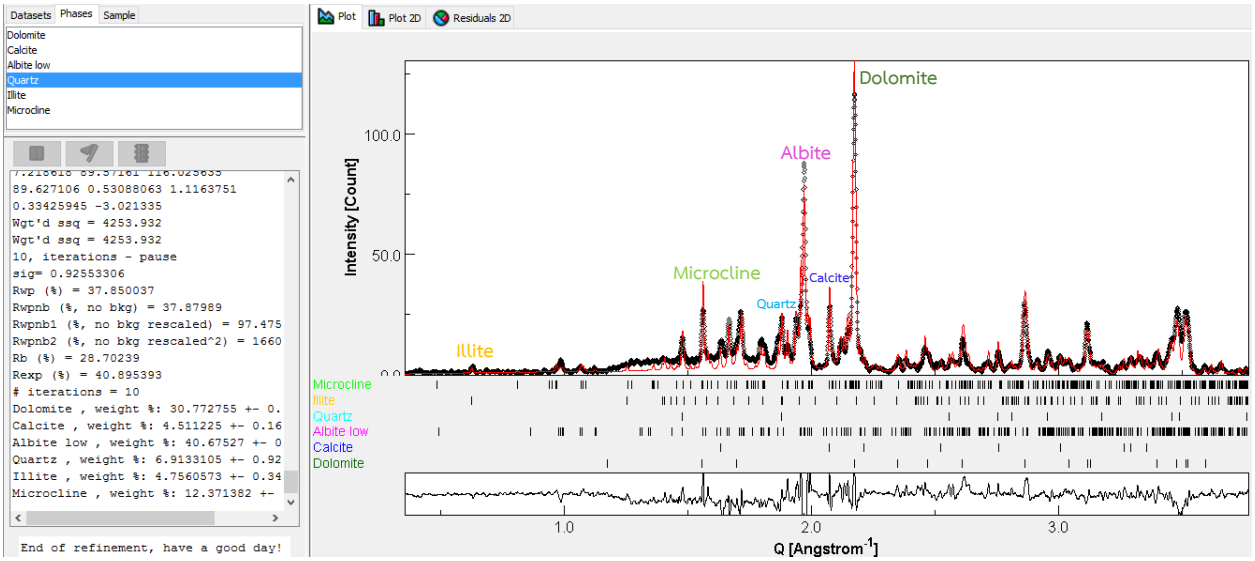

Sample name: TY 16

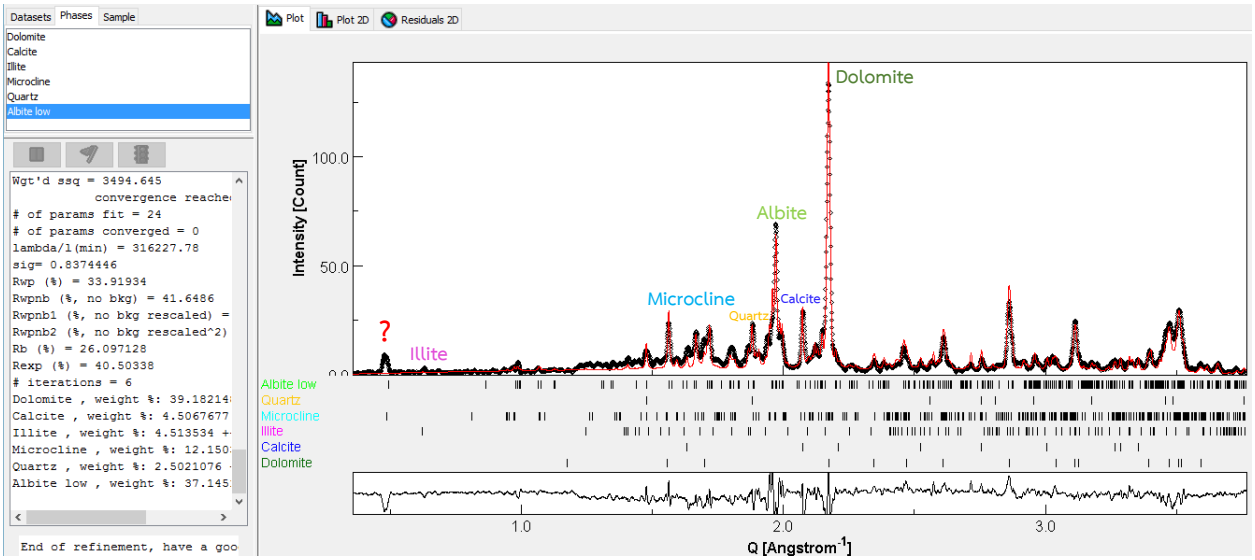

Sample name: TY 17

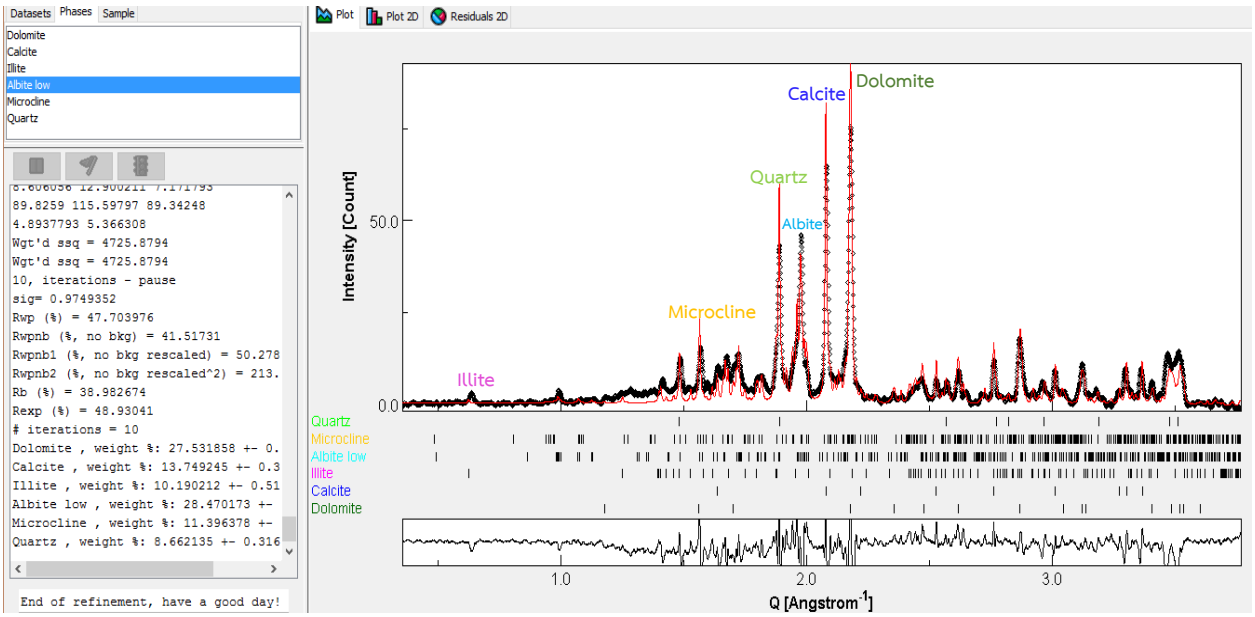

Sample name: TY 18

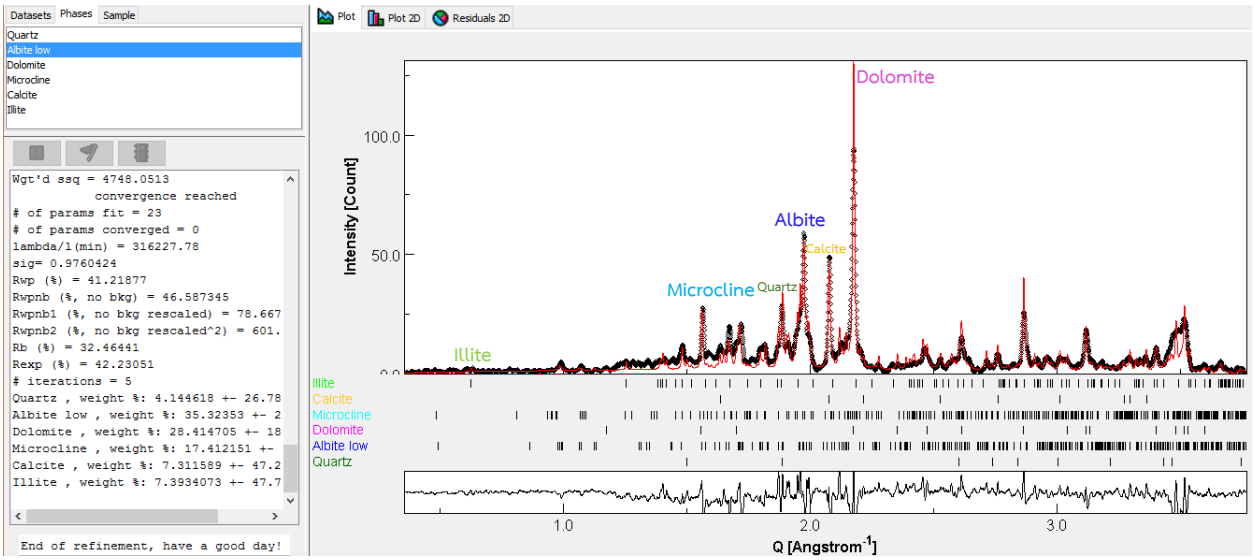

Sample name: TY 19

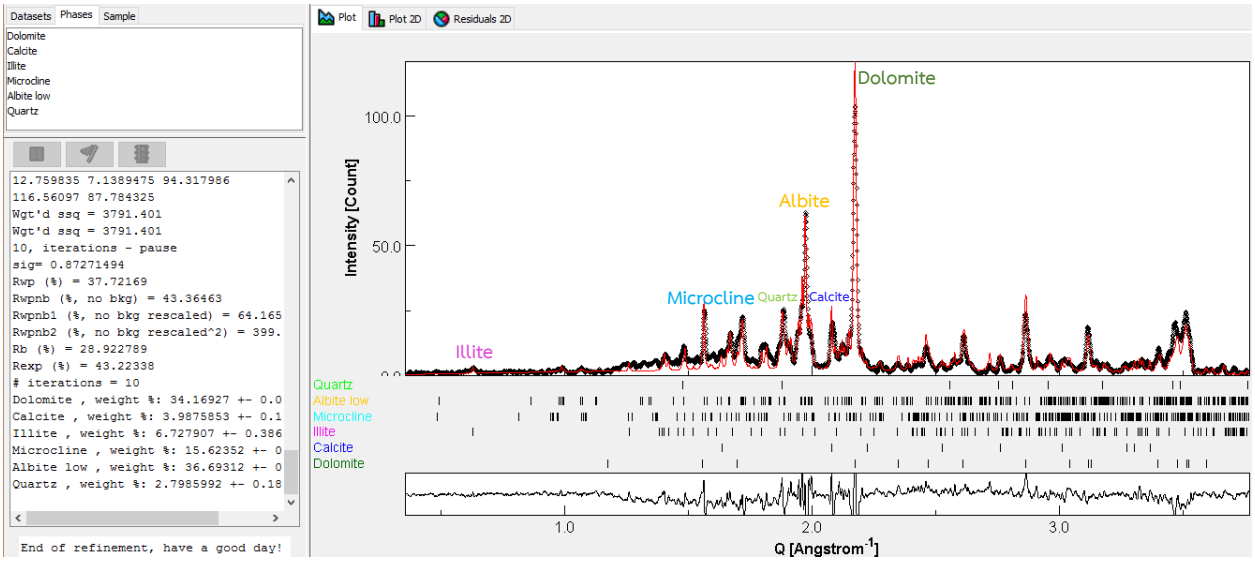

Sample name: TY 20

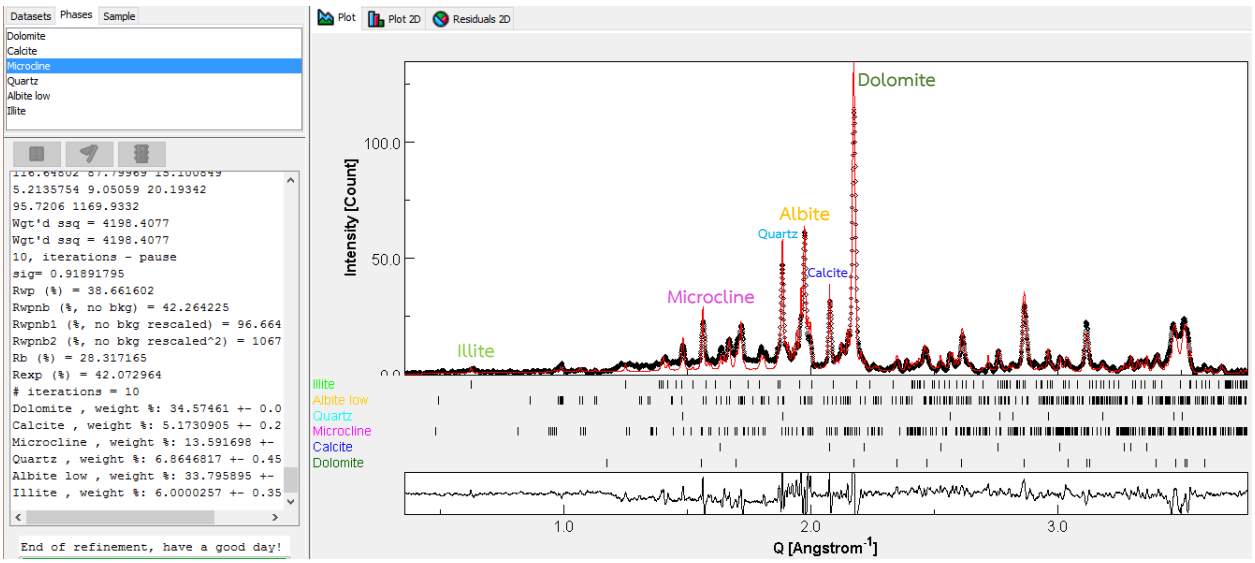

Sample name: TY 21

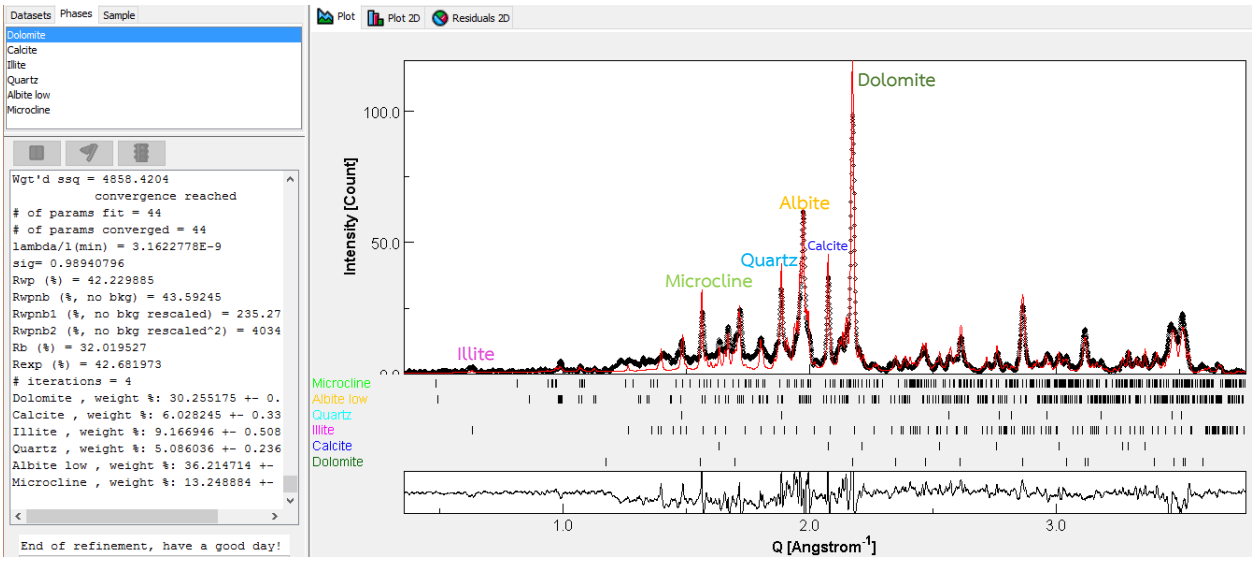

Sample name: TY 22

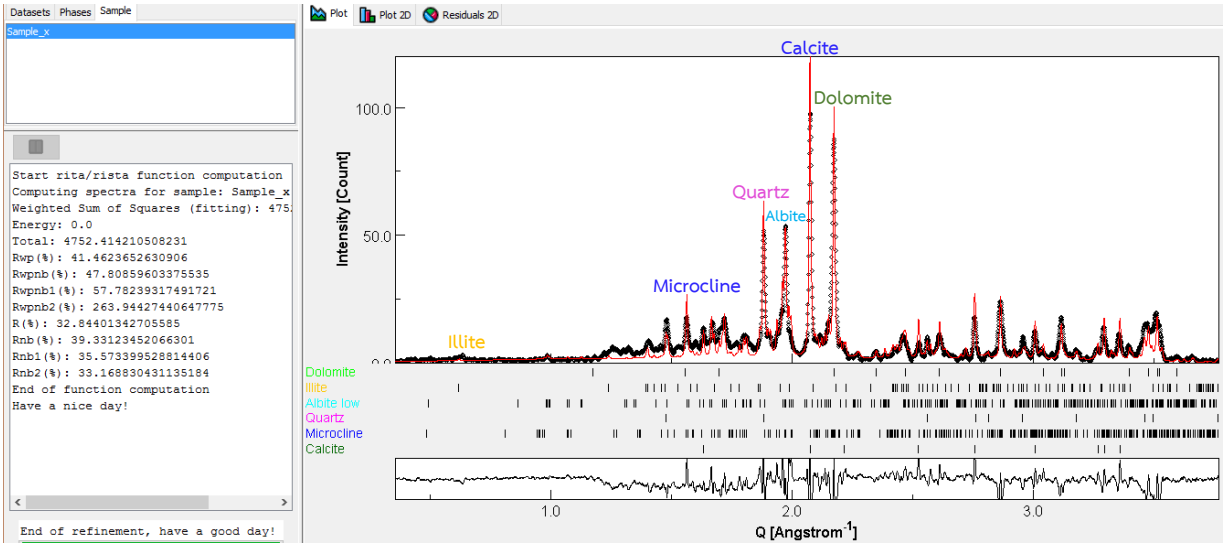

Sample name: TY 23

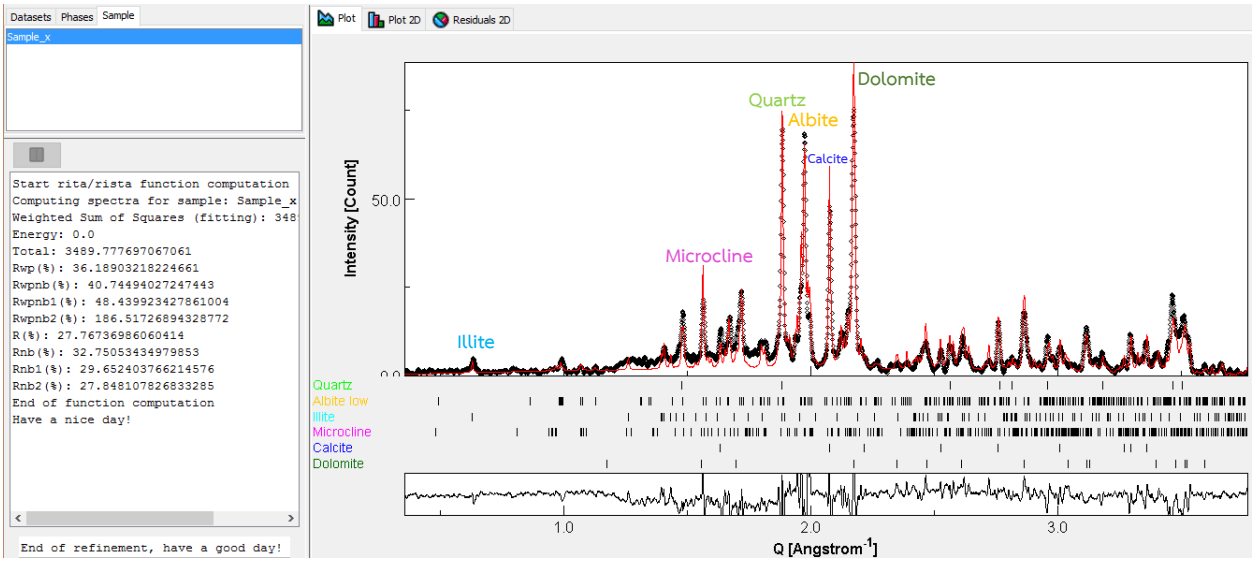

Sample name: TY 24

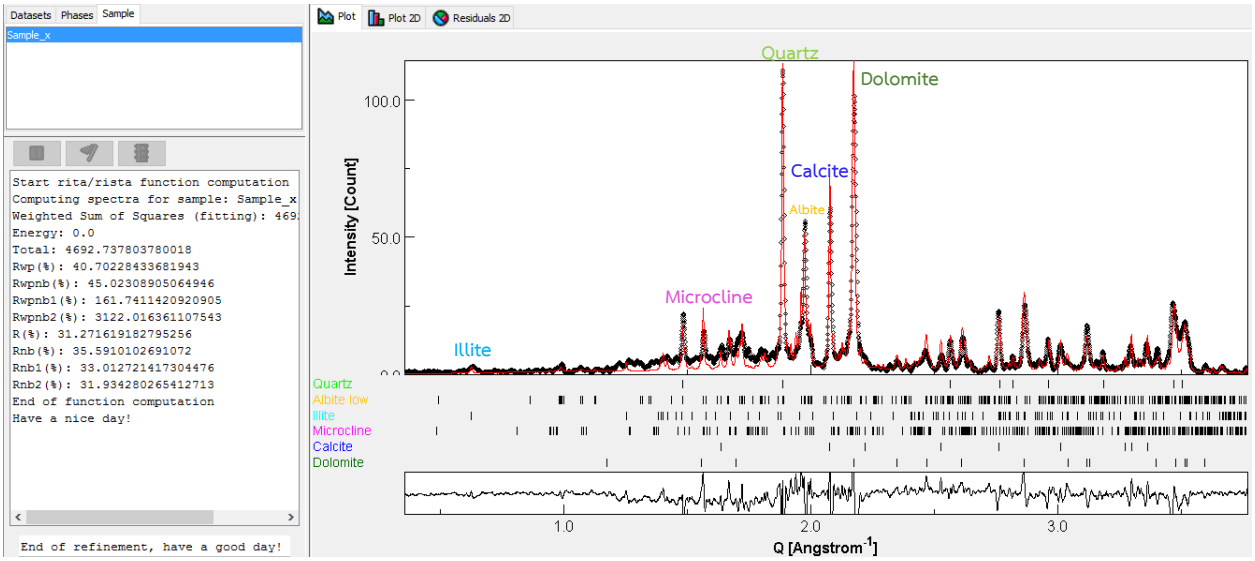

Sample name: TY 25

- Oriented XRD

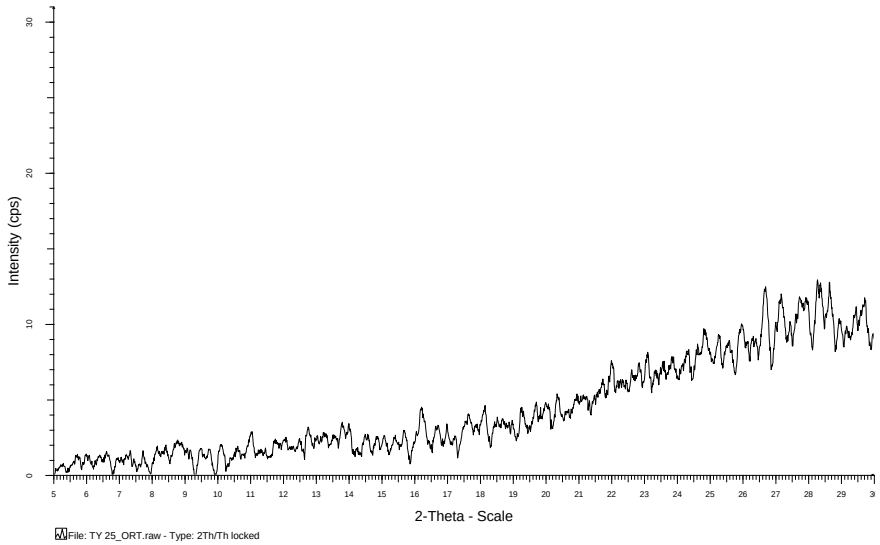

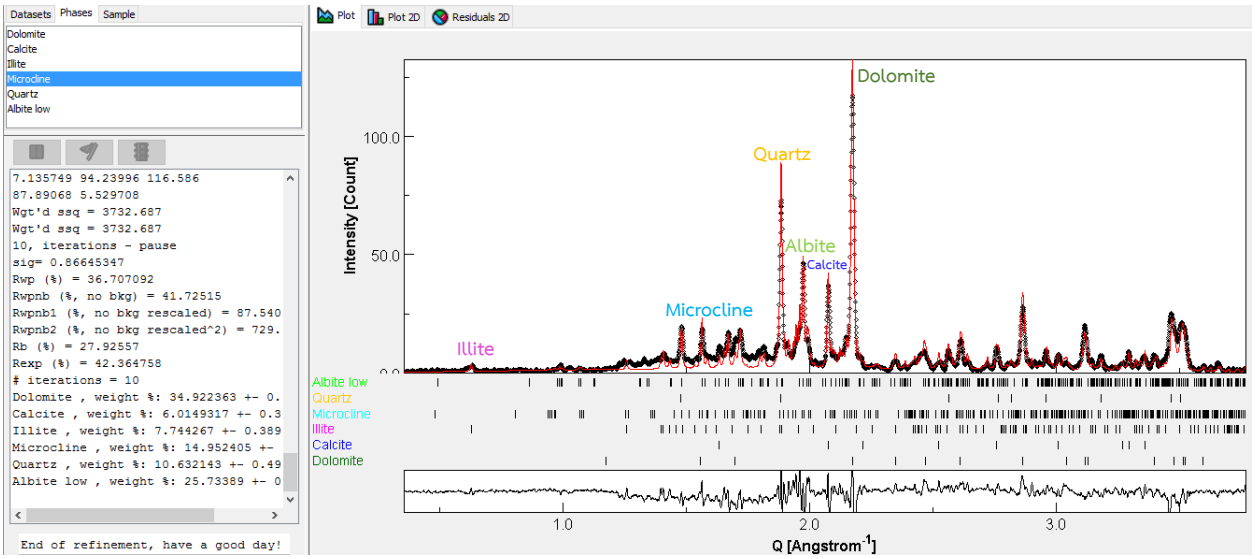

Appendix B: TOC & Rock-Eval pyrolysis results of the original and decarbonated samples

- The original Tat Yai samples

Company : GEN Labs
Well/Area : Student samples
Sample Type : Outcrops
File No. : BGM 16006

TABLE
ROCK-EVAL PYROLYSIS AND TOC CONTENT *

Sample ID	Lithology	TOC (wt.%)	mg/gm rock			Tmax (°C)	Oil Production Index (OPI)	Potential Yield (S_1+S_2)	Hydrogen Index	Oxygen Index
			S_1	S_2	S_3					
TY-1	brnsh gy, calc	1.92	0.22	0.03	0.24	301	0.88	0.25	2	13
TY-2	lt brnsh gy, calc	0.87								
TY-3	brnsh blk, calc	2.69	0.10	0.13	0.05	599	0.43	0.23	5	2
TY-4	brnsh blk, calc	2.75	0.10	0.12	0.49	601	0.45	0.22	4	18
TY-5	brnsh gy, calc	1.39	0.11	0.07	0.03	598	0.61	0.18	5	2
TY-6	brnsh gy, calc	1.24	0.06	0.06	0.02	597	0.50	0.12	5	2
TY-7	brnsh gy, calc	1.18	0.05	0.07	0.01	593	0.42	0.12	6	1
TY-8	brnsh gy, calc	1.36	0.04	0.07	0.03	598	0.36	0.11	5	2
TY-9	brnsh gy, calc	1.62	0.05	0.16	0.07	581	0.24	0.21	10	4
TY-10	brnsh blk, calc	2.25	0.03	0.10	0.05	600	0.23	0.13	4	2
TY-11	brnsh gy, calc	1.53	0.07	0.14	0.05	575	0.33	0.21	9	3
TY-12	lt brnsh gy, calc	0.93								
TY-13	lt brnsh gy, calc	0.47								
TY-14	brnsh gy, calc	1.23	0.09	0.06	0.11	598	0.60	0.15	5	9
TY-15	brnsh blk, calc	3.55	0.07	0.20	0.30	600	0.26	0.27	6	8
TY-16	brnsh blk, calc	2.70	0.13	0.25	0.04	582	0.34	0.38	9	1
TY-17	lt brnsh gy, calc	0.91								
TY-18	lt brnsh gy, calc	1.04	0.03	0.04	0.01	600	0.43	0.07	4	1
TY-19	brnsh blk, calc	2.27	0.04	0.09	0.25	600	0.31	0.13	4	11
TY-20	brnsh gy, calc	2.05	0.10	0.17	0.05	595	0.37	0.27	8	2

S_1 = Free Hydrocarbons
Oil Production Index = Transformation Ratio = $S_1/(S_1+S_2)$
* Pyrolysis by Rock Eval 6; TOC content by Leco Analyzer

S_2 = Pyrolysable Hydrocarbons
Tmax = Temperature of Maximum S_2
Hydrogen Index = $(S_2/TOC) \times 100$

S_3 = Organic CO_2
Oxygen Index = $(S_3/TOC) \times 100$

Company : GEN Labs
Well/Area : Student samples
Sample Type : Outcrops
File No. : BGM 16006

TABLE
ROCK-EVAL PYROLYSIS AND TOC CONTENT *

Sample ID	Lithology	TOC (wt.%)	mg/gm rock			Tmax (°C)	Oil Production Index (OPI)	Potential Yield (S_1+S_2)	Hydrogen Index	Oxygen Index
			S_1	S_2	S_3					
TY-21	brnsh gy, calc	1.88	0.06	0.09	0.04	599	0.40	0.15	5	2
TY-22	lt brnsh gy, calc	0.94								
TY-23	brnsh gy, calc	1.32	0.04	0.10	0.01	578	0.29	0.14	8	1
TY-24	brnsh gy, calc	1.42	0.04	0.12	0.02	582	0.25	0.16	8	1
TY-25	brnsh gy, calc	1.64	0.05	0.12	0.03	592	0.29	0.17	7	2

- Decarbonated samples

Job	Analysis	S1(mg/g)	S2(mg/g)	S3(mg/g)	S3CO(mg/g)	PC(%)	RC(%)	TOC(%)	MINC(%)	TpkS2(°C)	Tmax(°C)	Weight(mg)
ty01-25	ty_01.R00	0.08	0.01	0.07	0.03	0.01	2.55	2.56	0.02	362	324	60.5
ty01-25	ty_02.R00	0.03	0.03	0.05	0.01	0.01	1.35	1.35	0.02	646	608	60.2
ty01-25	ty_03.R00	0.13	0.07	0.07	0.01	0.02	4.26	4.28	0.02	646	608	60.0
ty01-25	ty_04.R00	0.09	0.13	0.31	0.05	0.04	4.45	4.49	0.03	646	608	60.6
ty01-25	ty_05.R00	0.10	0.05	0.10	0.01	0.02	2.23	2.25	0.03	341	303	59.8
ty01-25	ty_06.R00	0.06	0.04	0.05	0.02	0.01	1.97	1.98	0.02	342	304	59.9
ty01-25	ty_07.R00	0.14	0.03	0.03	0.03	0.02	1.70	1.72	0.01	500	462	60.5
ty01-25	ty_08.R00	0.10	0.05	0.06	0.02	0.02	2.27	2.29	0.03	645	607	60.4
ty01-25	ty_09.R00	0.18	0.17	0.05	0.02	0.03	2.77	2.80	0.02	640	602	60.7
ty01-25	ty_10.R00	0.12	0.02	0.10	0.02	0.02	3.19	3.21	0.02	321	283	60.6
ty01-25	ty_11.R00	0.20	0.15	0.04	0.01	0.03	2.26	2.29	0.02	644	606	60.9
ty01-25	ty_12.R00	0.09	0.05	0.03	0.02	0.02	1.37	1.39	0.01	644	606	60.2
ty01-25	ty_13.R00	0.09	0.00	0.04	0.00	0.01	0.82	0.83	0.01	344	306	60.5
ty01-25	ty_14.R00	0.11	0.01	0.04	0.02	0.01	1.62	1.63	0.01	342	304	60.1
ty01-25	ty_15.R00	0.27	0.48	0.36	0.20	0.09	5.82	5.91	0.03	645	607	59.9
ty01-25	ty_16.R00	0.25	0.52	0.08	0.04	0.07	4.81	4.88	0.02	636	598	60.4
ty01-25	ty_17.R00	0.09	0.06	0.05	0.01	0.02	1.41	1.43	0.01	646	608	60.9
ty01-25	ty_18.R00	0.06	0.02	0.05	0.01	0.01	1.52	1.53	0.01	413	375	60.3
ty01-25	ty_19.R00	0.19	0.19	0.29	0.05	0.05	3.74	3.79	0.03	645	607	60.2
ty01-25	ty_20.R00	0.27	0.20	0.05	0.02	0.04	3.71	3.75	0.02	646	608	60.4
ty01-25	ty_21.R00	0.15	0.02	0.06	0.02	0.02	2.93	2.95	0.02	363	325	60.5
ty01-25	ty_22.R00	0.07	0.03	0.06	0.01	0.01	1.48	1.49	0.01	646	608	59.9
ty01-25	ty_23.R00	0.08	0.05	0.03	0.02	0.01	1.88	1.89	0.01	646	608	61.0
ty01-25	ty_24.R00	0.17	0.14	0.05	0.01	0.03	2.53	2.56	0.01	646	608	60.0